June, 1969

Report ESL-R-387
M.I.T. DSR Project 76265
NASA Research Grant NGL-22-009(124)

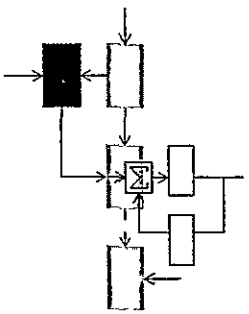

THE AERODYNAMIC SURFACE LOCATION PROBLEM IN OPTIMAL CONTROL OF FLEXIBLE AIRCRAFT

Timothy L. Johnson

Electronic Systems Laboratory

MASSACHUSETTS INSTITUTE OF TECHNOLOGY, CAMBRIDGE, MASSACHUSETTS 02139

Department of Electrical Engineering

June, 1969 Report ESL-R-387 Copy No._____

THE AERODYNAMIC SURFACE LOCATION PROBLEM IN OPTIMAL CONTROL OF FLEXIBLE AIRCRAFT

by

Timothy L. Johnson

This report consists of the unaltered thesis of Timothy Lee Johnson, submitted in partial fulfillment of the requirements for the degree of Master of Science at the Massachusetts Institute of Technology in May, 1969. This research was carried out at the M. I. T. Electronic Systems Laboratory with support extended by the National Aeronautic and Space Administration under Research Grant No. NGL-22-009(124), M. I. T. DSR Project No. 76265

Electronic Systems Laboratory
Department of Electrical Engineering
Massachusetts Institute of Technology
Cambridge, Massachusetts 02139

THE AERODYNAMIC SURFACE LOCATION PROBLEM IN OPTIMAL CONTROL OF FLEXIBLE AIRCRAFT

by

TIMOTHY LEE JOHNSON

SUBMITTED IN PARTIAL FULFILLMENT OF THE
REQUIREMENTS FOR THE DEGREE OF
MASTER OF SCIENCE

at the

MASSACHUSETTS INSTITUTE OF TECHNOLOGY
June, 1969

Signature of Author Timothy L. Johnson
Department of Electrical Engineering, May 23, 1969

Certified by Michael Athans
Thesis Supervisor

Accepted by
Chairman, Departmental Committee on Graduate Students

THE AERODYNAMIC SURFACE LOCATION PROBLEM IN OPTIMAL CONTROL OF FLEXIBLE AIRCRAFT

by

TIMOTHY LEE JOHNSON

Submitted to the Department of Electrical Engineering on May 23, 1969 in partial fulfillment of the requirements for the Degree of Master of Science.

ABSTRACT

The basic physical relationships involved in control of a flexible aircraft disturbed by random wind gusts were used in formulating the surface location problem as one in optimal control of a distributed system, using a limited number of point-force controllers. The three phases of this problem--estimation, control, and surface placement--were then solved by means of the matrix minimum principle and the calculus of variations. The variational equations were greatly simplified and the order of the problem considerably reduced by the use of optimal controllers at each stage in the search for optimal surface locations. These simplifications, plus advanced computational techniques made the general solution of the problem practically feasible.

Aircraft physics had to be investigated in great detail in order to obtain general equations expressing the distributed nature of the system exactly. A computer program was written which stored these equations and used them in sovling the surface location problem for a general aircraft.

This program was tested on a fourteenth order model of the Lockheed C-5A transport aircraft. As a guide for future applications, the derivation of the model parameters was carried through explicitly. The results of the optimization study were then analyzed in an attempt to recognize and develop a "strategy" for control surface placement.

A simple practical strategy was developed for systems with stress and stress rate responses and slightly simplified physics. This strategy, which was also verified for the C-5A model, has the two major advantages of (1) insight into the tradeoffs involved in surface location, and (2) partial insight into global solutions.

The major contributions of this thesis are (1) a computationally feasible general solution to the surface placement problem, (2) a practical application of optimal flexure control to a trial model of the C-5A transport, (3) implementation of efficient computational techniques for

solving state covariance and Riccati equations, and (4) recognition of the nature of the optimal solutions and presentation of a search strategy which makes use of the basic aircraft flexure physics.

Thesis Supervisor: Michael Athans

Title: Associate Professor of Electrical Engineering

ACKNOWLEDGEMENTS

Few thesis undertakings, I believe, have received such widespread cooperation from individuals and institutions as this one. I wish to sincerely thank each of those persons cited below for a gift far greater than the mere facts and innovations which appear in this manuscript proper -- the gift of knowledge. Behind each correct engineering approach there lie a dozen which have been tried and discarded; expert advice is often the force which suggests new approaches and pierces through inadequate ones. The institutions I wish to acknowledge have generously provided funds, facilities, and information without which this undertaking would not have been possible.

An individual for whom I hold great personal admiration, Dr. Grant B. Skelton, Supervisor of the Flight Mechanics Group at Honeywell's Systems and Research Center, has rendered essential assistance to this thesis project since its inception. Not only has Dr. Skelton provided for such resources as superb reference works and computational facilities, but also he has given strong personal support in the theoretical aspects of the project, from his recognition of the topic's significance to his suggestions for approaching a solution, and his aid in writing the preliminary report. As my thesis supervisor at Honeywell, Dr. Skelton has given me both the benefit of his brilliance in the control field, and of his deep insight on more personal but equally important issues such as ethics, responsibility, duty, and professional conduct. Dr. Skelton has been a mentor to me in the fullest sense of the word.

Professor Michael Athans, who has supervised this effort since my return to M.I.T., also deserves special citation. Few men could have taken over such a complex project in midstream and guided it so smoothly to a successful conclusion as Professor Athans; the revision of Sections I and II which was motivated by his suggestions has, I feel, considerably improved the final report. In addition to reading the thesis draft and offering constructive comments, Professor Athans has stimulated a continued growth of my knowledge and field of endeavor by suggestion some very promising areas of future study arising out of the ideas developed herein. I look forward to continued co-operation with Professor Athans in these areas.

Several other individuals have contributed significantly to various aspects of this thesis, particularly Mr. Michael Ward (computational techniques), Mr. C. R. Stone (aerodynamics), and Messrs. Lester Edinger and William Glasser (C-5A model construction). I also wish to thank members of the Flight Mechanics Group of the Honeywell Systems and Research Center, Mr. M. A. Bender of Honeywell, and Mr. R. L. McDougal of the Lockheed-Georgia Company for their co-operation.

In addition to this invaluable individual assistance, I must acknowledge the four organizations responsible for providing funds and facilities to support this research.

Honeywell, Inc., has fully supported this work from its inception, in terms of funds, computer facilities, information and indeed my own employment as an M.I.T. co-operative student. I cannot exaggerate the value of the experience which working for Honeywell has given me.

The Lockheed-Georgia Company has kindly permitted publication of the C-5A mathematical model which is developed in Section IV and appears in Appendix I. Although the model is based on preliminary (i.e., pre-flight test) data supplied by the company, I must strongly emphasize that the model developed in this thesis is purely the author's effort and purely his responsibility. The trial model is by no means complete and only represents in a very crude way the expected behavior of the aircraft. The Lockheed-Georgia Company accepts no responsibility for the validity of any of the results presented in this thesis.

I further acknowledge that this project has been partially supported by funds of the National Aeronautics and Space Administration under Grant No. (NASA)NGL-22-009(124) and is to appear shortly as a technical report by that agency. These funds provided computer time for obtaining results with the trial model of the C-5A and for prepartion of the final document.

Finally, I want to recognize the very generous support of the FANNIE AND JOHN HERTZ FOUNDATION, which has awarded the fellowship under which the later portion of this work was completed. Funds supplied by this foundation were crucial in permitting me to obtain the final and most significant computational results of the thesis.

My debts of gratitude would be incomplete without recognition of Mrs. Clara Conover for her superb job of typing this very detailed document and her unlimited patience with the numerous oversights in the manuscript. Mssrs. Harold Tonsing and Arthur Giordani have executed a flawless professional rendition of the numerous charts and diagrams which appear throughout this work.

CONTENTS

CONTENTS (Contd.)

INTRODUCTION

Historically the task of designing a flight control system has not included choosing the sizes or locations of the aerodynamic control surfaces. In many flight control problems the control designer has not even been free to choose the actuators which drive these surfaces. There has not been a need to give the designer these freedoms; surface locations and control authority are chosen for rigid body trim and maneuverability, and flight control designers have been designing rigid body control systems.

The advent of active flexure control has changed this picture. It is obvious from the flexure mode physics that no mode can be effectively controlled through a surface located near a node point. Outboard ailerons, for example, are evidently more effective for control of a wing torsion mode than elevator flaps. Clearly each directly controlled mode must be controllable, and some force producer locations will be more effective than others.

The freedom to choose control surface locations creates several new issues: How many control surfaces should be used; what are the trade-offs between them; can physically intuitive guidelines for surface placement be found; how much performance will added surfaces purchase, or will optimal positions change radically when new surfaces are added? These issues can be reduced to two fundamental questions:

1. What intuitive considerations (if any) are most significant in choosing control surface locations -- what are the fundamentals?

2. What degree of over-all performance improvement can be achieved by using the freedom to choose surface locations?

The primary concern of this thesis will be to answer the first question--how to identify the fundamentals of control surface location. By closely examining the flexure physics of the aircraft, one can understand the constraints posed by a limited number of control surfaces for a large number of vibration modes and develop a strategy for roughly estimating optimal locations. This rough estimation may be seen either as method of choosing initial locations for a search procedure, or as a "rule of thumb" to be used in lieu of an exact solution to the problem. In both cases the precise optimization problem serves as a check on the validity of the approximations used.

The C-5A transport (see Fig. 1) is an excellent vehicle for such investigations; structural flexure modes, being a significant factor in performance evaluation, can cause some control surface locations to be definitely superior to others. The great size of the C-5A makes it a ready candidate for multiple surfaces of many types -- ailerons, spoilers, canards, leading edge flaps, elevators, rudders, etc. Because of the many modes (15 modes have been calculated for both pitch and lateral models) and the possibility of so many types of multiple surfaces, the C-5A surface location problem definitely demands a control-theoretic treatment. The scale of the problem also permits proposed fundamentals to be adequately tested.

Optimal control theory will be shown to provide a qualitative framework for analyzing the performance of an aircraft with any specified set of control surfaces and surface locations. The success of programs such as Honeywell's Load Alleviation and Mode Stabilization

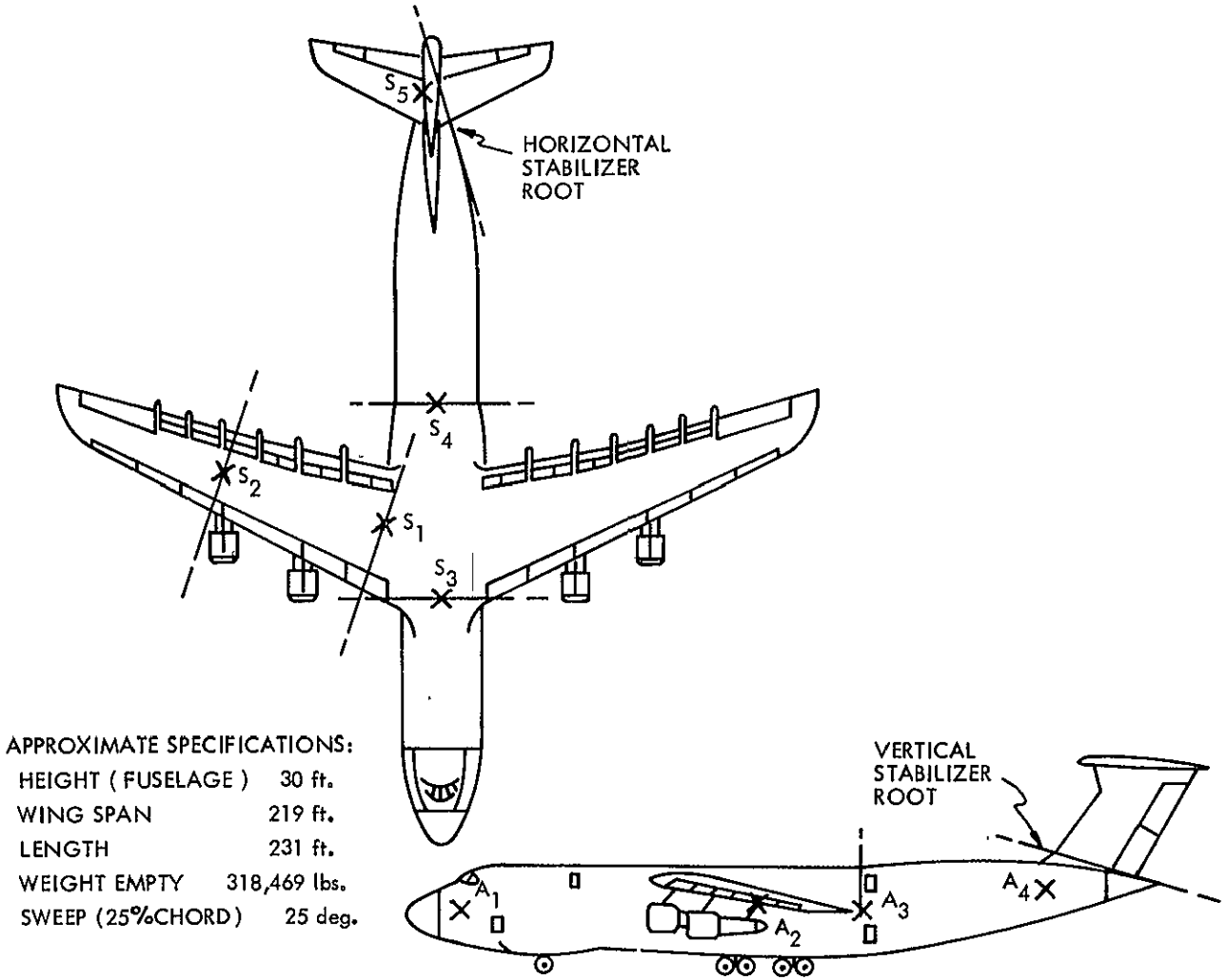

Fig. 1 Lockheed C-5A Transport Aircraft

System for the B-52[19] attests to the practicality of quadratic criteria in evaluating performance. Hence, the second question above may be answered by simply casting the relevant equations of the aircraft into an optimal control framework and evaluating the system performance by such measures as stresses and mean square accelerations.

The body of this thesis is organized around the three contributions which it makes:

1. Solution of the aerodynamic surface placement problem as a distributed-system problem in optimal control theory.
2. Practical implementation of the solution procedure; this includes a new representation of control forces as a function of position and description of a fast state-of-the-art computer program applicable to a wide variety of aircraft.
3. A strategy of surface placement -- an approximate method of choosing locations for a restricted class of problems.

The first section motivates the modelling process by describing the fundamentals of the physical system involved. Section II gives the formulation and solution of the theoretical problem. Section III describes implementation of the technique -- a precise mathematical model of the physics of typical aircraft, and a computational scheme for carrying out the desired calculations. Application of the computer program to a scaled-down model of a large transport aircraft, the C-5A, is given in Section IV. Section V explains a possible strategy of surface placement applicable to an important but restricted class of problems. The sections are written with a maximal amount of independence in order to accommodate readers with varying interests.

SECTION I

THE PHYSICAL SYSTEM

The introduction discusses surface location in an intuitive fashion--indeed the existence and nature of the control surface location problem are evident on such grounds. It is not evident, however, how to approach and organize the problem--in what ways does the solution depend on pure flexure properties of the aircraft, on dynamic properties of the rigid vehicle, on the probabilistic structure of gusts which strike the plane, or on the responses one chooses to evaluate. This section makes clear the physical relationships between these variables and motivates a state-variable description of the problem.

A. BASIC SYSTEM STRUCTURE

Because the aerodynamic forces which govern the motion of an aircraft in flight are basically nonlinear (Bernoulli's principle predicts a square-law dependence of forces on relative wind velocity), a reasonable control problem must treat the vehicle in one or more specified "flight conditions." A flight condition is generally specified by a steady velocity of the aircraft and its orientation with respect to the mean wind striking the vehicle, as well as the settings of throttle and control surfaces which maintain this condition of steady flight. The remainder of the thesis presumes that the primary "plant" is a large flexible aircraft whose motions are perturbed about such a steady flight condition. This assumption is reasonable since such vehicles are designed for long periods of steady flight.

The perturbing forces acting on an aircraft in steady flight are (1) random gust disturbances (relative to the mean wind, about which

all aerodynamic forces are linearized), and (2) control forces resulting from deflections of the aerodynamic surfaces. Because of its inefficiency, engine control is not considered in detail, although it can be readily incorporated into the framework of analysis presented.

The random excitations of the plant due to the gusts give rise to several undesirable responses, such as stresses and distributed torques which cause structural fatigue of the wings and tail, and accelerations affecting ride quality and safety of cargo. The objective of flexure control is to produce control forces in such a way as to counteract these undesirable effects of the stochastic gust inputs. Generally the control engineer is aware of certain locations on the vehicle where large responses are least desirable, e.g., weak points in the basic structure of the aircraft, crucial points such as those where engines are fixed to the wings, or passenger stations in the fuselage. In light of this information, response locations are assumed to be prespecified independently of control surface locations. This is possible because the basic structural properties of the vehicle are independent of surface location; aircraft designers specifically avoid major structural modifications for control surfaces, as these tend to weaken the overall vehicle. (Contrary to intuitive reasoning, it will be shown in Section III that the incidence of control forces is <u>not</u> at the hinge line of a flap--hence there are even more basic physical reasons for choosing response locations independently of control surface locations).

A fundamental though unproven tenet of control theory is that in order to control something, it must be measured. The problem of precisely <u>what</u> signals to sense appears to be quite complicated, as it involves a coupling of control and estimation problems which yields computationally intractable mathematics (with present technology),

so this thesis henceforth assumes sensor locations to be prespecified. Possible types of sensors include rate and position gyros, accelerometers, angle of attack probes, etc. These sensors pick up certain combinations of dynamic state and control variables such as flexure mode accelerations, pitch rate, control forces generated by aileron displacement, etc. An important distinction should be made between responses and sensed signals: sensor locations may be entirely different than response locations--in fact there is quite possibly no necessary connection whatsoever between responses and measured signals. Control of responses depends on their functional relation to the state of the system, and not on measurements of their exact values at a given time. Due to modelling uncertainty and component variations, sensed signals are customarily assumed to be corrupted to some extent. Sensor dynamics are generally ignored, as they are several orders of magnitude faster than aerodynamic and structural responses.

Measured signals, which often give only a partial measure of the state of the aircraft, are all that the control designer may use in constructing feedback signals to the control surfaces. Furthermore, hardware constraints demand that the control law have a minimum of dynamics and a relatively simple form. In effect this dictates (at most) constant gains on feedback of system states. The existence of adequate (though suboptimal) controllers with constant element values and relatively simple form convinces one that optimal controllers should be able to perform effectively within the same constraints.

The freedom to choose surface locations essentially expands the range of forces and moments that the control designer may exert on

the vehicle in order to damp out its responses. Presumably, this new freedom should allow him to do a better job with a specified set of responses and measured signals.

Figure 1 schematizes the basic system structure as described above.

B. MATHEMATICAL MODELLING OF THE SYSTEM

The most fundamental assumption underlying the modelling process is linearity. Linearity, in view of the valuable body of information on linear optimal control, is certainly desirable on a mathematical basis; the definition of the problem in the framework of a given flight condition has also made linearity a justifiable physical assumption. It should be noted that linearization has its costs--practical system designs require examination of many flight conditions and great expense in deriving coefficients for many linear models. If one makes the claim, however, that fatigue lifetimes are governed primarily by the constant flexing of an aircraft in normal (gusty) flight, linearized analyses are also a good way to attack the flexure control problem. In view of the fact that aerodynamic stresses over the cross section of a wing may vary by several tons in an average wind gust, this claim seems quite reasonable.

Another major assumption is that the distributed nature of the system may be adequately approximated by the use of a finite (and reasonably small) number of flexure modes. Although this assumption is well-justified in this problem (due to aerodynamic damping of higher modes), it poses formidable theoretical problems for distributed systems in general.

On the basis of the foregoing physical description and the assumption of linearity, one may model the functional relationships of a

SCHEMATIC DIAGRAM OF AIRCRAFT
FLEXURE CONTROL PROBLEM

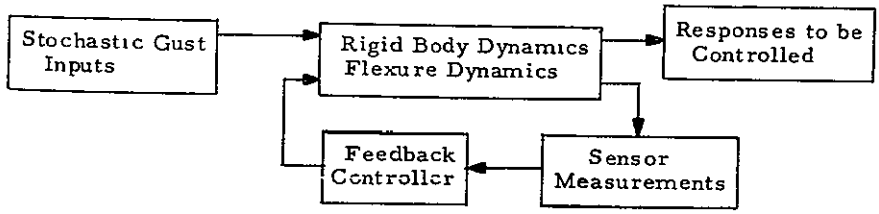

GENERATION OF GUSTS

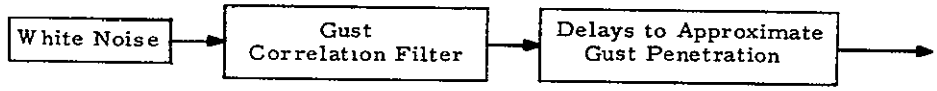

PLANT DYNAMICS

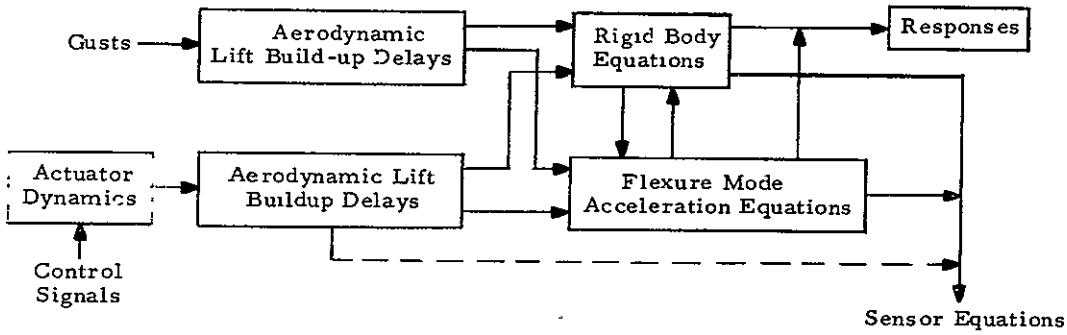

SENSOR EQUATIONS

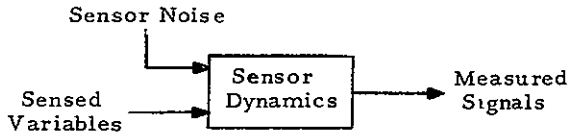

OPTIMAL FEEDBACK CONTROLLER

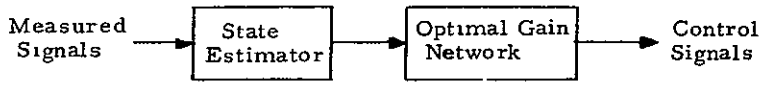

Figure 1

complete system by the equations and variables below.

Definition of Variables

$\underline{x}_1$ rigid body state (angle of attack, sideslip, roll, pitch and yaw rates, etc.)

$\underline{x}_2$ elastic state (mode deflections and rates)

$\underline{x}_3$ gust velocities generated by gust filter

$\underline{x}_4$ gust forces (aerodynamic effect of gusts)

$\underline{x}_5$ control forces (aerodynamic effect of control surface deflections --may be taken to include actuator dynamics)

$\underline{c}$ control signals (actuator drives)

$\underline{m}$ sensor measurements

$\underline{r}$ responses to be minimized

$\underline{\eta}_1$ white noise inputs to gust filter

$\underline{\eta}_2$ white noise inputs to sensor measurements

$\underline{y}$ vector of control surface locations

System Equations

$$\dot{\underline{x}}_1 = \underline{F}_1\underline{x}_1 + \underline{L}_1\underline{x}_2 + \underline{C}_1\underline{x}_4 + \underline{G}_1(\underline{y})\underline{x}_5 \quad \text{(Rigid Body Equations of Motion)} \tag{1}$$

$$\dot{\underline{x}}_2 = \underline{L}_2\underline{x}_1 + \underline{F}_2\underline{x}_2 + \underline{C}_2\underline{x}_4 + \underline{G}_2(\underline{y})\underline{x}_5 \quad \text{(Flexure Equations)} \tag{2}$$

$$\dot{\underline{x}}_3 = \underline{F}_3\underline{x}_3 + \underline{\eta}_1 \quad \text{(Gust Filter)} \tag{3}$$

$$\dot{\underline{x}}_4 = \underline{F}_4\underline{x}_4 + \underline{x}_3 \quad \text{(Gust Aerodynamics)} \tag{4}$$

$$\dot{\underline{x}}_5 = \underline{F}_5\underline{x}_5 + \underline{c} \quad \text{(Control Surface Aerodynamics)} \tag{5}$$

$$\underline{m} = \underline{A}_1\underline{x}_1 + \underline{A}_2\underline{x}_2 + \underline{A}_4\underline{x}_4 + \underline{B}_2\underline{\eta}_2 \quad \text{(Sensor Equations)} \tag{6}$$

$$\underline{r} = \underline{H}_1\underline{x}_1 + \underline{H}_2\underline{x}_2 + \underline{H}_4\underline{x}_4 + \underline{D}_5(\underline{y})\dot{\underline{x}}_5 \quad \text{(Response Equations)} \tag{7}$$

$$= \underline{H}_1\underline{x}_1 + \underline{H}_2\underline{x}_2 + \underline{H}_4\underline{x}_4 + \underline{D}_5(\underline{y})\underline{F}_5\underline{x}_5 + \underline{D}_5(\underline{y})\underline{c}$$

State augmentation

Define the new augmented states:

$$\underline{x}_o = \begin{bmatrix} \underline{x}_1 \\ \underline{x}_2 \\ \underline{x}_3 \\ \underline{x}_4 \end{bmatrix} \quad \underline{u} = [\underline{x}_5] \quad \underline{\eta} = \begin{bmatrix} \underline{\eta}_1 \\ \underline{\eta}_2 \end{bmatrix} \quad \hat{\underline{x}}_o = \begin{bmatrix} \hat{\underline{x}}_1 \\ \hat{\underline{x}}_2 \\ \hat{\underline{x}}_3 \\ \hat{\underline{x}}_4 \end{bmatrix} \quad \underline{x} = \begin{bmatrix} \underline{x}_o \\ \underline{u} \end{bmatrix}$$

The vector $\hat{\underline{x}}_o$ is taken to be the optimal linear estimator of the vector $\underline{x}_o$ based on the measured signals $\underline{m}$ (to be explained later). With these definitions, Eqs. 1 through 7 become:

$$\dot{\underline{x}} = \begin{bmatrix} \dot{\underline{x}}_o \\ \dot{\underline{u}} \end{bmatrix} = \underline{F}\,\underline{x} + \underline{G}\,\underline{c} + \underline{C}\,\underline{\eta} \tag{8}$$

$$\underline{m} = \underline{A}\,\underline{x} + \underline{B}\,\underline{\eta} \tag{9}$$

$$\underline{r} = \underline{H}\underline{x} + \underline{D}\,\underline{c} \tag{10}$$

where

$$\underline{F} = \begin{bmatrix} \underline{F}_1 & \underline{L}_1 & \underline{0} & \underline{C}_1 & \underline{G}_1(y) \\ \underline{L}_2 & \underline{F}_2 & \underline{0} & \underline{C}_2 & \underline{G}_2(y) \\ \underline{0} & \underline{0} & \underline{F}_3 & \underline{0} & \underline{0} \\ \underline{0} & \underline{0} & \underline{I} & \underline{F}_4 & \underline{0} \\ \underline{0} & \underline{0} & \underline{0} & \underline{0} & \underline{F}_5 \end{bmatrix} \quad \underline{G} = \begin{bmatrix} \underline{0} \\ \underline{0} \\ \underline{0} \\ \underline{0} \\ \underline{I} \end{bmatrix} \quad \underline{C} = \begin{bmatrix} \underline{0} & \underline{0} \\ \underline{0} & \underline{0} \\ \underline{I} & \underline{0} \\ \underline{0} & \underline{0} \\ \underline{0} & \underline{0} \end{bmatrix}$$

$$\underline{A} = [\underline{A}_1 \; \underline{A}_2 \; \underline{0} \; \underline{A}_4 \; \underline{0}] \qquad \underline{B} = [\underline{0} \; \underline{B}_2]$$

$$\underline{H} = [\underline{H}_1 \; \underline{H}_2 \; \underline{0} \; \underline{H}_4 \; \underline{D}_5(y)\underline{F}_5] \qquad \underline{D} = [\underline{D}_5(y)]$$

Control Problem

According to the model, one has perfect knowledge of the state $\underline{x}_5$ (aerodynamic forces due to control signals), since $\underline{c}$, the control signals, are generated directly by whatever feedback system is used.

These signals are the only inputs to $\underline{x}_5$. So given $\underline{c}$, one can in theory calculate $\underline{x}_5$, and if any measurements were to contain $\underline{x}_5$, it could be subtracted out exactly to obtain a set of modified signals independent of $\underline{x}_5$; note that this assumption has been implemented in Eq. 6 by making $\underline{m}$ independent of $\underline{x}_5$.

If one knew the remaining states of the system, $\underline{x}_o$, he would wish to use a control law of the form

$$\underline{c} = \underline{K}(\underline{y})\underline{x} \tag{11}$$

since $\underline{x}$ by definition contains all information on the state of the system. $\underline{K}(\underline{y})$ is chosen to be constant rather than time-varying because a time-varying gain would be too difficult to implement; it will later be shown that for long flight times (which is certainly the case), a constant gain $\underline{K}(y)$ is optimal at any rate.

But $\underline{x}_o$ is not completely known, in general, since the system can only be measured by a limited number of stochastically disturbed sensors, for economic and practical reasons. Therefore, one hopes to use a linear estimate, $\hat{\underline{x}}_o$, which (in a way to be defined in Section II) best approximates $\underline{x}_o$. Intuition readily tells one that $\hat{\underline{x}}_o$ must satisfy an equation of the form

$$\dot{\hat{\underline{x}}}_o = \underline{F}_o \hat{\underline{x}}_o + \underline{G}_o \underline{m} \quad *$$

since this is the most general linear dynamic system making use of the measurements available. In practice, this system (the Kalman filter) will not be easy to build. It will be used in this thesis, however, because of its optimality properties; it provides a justifiable standard

---

* If $\underline{m}$ should include $\underline{x}_5$, the author has shown that the Kalman filter will perfectly estimate this state anyway.

by which to compare end results of the location problem. By analogy with (11), one now tries to choose a set of gains so that

$$\underline{c} = \hat{\underline{K}}(\underline{y}) \begin{bmatrix} \hat{\underline{x}}_o \\ \underline{x}_5 \end{bmatrix}$$

For a given set of control surface locations, $\hat{\underline{K}}(\underline{y})$ is chosen to minimize some weighted, quadratic measure of the responses (e.g., their r.m.s. values) over all time.

But if $\underline{y}$ is fixed, the optimum is constrained in comparison to the values it might attain for some other $\underline{y}$. The surface location problem is to find the value or values of $\underline{y}$ which yield the best performance of the vehicle. The modified Newton-Raphson search procedure derived in the following section is a simple algorithm designed to accomplish this complicated task.

SECTION II

THE MATHEMATICAL PROBLEM

This segment of the thesis solves the mathematical version of the control surface location problem motivated by the discussion in Section I. A rigorous mathematical formulation of the problem is stated in the first subsection; the remaining subsections deal with the estimation, control, and search problems, respectively. Detailed calculations have been relegated to appendices.

A. PROBLEM STATEMENT

The linear, time-invariant system to be investigated in this thesis takes the following form:

$$\dot{\underline{x}}(\underline{y},t) = \underline{F}(\underline{y})\,\underline{x}(\underline{y},t) + \underline{G}\,\underline{c}(\underline{y},t) + \underline{C}\,\underline{\eta}(t) \qquad (1)$$

where $\underline{x}(\underline{y},t)$ is the state of the (distributed) system

$\underline{c}(\underline{y},t)$ are control signals to the aerodynamic surfaces

$\underline{\eta}(t)$ is a vector of white noise system distrubances.

$\underline{y}$ is a vector of control surface locations

and $\underline{x}$, $\underline{c}$, $\underline{\eta}$, and $\underline{y}$ are of dimension $(n_o + n_1)$, n_c, n_η and n_y, respectively.

The vector $\underline{\eta}(t)$ is zero-mean with covariance matrix

$$\underline{E}\,(\underline{\eta}(t)\underline{\eta}'(\tau)) = \underline{N}\,\delta(t-\tau)$$

where $\underline{N}$ is a positive definite and symmetric matrix. Because $\underline{N}$ is time-invariant and the system itself is time-invariant, all time-varying signals will become very nearly ergodic shortly after $t=0$, regardless of initial conditions (which are left unspecified for this reason)

and the problem will become an algebraic one in the covariance matrices of the state variables.

The state $\underline{x}(\underline{y},t)$ of the system and the noise $\underline{\eta}(t)$ are assumed to be of the form

$$\underline{x}(\underline{y},t) = \begin{bmatrix} \underline{x}_o(\underline{y},t) \\ \underline{x}_1(\underline{y},t) \end{bmatrix} \quad ; \quad \underline{\eta}(t) = \begin{bmatrix} \underline{\eta}_o(t) \\ \underline{\eta}_2(t) \end{bmatrix}$$

where $\underline{x}_o, \underline{x}_1, \underline{\eta}_o, \underline{\eta}_2$ are of dimension n_o, n_1, n_o , and n_m, respectively, and the plant and noise matrices are decomposed as follows:

$$\underline{F}(\underline{y}) = \begin{bmatrix} \underline{F}_o & \underline{G}_o(\underline{y}) \\ \underline{0} & \underline{F}_1 \end{bmatrix} \quad ; \quad \underline{G} = \begin{bmatrix} \underline{0} \\ \underline{I} \end{bmatrix} \quad ; \quad \underline{C} = \begin{bmatrix} \underline{C}_o & \underline{0} \\ \underline{0} & \underline{0} \end{bmatrix} \quad ; \quad \underline{N} = \begin{bmatrix} \underline{N}_o & \underline{0} \\ \underline{0} & \underline{N}_2 \end{bmatrix}$$

The matrix $\underline{G}_o(\underline{y})$ is assumed to be continuous and differentiable in each dimension of $\underline{y}$. ($\underline{I}$ is the identity matrix.)

The measurements of the state take the form

$$\underline{m}(\underline{y},t) = \underline{A}\,\underline{x}(\underline{y},t) + \underline{B}\,\eta(t) \tag{2}$$

In accordance with the above partitioning, $\underline{A}$ and $\underline{B}$ are written:

$$\underline{A} = [\underline{A}_o \quad \underline{0}] \quad ; \quad \underline{B} = [\underline{0} \quad \underline{B}_o]$$

$\underline{B}_o$ is assumed to be of full rank, $n_m < n_o$, for cases of interest.

The responses to be minimized contain state and control variables:

$$\underline{r}(\underline{y},t) = \underline{H}(\underline{y})\underline{x}(\underline{y},t) + \underline{D}(\underline{y})\underline{c}(\underline{y},t) \tag{3}$$

The dimension of $\underline{r}(\underline{y},t)$ is n_r, and $\underline{H}(\underline{y})$ is partitioned as follows:

$$\underline{H}(\underline{y}) = [\underline{H}_o \; \underline{D}(\underline{y})\underline{F}_1]$$

Again, $\underline{D}(\underline{y})$ is assumed continuous and differentiable in $\underline{y}$.

The objective is to find a linear time-invariant control law of the form

$$\hat{\underline{c}}(\underline{y},t) = \hat{\underline{K}}(\hat{\underline{y}})\hat{\underline{x}}(\hat{\underline{y}},t) \quad , \quad \hat{\underline{x}}(\underline{y},t) = \begin{bmatrix} \hat{\underline{x}}_o(\underline{y},t) \\ \underline{x}_1(\underline{y},t) \end{bmatrix} \tag{4}$$

where $\hat{\underline{x}}_o(\underline{y},t)$ is the conditional minimum-variance unbiased linear estimate of $\underline{x}_o(\underline{y},t)$ given $\underline{m}(\underline{y},t)$, and $\hat{\underline{K}}(\underline{y})$ is chosen so as to minimize the following quadratic criterion in the responses

$$J(\underline{y}) = \lim_{T\to\infty} \frac{1}{T}\int_0^T (\underline{r}'(\underline{y},t)\underline{Q}\,\underline{r}(\underline{y},t))dt \tag{5}$$

where $\underline{Q}$ is a positive definite symmetric weighting matrix on the responses. The surface locations, $\hat{\underline{y}}$, are chosen so that

$$J^*(\hat{\underline{y}}) \leq J^*(\underline{y}) \quad \text{for all } \underline{y} \text{ in the domain}$$

where $\underline{y}$ is defined (assumed to be convex and simply-connected), and where $J^*(\underline{y})$ is the minimum value of the cost functional for a fixed $\underline{y}$.

In summary, the solution of the problem consists of three steps:

(1) Find $\hat{\underline{x}}_o(\underline{y},t)$

(2) Find $\hat{\underline{K}}(\underline{y})$ for a specified $\underline{y}$

(3) Find $\hat{\underline{y}}$

The following subsections treat these problems in order as the estimation, control, and search problems. For the sake of legibility all $\underline{y}$ and t dependences will be assumed implicitly in the following derivations.

B. SOLUTION OF THE ESTIMATION PROBLEM

Kalman[1] has shown the existence of a linear minimum-variance unbiased estimator $\hat{\underline{x}}$ of the state $\underline{x}$. The estimation problem may be

[1] Kalman, R. E., and Bucy, R. S., "New Results in Linear Filtering and Prediction Theory," Journal of Basic Engineering, March, 1961, pp. 95-108.

described as follows:

Given the system (1) and the measurements (2), find the estimator of the form

$$\hat{\underline{x}}(\underline{y}, t) = \int_0^t \underline{L}(\underline{y}, t, \tau)\, \underline{m}(\underline{y}, \tau)\, d\tau \tag{6}$$

which minimizes the criterion

$$J(\underline{x}) = TR\left[E\{(\underline{x}-\hat{\underline{x}})'(\underline{x}-\hat{\underline{x}})\}\right] \tag{7}$$

assuming the control $\underline{c}$ to be of the form $\underline{c} = \underline{K}(\underline{y})\hat{\underline{x}}(\underline{y}, t)$.

Make the definitions

(i) $\tilde{\underline{x}} = \underline{x} - \hat{\underline{x}}$ = estimation error

(ii) $E\{\underline{x}\underline{x}'\} = \underline{X}$ = state second moment matrix

(iii) $E\{\hat{\underline{x}}\hat{\underline{x}}'\} = \hat{\underline{X}}$ = state estimate second moment matrix

(iv) $E\{\tilde{\underline{x}}\tilde{\underline{x}}'\} = \tilde{\underline{X}}$ = error covariance matrix

One then obtains the well-known equations for the Kalman-Bucy optimal filter $\hat{\underline{L}}(t, \tau)$:

$$\partial\hat{\underline{L}}(t, \tau)/\partial t = [\underline{F} + \underline{G}\underline{K} - \hat{\underline{L}}(t, t)\underline{A}]\hat{\underline{L}}(t, \tau) \tag{8}$$

where $\hat{\underline{L}}(t, t) = [\tilde{\underline{X}}\underline{A}' + \underline{C}\underline{N}\underline{B}'](\underline{B}\underline{N}\underline{B}')^{-1}$ (9)

and $\tilde{\underline{X}}$ is the solution of the steady-state error-covariance equation:

$$\dot{\tilde{\underline{X}}} = (\underline{F} - \underline{C}\underline{N}\underline{B}'(\underline{B}\underline{N}\underline{B}')^{-1}\underline{A})\tilde{\underline{X}} + \tilde{\underline{X}}(\underline{F} - \underline{C}\underline{N}\underline{B}'(\underline{B}\underline{N}\underline{B}')^{-1}\underline{A})'$$

$$-\tilde{\underline{X}}\underline{A}'(\underline{B}\underline{N}\underline{B}')^{-1}\underline{A}\tilde{\underline{X}} + \underline{C}(\underline{N} - \underline{N}\underline{B}'(\underline{B}\underline{N}\underline{B}')^{-1}\underline{B}\underline{N})\underline{C}' = \underline{0} \tag{10}$$

As a side result, when this filter is used, the estimation error has the property that

$$E\{\hat{\underline{x}}(\underline{y}, t)\tilde{\underline{x}}'(y, t)\} = \underline{0} \tag{11}$$

which is a result of the orthogonal projection lemma.[1] This in turn implies that

[1] Kalman, R.E., and Bucy, R.S., "New Results in Linear Filtering and Prediction Theory," Journal of Basic Engineering, March, 1961, pp. 95-108.

$$\underline{X} = \hat{\underline{X}} + \tilde{\underline{X}} \qquad (12)$$

Coming back to Eq. 10 and using the partitioned matrices given in Section A, one sees that $\tilde{\underline{X}}$ must be of the form

$$\tilde{\underline{X}} = \begin{bmatrix} \tilde{\underline{X}}_o & \underline{0} \\ \underline{0} & \underline{0} \end{bmatrix}$$

where $\tilde{\underline{X}}_o$ satisfies the matrix Riccati equation:

$$\underline{F}_o\tilde{\underline{X}}_o + \tilde{\underline{X}}_o\underline{F}_o' - \tilde{\underline{X}}_o\underline{A}_o'(\underline{B}_o\underline{N}_2\underline{B}_o')^{-1}\underline{A}_o\tilde{\underline{X}}_o + \underline{C}\underline{N}_0\underline{C}' = 0 \qquad (13)$$

This equation is independent of $\underline{y}$, a fact of considerable importance, it will turn out. In Appendix A it is shown that the state covariance equation can be expressed in terms of $\hat{\underline{X}}(y,t)$ and $\tilde{\underline{X}}$, a constant matrix. The net effect of this is that, via (12) there is a separation of control and estimation problems and via (13) there is furthermore a separation of search and estimation problems! Equation 13 may be solved once and for all and Eqs. 8 and 9 need only be evaluated after $\hat{\underline{y}}$ and $\hat{\underline{K}}(\hat{\underline{y}},t)$ are found--they play no further role in the problem solution. These side benefits of optimality show that use of the Kalman filter is justified not only by the fact that it serves as a standard of optimality but also by the great savings it yields in computational effort.

C. SOLUTION OF THE CONTROL PROBLEM

First, Eq. 5 is transformed in order to put the criterion in a form which is easier to manipulate.

$$J(\underline{y}) = \lim_{T\to\infty} \frac{1}{T}\int_0^T (\underline{r}'\underline{Q}\,\underline{r})dt$$

$$= \sum_{i=1}^{n_r}\sum_{j=1}^{n_r} Q_{ij} \lim_{T\to\infty} \frac{1}{T}\int_0^T (r_i r_j)dt$$

$$= \sum_{i=1}^{n_r} \sum_{j=1}^{n_r} Q_{ij} E\{r_i r_j\}, \text{ via the ergodicity assumption}$$

$$= \sum_{i=1}^{n_r} \sum_{j=1}^{n_r} Q_{ij} R_{ij}, \text{ where } \underline{R} \doteq E\{\underline{r}\,\underline{r}'\} \text{ is the response second moment matrix}$$

$$J(\underline{y}) = TR[\underline{Q}\,\underline{R}] \tag{14}$$

But $\underline{R} = E\{\underline{r}\,\underline{r}'\} = E\{(\underline{H}\,\underline{x} + \underline{D}\,\underline{c})(\underline{x}'\underline{H}' + \underline{c}'\underline{D}')\}$

$$= E\{[(\underline{H} + \underline{D}\underline{K})\hat{\underline{x}} + \underline{H}\tilde{\underline{x}}][\tilde{\underline{x}}'\underline{H}' + \hat{\underline{x}}'(\underline{H} + \underline{D}\underline{K})']\}$$

$$= (\underline{H} + \underline{D}\underline{K})\hat{\underline{X}}(\underline{H} + \underline{D}\underline{K})' + \underline{H}\tilde{\underline{X}}\underline{H}'$$

Thus the criterion may be written

$$J(\underline{y}) = TR[\hat{\underline{X}}(\underline{H} + \underline{D}\underline{K})'\underline{Q}(\underline{H}+\underline{D}\underline{K}) + \tilde{\underline{X}}\underline{H}'\underline{Q}\underline{H}] \tag{15}$$

In Appendix B, the optimal control law $\hat{\underline{K}}$ is derived via the matrix minimum principle.[2] The result is:

$$\hat{\underline{K}} = -(\underline{D}'\underline{Q}\underline{D})^{-1}(\underline{D}'\underline{Q}\underline{H} + \underline{G}'\underline{S}) \tag{16}$$

where $\underline{S}$ is the solution of the costate equation,

$$(\underline{F} - \underline{G}(\underline{D}'\underline{Q}\underline{D})^{-1}\underline{D}'\underline{Q}\underline{H})'\underline{S} + \underline{S}(\underline{F} - \underline{G}(\underline{D}'\underline{Q}\underline{D})^{-1}\underline{D}'\underline{Q}\underline{H}) - \underline{S}\underline{G}(\underline{D}'\underline{Q}\underline{D})^{-1}\underline{G}'\underline{S}$$
$$+ \underline{H}'(\underline{Q} - \underline{Q}\underline{D}(\underline{D}'\underline{Q}\underline{D})^{-1}\underline{D}'\underline{Q})\underline{H} = \underline{0} \tag{17}$$

The state covariance equation for the optimally-controlled system is

$$(\underline{F} + \underline{G}\hat{\underline{K}})\hat{\underline{X}} + \hat{\underline{X}}(\underline{F} + \underline{G}\hat{\underline{K}})' + \underline{F}\tilde{\underline{X}} + \tilde{\underline{X}}\underline{F}' + \underline{C}\underline{N}\underline{C}' = \underline{0} \tag{18}$$

The Riccati equation (17) is solved first, yielding $\hat{\underline{K}}$ which allows one to solve (18) for $\hat{\underline{X}}$. All of this is carried out at each location $\underline{y}$ to be examined. The search problem dictates which $\underline{y}$ are selected.

---

[2] Athans, Michael, "The Matrix Minimum Principle," Information and Control, Vol. 11, No. 5, pp.592-605.

D. SOLUTION OF THE SEARCH PROBLEM

Consider a scalar-valued function of a vector, $J(\underline{y})$ which is everywhere continuous and twice-differentiable. If $\underline{y}_o$ is a local relative minimum of $J(\underline{y})$, the function may be expanded about this value to give

$$J(\underline{y}) = J(\underline{y}_o) + \underline{J}_1'(\underline{y}_o)(\underline{y}-\underline{y}_o) + (\underline{y}-\underline{y}_o)'\underline{J}_2(\underline{y}_o)(\underline{y}-\underline{y}_o) \tag{19}$$

where $\underline{J}_1(\underline{y}_o)$ is a vector whose i^{th} element $(i=1,\ldots,n_y)$ is

$$J_{1i}(\underline{y}_o) = [\partial J(\underline{y})/\partial y_i]_{\underline{y}=\underline{y}_o} \tag{20}$$

And $\underline{J}_2(\underline{y}_o)$ is a matrix with i,j^{th} entry $(i,j=1\ldots n_y)$:

$$J_{2ij}(\underline{y}_o) = \frac{1}{2}[\partial^2 J(\underline{y})/\partial y_i \partial y_j]_{\underline{y}=\underline{y}_o} \tag{21}$$

This "element differentiation" notation will be used throughout the thesis in a similar fashion for expansion of matrices about any nominal value of $\underline{y}$. The subscripts (1i) and (2ij) on matrices denote differentiation of each element by y_i and y_i and y_j, respectively. For deterministic matrices (e.g., $\underline{F}(\underline{y})$, $\underline{G}_o(\underline{y})$, etc.) the variations of $\underline{y}$ are independent in each dimension, whereas for stochastic variables ($\underline{S}(\underline{y})$, $\underline{K}(\underline{y})$, $\hat{\underline{X}}(\underline{y})$) the variations are taken *mutatis mutandis* so that if y_i is varied, y_j, $j \neq i$ are adjusted to maintain optimal control.

Returning to (19), the conditions for a minimum $\underline{y}_o$ are:

$$\text{(i)} \quad \underline{J}_1(\underline{y}_o), = \underline{0}, \tag{22}$$

and

$$\text{(ii)} \quad (\underline{y}-\underline{y}_o)' \underline{J}_2(\underline{y}_o)(\underline{y}-\underline{y}_o) \geq 0 \tag{23}$$

for all $\underline{y}$ in the neighborhood of $\underline{y}_o$ (this implies that $\underline{J}_2(\underline{y}_o)$ must be positive semidefinite). Assume that one has selected a point $\underline{y}^k$ which he presumes to be in the neighborhood of $\underline{y}_o$ and he wants to determine a $\Delta\underline{y}^k$ such that $\underline{y}^k + \Delta\underline{y}^k = \underline{y}_o$. One method of determining $\Delta\underline{y}^k$ is

the Newton-Raphson method, which proceeds as follows:

Expand $\underline{J}_1(\underline{y}_o)$ about $\underline{y}_o$:

$$\underline{J}_1(\underline{y}^k) \simeq \underline{J}_1(\underline{y}_o) - \underline{J}_2(\underline{y}_o)\Delta\underline{y}^k$$

$$\simeq \underline{J}_1(\underline{y}_o) - \underline{J}_2(\underline{y}^k)\Delta\underline{y}^k$$

since $\underline{J}_2(\underline{y}^k)$ differs from $\underline{J}_2(\underline{y}_o)$ by second order in $\Delta\underline{y}^k$. But $\underline{J}_1(\underline{y}_o) = \underline{0}$, so one can write

$$\Delta\underline{y}^k \simeq - [\underline{J}_2(\underline{y}^k)]^{-1} \underline{J}_1(\underline{y}^k) \tag{24}$$

providing the inverse exists, which will occur if $\underline{y}^k$ is in a neighborhood sufficiently close to $\underline{y}_o$. Positive definiteness of $\underline{J}_2(\underline{y}^k)$ can be shown a sufficient condition for convergence of the algorithm

$$\underline{y}^{k+1} = \underline{y}^k + \Delta\underline{y}^k \tag{25}$$

to the desired value of $\underline{y}_o$. The algorithm will give rapid error-free convergence to local minima provided that $\underline{J}_2(\underline{y})$ is smooth enough near $\underline{y}_o$ to assure a large neighborhood of convergence. If convergence conditions are not satisfied one must use a gradient or other method to bring $\underline{y}^k$ into the relevant neighborhood, resulting in a so-called "modified" Newton-Raphson search. In aircraft problems, scrutiny of Section III will reveal that the requisite smoothness properties may be directly related to the smoothness of the mode slope derivates, which are in turn related to the smoothness of the elastic modulus as a function of position on the aircraft. Further discussion of this point is postponed to Section V.

The search procedure used in this thesis is constrained in that one demands an optimal controller be used at each $\underline{y}^k$; this reduces the criterion J from a functional in the two quantities $\underline{y}$ and $\underline{K}$ to a functional in $\underline{y}$ alone by setting $\underline{K} = \hat{\underline{K}}(\underline{y})$. The constraint equations are

derived in Appendix C, while the criterion variations are found in Appendix D; the results are:

$$J_{1i} = -TR[\underline{S}_{1i}(\underline{F}\tilde{\underline{X}} + \tilde{\underline{X}}\underline{F}' + \underline{C}\underline{N}\underline{C}')] \tag{26}$$

and $$J_{2ij} = 2TR\{[(\underline{S}\underline{F}_{2ij}+\underline{S}_{1j}\underline{F}_{1i} + \underline{S}_{1i}\underline{F}_{1j}+(\underline{H}+\underline{D}\underline{K})'\underline{Q}(\underline{H}_{2ij}+\underline{D}_{2ij}\underline{K})$$
$$+(\underline{H}_{1j}+\underline{D}_{1j}\underline{K})'\underline{Q}(\underline{H}_{1i}+\underline{D}_{1i}\underline{K}) - \underline{K}_{1j}'(\underline{D}'\underline{Q}\underline{D})\underline{K}_{1i}]\hat{\underline{X}}\}, \tag{27}$$

where $\underline{S}_{1i}$ is the solution of the equation:

$$(\underline{F}+\underline{G}\underline{K})'\underline{S}_{1i} + \underline{S}_{1i}(\underline{F}+\underline{G}\underline{K})+\underline{F}_{1i}'\underline{S}+\underline{S}\underline{F}_{1i}+(\underline{H}_{1i}+\underline{D}_{1i}\underline{K})'\underline{Q}(\underline{H}+\underline{D}\underline{K})$$
$$+(\underline{H}+\underline{D}\underline{K})'\underline{Q}(\underline{H}_{1i}+\underline{D}_{1i}\underline{K}) = \underline{0} \tag{28}$$

and $$\underline{K}_{1i} = -(\underline{D}'\underline{Q}\underline{D})^{-1}[\underline{D}_{1i}'\underline{Q}(\underline{H}+\underline{D}\underline{K})+\underline{D}'\underline{Q}(\underline{H}_{1i}+\underline{D}_{1i}\underline{K}) + \underline{G}'\underline{S}_{1i}] \tag{29}$$

The matrices $\underline{S}$, $\underline{K}$ and $\hat{\underline{X}}$ are the solutions of Eqs. 16-18 for $\underline{y}=\underline{y}^k$.

In summary, the complete solution of the problem is given by Eqs. 13, 16-18, and 26-29 and the search algorithm defined by (24) and (25). The implementation of this procedure on the computer is discussed in Section III-B.

SECTION III

IMPLEMENTATION OF THE SOLUTION TECHNIQUE

The practicality of the proposed solution technique rests on two factors. First, it must be possible to describe the two matrix functions of a vector $\underline{G}_o(\underline{y})$ and $\underline{D}(\underline{y})$ for a general aircraft in such a way that readily available vehicle data can be easily utilized in the search algorithm; otherwise each application would require too much "accounting" engineering to be worthwhile. Secondly, an efficient, fast, generally applicable computational scheme must be written in order that answers are economically obtainable. Both phases of implementation are described in this section.

A. VEHICLE DESCRIPTION

In modern applications, it is reasonable to assume the availability of linearized equations of motion and linear modal analysis of flexure properties of large aircraft. The following discussion will demonstrate that this information, plus some evident parameters of the vehicle, are sufficient to determine all of the variables needed in the proposed optimization scheme.

A.1 Specification of Control Surface Types and Positions

The aircraft is broken into four segments: (1) wing, (2) fuselage, (3) vertical tail, and (4) horizontal tail -- this numbering sequence is followed throughout the thesis. All coordinates are referred to the orthogonal axis system below.

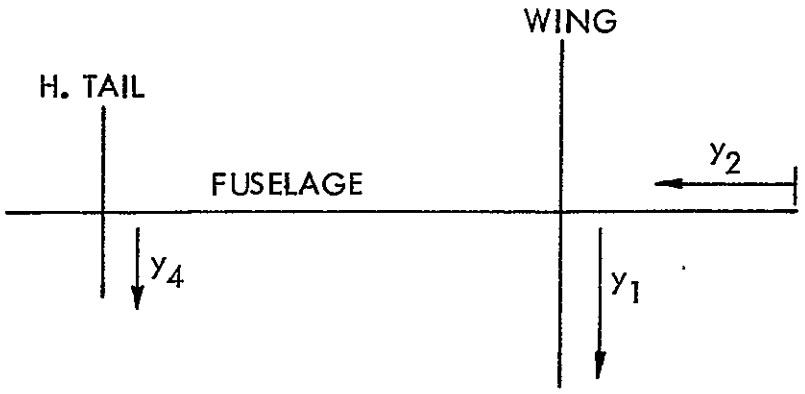

(a) TOP VIEW

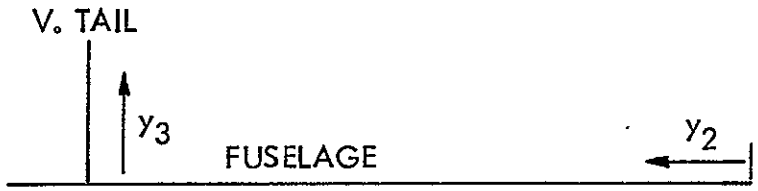

(b) SIDE VIEW

Figure 1

The true aircraft axes need not correspond to these axes, of course, but positions on the true axis system are defined by their projections onto these axes rather than by measurement of lengths directly along the true axes. Customary units are inches; the end point of an axis need not correspond to a zero co-ordinate value (for example, the zero of the fuselage axis may correspond to the tip of a nose probe rather than to the actual nose of the airplane)--for this reason two vectors, $YO = (y_{10}, y_{20}, y_{30}, y_{40})'$ and $YEND = (y_{1e}, y_{2e}, y_{3e}, y_{4e})'$ define the dimensions of the aircraft.

The vector $\underline{y}$ actually consists of the positions of each control surface which is to be optimally located. The following control surfaces are permitted (again, numbering corresponds to the code used in the optimization program):*

(1) Combined ailerons

(2) Differential ailerons

(3) Combined leading edge slats

(4) Differential leading edge slats

(5) Combined spoilers

(6) Differential spoilers

(7) Combined elevators

(8) Differential elevators

(9) Rudder

Positive deflections should be defined in the positive axis directions according to rigid body coordinates for the given vehicle, e.g., if Y were out the right wing and Z were down, differential aileron deflection would be positive for right aileron down, etc.

Each of the five types of control surfaces listed above is assigned an axis which is assumed to be a straight line and is specified by two quantities, its angle of intersection with the fuselage (AXANG) in radians and the distance (AXX) of its root from the center of gravity (forward being positive). The set of force producers to be varied and their positions at a given point in the computer program are specified by the following vectors and matrices:

---

* Henceforth, unless otherwise noted, subscripts on the variable y refer to the surface types as denumerated here (where y_i is presumed to be with reference to the proper body axis), and not to the body reference axis system (y_1, y_2, y_3, y_4) outlined above.

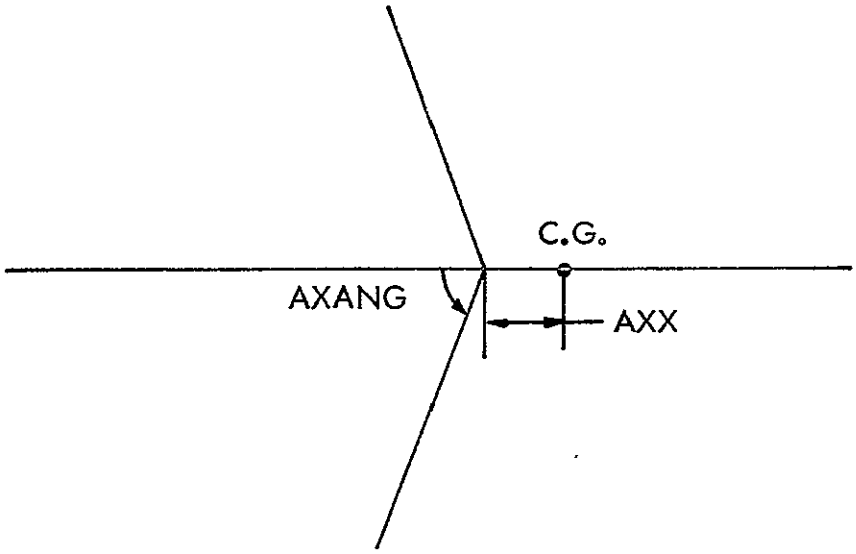

(a) AILERONS, SPOILERS, OR LEADING EDGE SLATS (TOP VIEW)

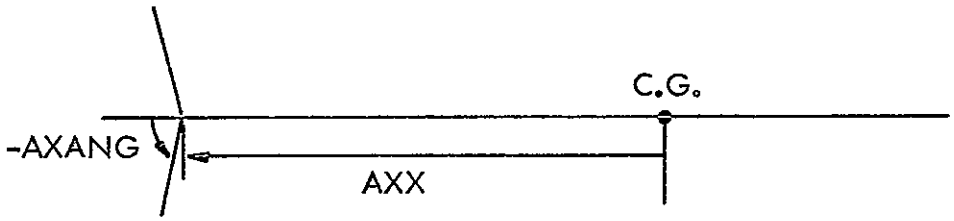

(b) ELEVATORS (TOP VIEW)

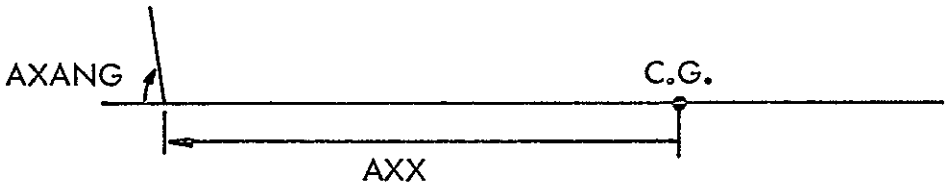

(c) RUDDERS (SIDE VIEW)

Figure 2

NFP(I), I=1, NT --number of force producers of type I to be positioned, where I corresponds to the numbering above, e.g., if NFP(2) = 3, three sets of (differential) ailerons are to be positioned. If there are no control surfaces of a given type, or if their positions are to remain fixed, NFP for that type must be zero.

LOC(I), I=1, NT --axis (y_1, y_2, y_3, or y_4) to which type I control surface is to be referred. If rudder position is to be optimized, for instance, LOC(9) = 3, since rudder position is referred to the vertical axis, y_3, and the rudder is control surface type 9. LOC(I) may be zero if the I^{th} surface position isn't optimized or remains fixed. To facilitate added types of control surfaces (e.g., canards) the dimension of NFP and LOC is specified as NT rather than 9 throughout the program.

YFP(I, J), I=1, NT; J=1, NMAX --position of J^{th} control surface of type I, referred to the axis as specified by LOC(I). Aileron, leading edge flap and spoiler positions are referred to wing coordinates (y_1), elevators to horizontal tail coordinates (y_4), and rudders to vertical tail coordinates (y_3).

AXANG(I), I=1, NT --angle between fuselage and axis along which the influence of surface type I is felt (see Appendix G.3)

AXX(I), I=1, NT --distance of root of axis of control surface type I fore of the C.G. (AXX for the elevator would be negative, for example). This parameter is often called $-\ell_T$ in aerodynamic literature.

This completes the specification of aircraft geometry and control surface locations. The control and response matrices, $\underline{G}_o$ and $\underline{D}$, depend on these positions in four important ways: (1) through the flexure

physics, (2) through diminished lift effectiveness of outboard surfaces, (3) through increasing torque arms of outboard surfaces, and (4) through modal acceleration contributions to responses. The following sections derive these effects from the basic physics of the aircraft in flight. The casual reader is advised to skip to the summary following Section III.A.4 at this point.

A.2 Airframe Flexure Physics

This section outlines some of the significant aspects of airframe flexure physics. The discussion is based on Bisplinghoff's statement of the problem[2] and on discussions with C. R. Stone of the Honeywell Systems and Research staff.

Since discussion will be focused on the y-dependence of the $\underline{G}_o$ and $\underline{D}$ matrices in the plant and response equations, viz., the dependence of forces and responses on outboard control surface location, fuselage dynamics will not be treated in detail. Although mode shapes include fuselage displacement, the analysis of wing, horizontal and vertical tail dynamics is the major issue of aircraft flexure physics. Each of these segments may be modelled as a tapered slender beam fixed at one end to the aircraft body. For such a structure, two types of motions may be distinguished (a) torsion about the axis of the beam and (b) bending about an axis perpendicular to the beam in the plane of the wing surface (see Fig. 3). Taking y as the co-ordinate out the axis of the beam, the dominant characteristics of each flexure mode are described by stating torsional and vertical deflections of the beam structure as a function of y. For slender slightly-swept or unswept wings the pure mechanics of vibration are well approximated by Hooke's Law and St. Venant's theory of torsion. Only when the

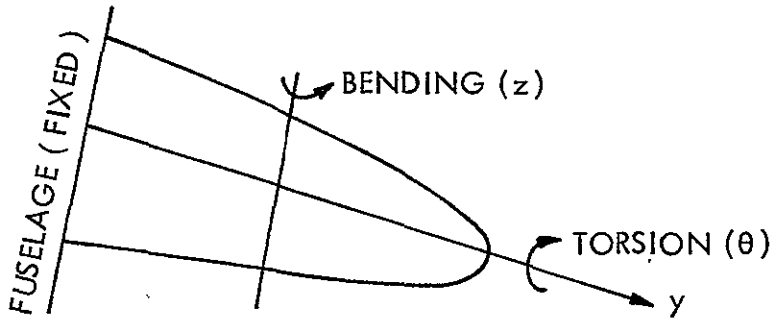

Figure 3

torsional elastic axis passes through the center of gravity of each chordwise wing segment, however, do torsional and bending motions become decoupled. Figure 4 portrays the physical variables of the flexure equations:

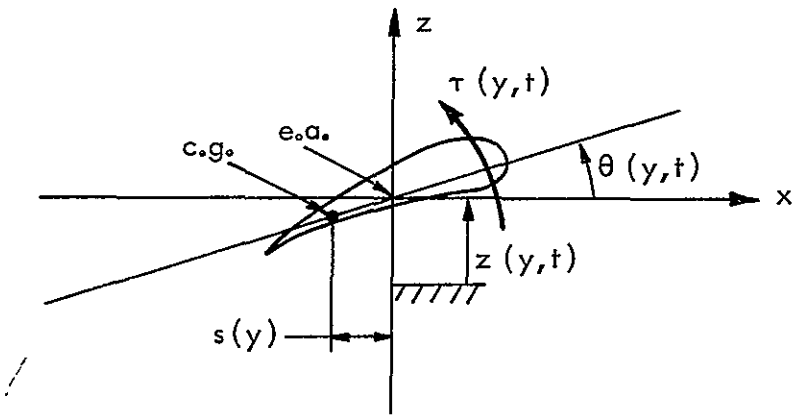

Figure 4

modes $F_z(y,t)$ and $\tau(y,t)$ arise due to structural coupling and damping--these effects are explained in Appendix I; for simplicity they are neglected in the following derivation. When F_z and τ are set to zero, the solutions are separable functions of space and time:

$$z(y,t) = \xi(y)\, T(t) \tag{3}$$

$$\theta(y,t) = \phi(y)\, T(t) \tag{4}$$

The flexure equations become:

$$m(y)(\xi(y)-s(y)\phi(y))\ddot{T}(t)+(EI(y)\xi''(y))''T(t) = 0 \tag{5}$$

$$(I_y(y)\phi(y)-s(y)m(y)\xi(y))\ddot{T}(t)-(GJ(y)\phi'(y))'T(t) = 0 \tag{6}$$

If $\ddot{T}(t) + \omega^2 T(t) = 0$, then the spatial equations may be written:

$$\begin{bmatrix} \xi''' \\ \xi'' \\ \xi' \\ \xi \\ \phi \\ \phi \end{bmatrix}' = \begin{bmatrix} -\frac{2EI'}{EI} & -\frac{EI''}{EI} & 0 & \frac{m\omega^2}{EI} & 0 & \frac{-ms\omega^2}{EI} \\ 1 & 0 & 0 & 0 & 0 & 0 \\ 0 & 1 & 0 & 0 & 0 & 0 \\ 0 & 0 & 1 & 0 & 0 & 0 \\ 0 & 0 & 0 & \frac{ms\omega^2}{GJ} & \frac{-GJ'}{GJ} & \frac{-I_y\omega^2}{GJ} \\ 0 & 0 & 0 & 0 & 1 & 0 \end{bmatrix} \begin{bmatrix} \xi''' \\ \xi'' \\ \xi' \\ \xi \\ \phi' \\ \phi \end{bmatrix}$$

For specified boundary conditions at either end of the wing,* these equations have solutions for an infinite sequence $\omega = \omega_1, \omega_2, \omega_3 \ldots$ of natural frequencies. The solution corresponding to $\omega=\omega_i$, consisting of $\xi(y)\doteq\xi_i(y)$ and $\phi(y)\doteq\phi_i(y)$, defines the i^{th} natural mode shape of the wing.

The distributed force problem is solved by assuming the flexure pattern to be a linear combination of natural modes: $z(y,t)=\sum_{i=1}^{\infty} \xi_i(y)\eta_i(t)$ and $\theta(y,t)=\sum_{i=1}^{\infty} \phi_i(y)\eta_i(t)$ where $\eta_i(t)$ is the normal co-ordinate

---

* See Appendix F.

specifying displacement of the i^{th} natural mode. Inserting these proposed solutions into Eqs. 1 and 2 and using the orthogonality condition* that

$$M_j \delta_{ij} = \int_0^{\ell} [m(y)\xi_i(y)\xi_j(y) - m(y)s(y)[\phi_i(y)\xi_j(y) + \phi_j(y)\xi_i(y)] + I_y(y)\phi_i(y)\phi_j(y)]\, dy$$

where ℓ is the length of the wing, it is possible to find equations for the $\eta_i(t)$:

$$M_j \ddot{\eta}_j(t) + M_j \omega_j^2 \eta_j(t) = \int_0^{\ell} (F_z(y,t)\xi_j(y) + \tau(y,t)\phi_j(y))\, dy \doteq X_j \qquad (7)$$

In practical applications the engineer is usually given the $\xi_i(y)$ and $\phi_i(y)$, or similar quantities.** The Eqs. 7 for the $\eta_i(t)$ are then appended to the plant equations in the model. The computer program models the direct forces due to control surfaces (flaps) on a wing as point forces. This means that the force from a flap centered at y_o will be approximately written $F_z(y,t) = F_o(t)\delta(y-y_o)$ and $\tau(y,t) = T_o(t)\delta(y-y_o)$. The above force term thus becomes:

$$X_j \tilde{=} F_o(t)\, \xi_j(y_o) + T_o(t)\phi_j(y_o) \qquad (8)$$

To a first approximation the forces F_o and the torques T_o are due to the change in lift resulting from a unit deflection of a flap of unit length--this may be found from tabulated section lift curves as a function of y_o. The forces are related to the control signal $u(t)$ through actuator dynamics and Kussner lift buildup of aerodynamic forces, as described in Section I. The y-dependence of the mode forcing terms requires storage of vertical and torsional natural mode

---

* See Appendix F.

** See Appendix I.

shapes. Since the variational procedure requires the second derivative of these terms, an accurate spline fit procedure is used to generate second derivatives, which are then Fourier decomposed for computer storage. Mode shapes and their derivatives are easily generated to an accuracy of better than one percent using only two hundred storage locations per mode.

A.3 Forces Depending on Control Surface Position

The force matrix $\underline{G}_o(y)$ picks up its dependence on control surface locations in three ways. (1) The rigid body equations of motion include the direct lift and moment effects of surface deflections--some of the moment arms are functions of control surface location; (2) the extent to which a given flexure mode acceleration is excited depends on where the force producers are located; (3) rigid body and flexure modes are generally not decoupled--vertical acceleration at the center of gravity, for instance, may include rigid body acceleration plus that due to each modal acceleration.

(1) Rigid Body Effects.* The rigid body equations of motion are assumed to be stated in terms of a subset of the coordinates,

(a) $\ddot{z}$ - vertical acceleration

(b) $\ddot{\theta}$ - pitch acceleration

(c) $\ddot{y}$ - side acceleration

(d) $\ddot{\psi}$ - yaw acceleration

(e) $\ddot{\phi}$ - roll acceleration

(f) $\ddot{x}$ - forward acceleration

---

* The linearized equations of motion are derived from first principles in Appendix E.

All of these quantities are assumed to be evaluated at the center of gravity. For cases (such as the C-5A) where these are not the coordinates of the available model, it is usually easy to form the requisite linear combinations of these coordinates or to adjust the coefficient matrices to account for changes of scale.

(a) Vertical acceleration: The total vertical force due to a unit combined aileron, spoiler, leading edge flap or elevator deflection is to first approximation due to the altered airflow pattern over that section of wing or tail. The effect of a deflection is to change the mean camber line, hence the effective angle of attack, hence the lift of that section. The magnitude of the resulting vertical force depends on (of course) the amount of deflection, the depth of the hinge line into the wing, and the local chord of the wing, which is a function of y_1. Thus for a flap of unit length and given percentage of local chord in depth, the total lift per unit angular deflection decreases as the chord becomes shorter, i.e., as the flap is moved outboard (see Fig. 5, curve a).

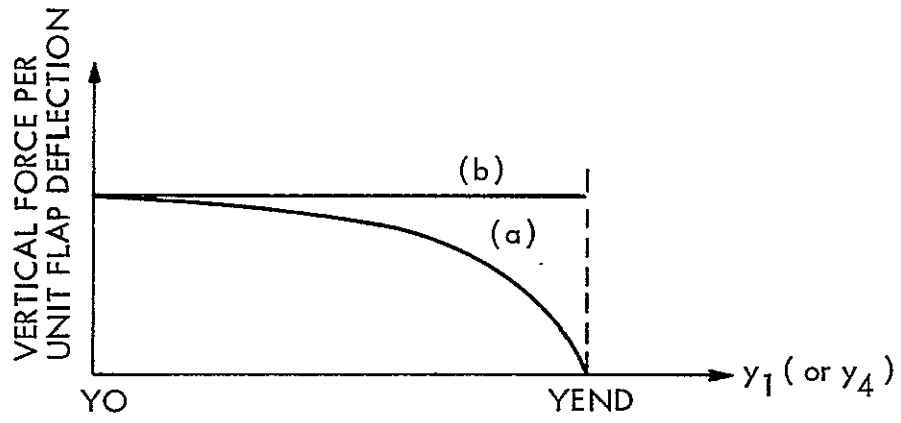

Figure 5

To allow for chord variation and flap design this curve is specified for wing and tail as a Fourier series. For instance, if one wanted the same force per unit deflection all the way out the wing (see curve b above), the flap area would have to be increased for outboard surfaces. The shape of this curve thus embodies the flap design assumptions built into the program--curve (a) is for "uniform" flap size, while curve (b) is for uniform authority per unit deflection (but nonuniform flap size). Curve (b) is likely to be more useful for study purposes (a point force of constant strength being easiest to visualize), while (a) may be more suited to trial design work. The shape of this curve will influence the optimization results, however. It is assumed that the same curve applies to all control surfaces on the wing (exept for a constant scale factor). Letting δ_i be the deflection of the i^{th} control surface (see Section III.A.1), the y-dependent part of $\ddot{z}$ may be written

$$\ddot{z}_y = \sum_{i=1,3,5,7} C_{L_i}(y_i)\delta_i + M.A. \qquad (9)$$

$$C_{L_i}(y_i) = CLC(i) \cdot C_L(y_i)$$

CLC(i) = scale factor for i^{th} surface

$C_L(y)$ = section lift curve for wing or tail (see above); C_L is one function for i=1,3,5 and another for i=7

M.A. = modal accelerations at the center of gravity

(b) Pitch acceleration: Because of swept wing structure, as a control surface is moved out the wing or tail it is farther aft of the center of gravity, producing (along with the vertical force effect) a pitching moment which is just the product of the vertical force times the length of the lever arm,as shown in Fig. 6.

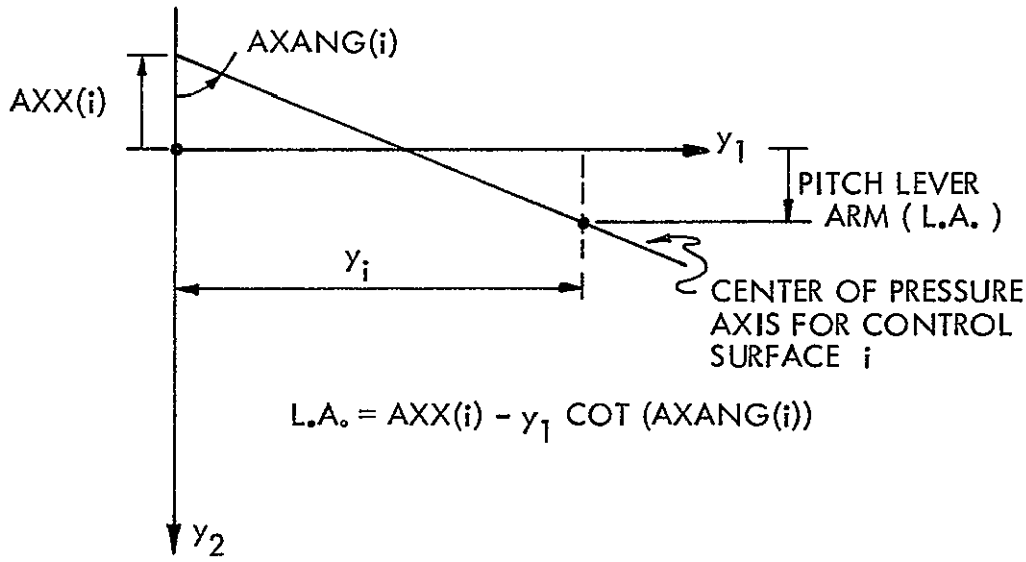

Figure 6

Hence

$$\ddot{\theta}_y = \sum_{i=1,3,5,7} C_{L_i}(y_i)[\,AXX(i)-y_i/TAN(AXANG(i))\,]\,\delta_i + M.A. \qquad (10)$$

Note that in calculating the lever arm AXX is taken to be negative if the root of the center of pressure axis of the i^{th} control surface is aft of the center of gravity. The same diagram holds for the horizontal tail, AXX(7) being greater in magnitude.

(c) Lateral acceleration: Since no set of control surfaces can exert a balanced couple of side forces, there are no direct effects of either combined or differential control surfaces on lateral accelrations. Since lateral flexure mode accelerations at the center of gravity are small, they have been neglected--few practical flexure models include lateral accelerations of the various modes.

(d) Yaw acceleration: All differential control surfaces give rise to yawing moments due to differential drag effects of up vs. down deflections; rudder deflections also contribute. The expressions for the moment arms are shown in Fig. 7.

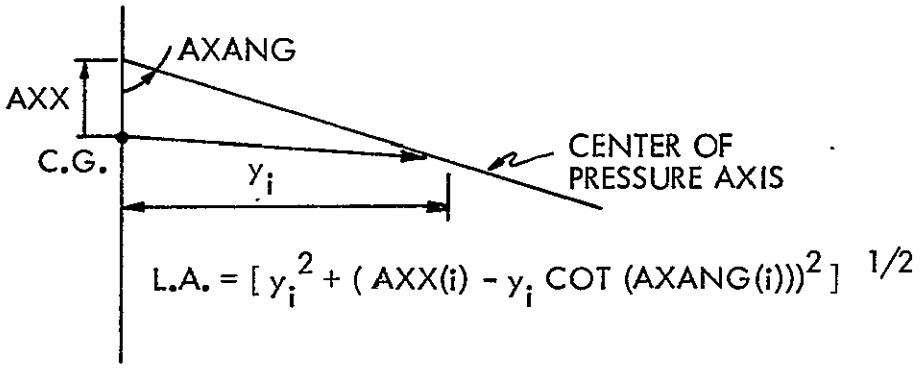

(a) WING CONTROL SURFACES

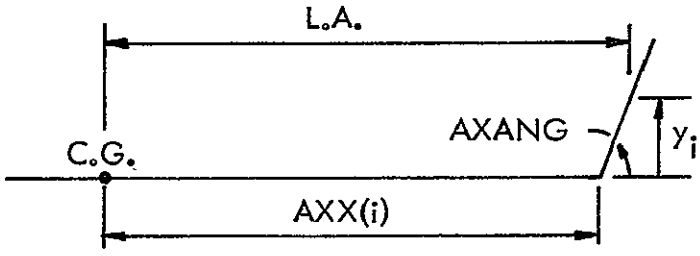

L.A. = AXX(8) - y_8 COT (AXANG(8))

(b) RUDDERS

Figure 7

Thus the direct effects of control surfaces on yaw acceleration are:

$$\ddot{\psi}_y = \sum_{i=2,4,6} C_{D_i}(y)[AXX(i)^2 + y_i^2(1+1/TAN^2(AXANG(i))) - 2y_i AXX(i)/TAN(AXANG(i))]^{1/2}\delta_i + C_{N_9}[AXX(9) + y_9/TAN(AXANG(9))] \quad (11)$$

where

$C_{D_i}(y) = GSTOCK(\ddot{\psi}, y_i) \cdot C_{L_{i-1}}(y)$, is the drag coefficient and $C_{L_{i-1}}$ is obtained from the vertical acceleration equation.

$$C_{N_9} \tilde{=} GSTOCK(\ddot{\psi}, y_9)$$

Note that the section lift curve ($C_{L_{i-1}}$) for each type of control surface is used in approximating the differential drag (C_{D_i}), the constant coefficient term being stored in a reference matrix GSTOCK (explained in Appendix G.3). Since the sweep of the horizontal tail is negligible, the effect of differential elevator drag has been assumed independent of y.

(e) Roll acceleration: Rudder deflection and all differential control surface deflections produce rolling moments. For rudder and wing control surfaces, the moment arms are merely the y-coordinate values for those surfaces. The diagram for the elevator roll moment arm is shown in Fig. 8. Hence roll acceleration is given by

$$\ddot{\phi}_y = \sum_{i=2,4,6,9} C_{P_i}(y_i) y_i \delta_i + C_{P_8}(y_8)[y_{VT}^2 + y_8^2]^{1/2}\delta_8 + M.A. \quad (12)$$

where

$$C_{P_i} = GSTOCK(\ddot{\phi}, y_i) \cdot C_{L_{i-1}}(y_i) \qquad i=2, 4, 6$$

$$C_{P_9} = GSTOCK(\ddot{\phi}, y_9)$$

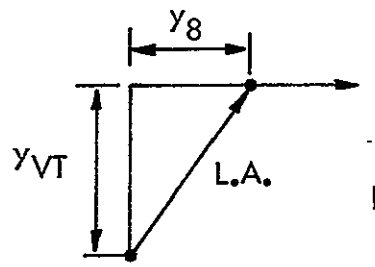

$$L.A. = [(YEND - YO)_3^2 + y_8^2]^{1/2}$$

Figure 8

(f) Forward acceleration: The drag due to both combined and differential surface deflections depends on local chord and is hence a function of y_1. For a given flight condition and control surface, the drag coefficient is assumed to be in constant proportion to the lift coefficient. Hence the y-dependent portion of the x acceleration equation is written

$$\ddot{x}_y = \sum_{i=1}^{9} C_{D_i}(y_i)\delta_i \tag{13}$$

$$C_{D_i}(y_i) = GSTOCK(\ddot{x}, y_i) \cdot C_{L_i}(y_i)$$

where

$GSTOCK(\ddot{x}, y_i)$ = constant coefficient for $\ddot{x}$ equation, i^{th} control surface

(2) The forcing functions for the mode acceleration equations depend on force producer locations. This dependence is described in Section III.A.2, where the following theoretical results are derived:

$$\ddot{\eta}_j(t) + 2\xi\omega_j\dot{\eta}_j(t) + \omega_j^2\,\eta_j(t) = (F_{AERO}+X_j)/M_j \qquad (14)$$

where $\ddot{\eta}_j$ = j^{th} modal acceleration

ξ = structural damping (.01-.03)*

ω_j = j^{th} modal frequency

F_{AERO} = aerodynamic forces consisting of combinations of other A/C state variables (independent of y)**

$\frac{X_j}{M_j}$ = aerodynamic accelerations due to control surface displacements

$$\tilde{=} \sum_{i=1}^{9} \frac{C_{L_i}(y_i)}{M_j/M}\left[\xi_j(y_i) + d(y_i)\phi_j(y_i)\right]\delta_i$$

where $\xi_j(y_i)$=vertical displacement of j^{th} mode at position of i^{th} force producer

$d(y_i)$= moment arm between center of pressure and elastic axis at i^{th} force producer position (formerly referred to as s(y))

$\phi_j(y_i)$=torsional displacement of j^{th} mode at position of i^{th} force producer

M_j = modal mass of j^{th} mode**

---

*Observe that structural damping ($2\xi\omega_j\dot{\eta}_j(t)$) and aerodynamic force terms have been added to the equations given in Section III.A.2. In addition, the terms F_o and T_o have been replaced by $C_{L_i}(y_i)\delta_i(t)$ and $C_{L_i}(y_i)d(y_i)\delta_i(t)$ respectively.

**The generalized masses are input as the constants Z2M(j). When the aircraft is approximated by a lumped parameter model with masses $m(y_k) = m_k$ and lever arms $s(y_k) = s_k$, I(y) becomes $I(y_k)=s_k^2 m_k$. The expression for M_j becomes

$$M_j = Z2M(j) = \sum_k m_k(\xi_j^2(y_k) - 2s_k\phi_j(y_k)\xi_j(y_k) + s_k^2\phi_j^2(y_k))$$

(Continued on bottom of next page)

$$= \int_{\text{aircraft}} [\, m(y)\xi_j^2(y) - 2m(y)s(y)(\phi_j(y)\xi_j(y)) + I_y(y)] \, dy$$

M = mass of aircraft

The y-dependent forcing terms, X_j/M_j, are computed by a subroutine GD. The equation and geometry for $d(y_i)$ are shown in Fig. 9.

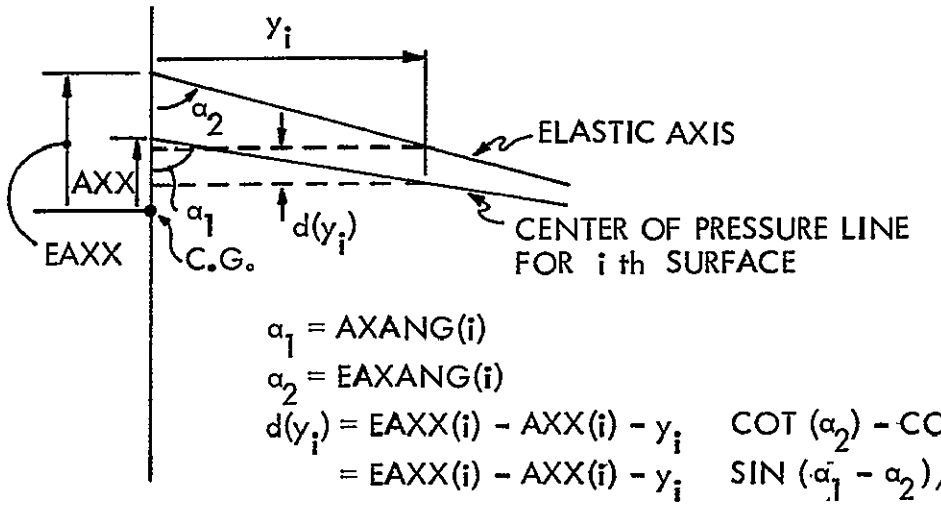

Figure 9

**Since the lift coefficients C_{L_i} are computed for accelerations, it is necessary to multiply through by the aircraft mass (M) to achieve dimensional agreement or equivalently, to divide M_j by M. Thus the constants Z2M(j) = M_j/M, with units of (length)^{2j} are the actual input parameters of the program.

In the C-5A case, the mode shape data includes masses m_k (26 for wing, 25 for fuselage, 11 for vertical tail, and 10 for horizontal tail) and modal deflections for eack y_k corresponding to m_k for each mode.

In summary, the y-dependent terms for the mode acceleration equations are

$$\ddot{\eta}_{j_y} = \frac{X_j}{Z2M(j)} = \sum_{i=1}^{9} \frac{C_{L_i}(y_i)}{M_j/M} [\xi_j(y_i) + d(y_i)\phi_j(y_i)]\,\delta_i \qquad (15)$$

(3) Mode Acceleration Contribution to Rigid Body Variables: As noted in the rigid body equation descriptions (1), the $\ddot{z}$, $\ddot{\phi}$ and $\ddot{\theta}$ equations contain contributions from the mode accelerations at the center of gravity.* The $\ddot{z}$ equation simply picks up vertical accelerations ($\ddot{\eta}_j$) at that point; hence the mode acceleration term of the $\underline{G}_o(\underline{y})$ matrix is

$$\ddot{z}_y(\text{M.A.}) = \sum_j \xi_j(y_{CG})\,[X_j/Z2M(j)] \qquad (16)$$

where y_{CG} = center of gravity location and $X_j/Z2M(j)$ is given above.

The $\ddot{\theta}$ variable picks up the mode slopes along the fuselage (nonzero for symmetric modes only), hence

$$\ddot{\theta}_y(\text{M.A.}) = \sum_j \frac{\partial \xi_j}{\partial y_2}(y_{\text{C.G.}})\,[X_j/Z2M(j)] \qquad (17)$$

y_2 = fuselage axis

The roll ($\ddot{\phi}$) equation picks up mode slopes across the wings (nonzero for antisymmetric modes only), giving

$$\ddot{\phi}_y(\text{M.A.}) = \sum_j \frac{\partial \xi_j}{\partial y_1}(y_{o_1})\,X_j/Z2M(j) \qquad (18)$$

For reference and comment, the relevant equations are summarized here:

---

*See Appendix E.

(1) Vertical Acceleration:

$$\ddot{z}_y = \sum_{i=1,3,5,7} [C_{L_i}(y_i) + \sum_{j=1}^{NI} \xi_j(y_{CG}) X_j(y_i)/Z2M(j)]\delta_i \qquad (19)$$

(2) Pitch Acceleration:

$$\ddot{\theta}_y = \sum_{i=1,3,5,7} [C_{L_i}(y_i)[AXX(i) - y_i/TAN(AXANG(i))]$$

$$+ \sum_{j=1}^{NI} \frac{\partial \xi_j}{\partial y_2} (y_{CG}) X_j(y_i)/Z2M(j)]\delta_i$$

(3) Side Acceleration:

$$\ddot{Y}_y = 0 \qquad (21)$$

(4) Yaw Acceleration:

$$\ddot{\psi}_y = \sum_{i=2,4,6} C_{D_i} C_{L_{i-1}}(y_i)[AXX^2(i) + y_i^2(1+COT^2(AXANG(i)))$$

$$-2y_i AXX(i)COT(AXANG(i))]^{1/2}\delta_i$$

$$+ C_{D_9}[AXX(9) + y_9 COT(AXANG(9))]\delta_9 \qquad (22)$$

(5) Roll Acceleration:

$$\ddot{\phi}_y = \sum_{i=2,4,6,9} [C_{P_i} C_{L_{i-1}}(y_i) y_i + \sum_{j=1}^{NI} \frac{\partial \xi_j(y_{CG})}{\partial y_1} X_j(y_i)/Z2M(j)]\delta_i$$

$$+ [C_{P_8} C_{L_7}(y_8)[y_{VT}^2 + y_8^2]^{1/2}$$

$$+ \sum_{j=1}^{NI} \frac{\partial \xi_j(y_{CG})}{\partial y_1} X_j(y_8)/Z2M(y_j)]\delta_8 \qquad (23)$$

(6) Forward Acceleration:

$$\ddot{x}_y = \sum_{i=1,3,5,7} C_{D_i} C_{L_i}(y_i)\delta_i + \sum_{i=2,4,6,8} C_{D_i} C_{L_{i-1}}(y_i)\delta_i + C_{D_9}\delta_9$$

(24)

A.4 Responses Depending on Control Surface Position

The y-dependence of the response matrix, $\underline{D}(\underline{y})$, is due only to acceleration responses; stresses and stress rates depend only on mode shape values at given response stations and on the modal displacements, which are functions of time alone. Stresses, for instance, may be written:

$$\begin{aligned} s(y_r) &= k \cdot (\text{bending moment at } y_r) \\ &= k \cdot EI(y_r) \sum_i \xi_i''(y_r,t) \\ &= k \cdot EI(y_r) \cdot \sum_i \eta_i(t) \xi_i''(y_r) \end{aligned} \tag{25}$$

where

k = constant depending on stress station

$EI(y_r)$ = stiffness modulus at response station y_r

$\eta_i(t)$ = displacement of i^{th} mode

$\xi_i''(y_r)$ = mode slope derivative of i^{th} mode evaluated at response station y_r

Since the $\eta_i(t)$ (and $\dot{\eta}_i(t)$, for stress rates) appear in the plant state vector $(\underline{x}_1)$ and the y_r are fixed, the stress equations have no y-dependent terms.

Acceleration responses, however, may be written

$$\ddot{z}_y(y_r) = R.B._y(y_r) + \sum_i \xi_i(y_r) \ddot{\eta}_{y_i}(t) \tag{26}$$

where

R.B. = rigid body terms

$\xi_i(y_r)$ = i^{th} mode shape evaluated at response station y_r

$\ddot{\eta}_{y_i}(t)$ = modal acceleration of i^{th} mode

Since only vertical acceleration responses are to be considered, the rigid body variables Y, ψ and x contribute nothing. If y_r is on the fuselage, ϕ may also be ignored. For y_r on wings or tail

$$R.B._y(y_r) = \ddot{z}_y(y_r) + \ddot{\phi}_y y_r - \ddot{\theta}_y x_r$$

For y_r on the fuselage.

$$R.B._y(y_r) = \ddot{z}_y(y_r) - \ddot{\theta}_y x_r$$

where x_r is the distance of the response location fore of the center of gravity (i.e., x_r is negative for response locations aft of the center of gravity). For y_r on the fuselage this is $x_r = y_{CG} - y_r$ and for y_r on the other segments of the aircraft it is $x_r = EAXX - y_r \cdot COT(EAXANG)$, where EAXX and EAXANG are for the appropriate segment. This assumes that response locations will be located on the elastic axis.

The modal acceleration terms $\ddot{\eta}_{y_i}(t)$ are explained above. Note that once the y-dependent terms of $\underline{G}_o$ have been computed, they may be used directly in forming the $\underline{D}$ matrix. If $\ddot{z}_y$ is not measured in the same units as the $\ddot{\eta}_i$ and rigid body variables, the appropriate elements of DSTOCK can be used for conversion factors.

A.5 Summary of Section III.A

The preceding derivations appear exceedingly complex because they attempt to treat a large class of aircraft models and use standard aerodynamic conventions (which are intrinsically confusing to the non-initiated) so that the parameters of available linearized models may be conveniently inserted into the computer program. The approach and the physics, however, are basically simple. The approach is summarized as follows: the $\underline{G}_o$ matrix has the force coefficients corresponding to a given equation of motion along each row and the forces generated by each type of control surface down each comumn (see Fig. 10). The

preceding derivation simply passes from element to element, giving formulas for the nonzero elements.

Equation of Motion ($\underline{x}_o$) \ Control Surface Type ($\underline{c}$)	1	2	3	4	5	6	7	8	9
$\ddot{z}$	×	0	×	0	×	0	×	0	0
$\ddot{y}$	0	0	0	0	0	0	0	0	0
$\ddot{x}$	×	×	×	×	×	×	×	×	×
$\ddot{\theta}$	×	0	×	0	×	0	×	0	0
$\ddot{\psi}$	0	×	0	×	0	×	0	0	×
$\ddot{\phi}$	0	×	0	×	0	×	0	×	×
$\ddot{\eta}_i$(sym)	×	0	×	0	×	0	×	0	0
$\ddot{\eta}_j$(asym)	0	×	0	×	0	×	0	×	×

General $\underline{G}_o$ matrix*

(x denotes $\underline{y}$-dependent term; 0 denotes no $\underline{y}$-dependence)

Figure 10

A similar procedure is followed for the $\underline{D}$ matrix. The physical effects are basically simple also. The y-dependent terms occur in (1) the forcing functions for the flexure modes, (2) the torque moment arms, and (3) accelerations (either at response locations or at the center of gravity) at any point on the aircraft. The first effect utilizes the mode shape data, while the second effect uses basic aircraft geometry; the third effect combines both data inputs. In addition, depending on the way one wishes to specify flap design assumptions, there may be a y-dependent attenuation factor due to decreasing lift effectiveness of outboard control surfaces. Appendix G.3 describes how the various terms are computed.

---

*See Section III.A.1 for definition of control surface types.

B. COMPUTATIONAL SCHEME

The computer program which implements the proposed method has been written for full-scale investigation of the location problem rather than demonstration purposes. The input data consists of plant parameters derived from the aircraft equations of motion, gust model parameters, Fourier series coefficients for mode slope derivatives, and certain parameters specifying aircraft dimensions and control surfaces to be studied. The model may include lateral and/or longitudinal equations of motion and symmetric and/or antisymmetric flexure modes. Provision is made for the following control surfaces: elevator, rudder, spoiler flaps, leading edge flaps and ailerons (all surfaces operated in combined and/or differential mode). Most types of state augmentation may be accomplished with ease--e.g., actuator dynamics, unsteady aerodynamics, etc.

The structure of the program consists of an executive module which forms the coefficients of the filter equation (Section II.B.1), the optimal control equations (Appendix B), and the variational equations (Appendices C and D), and a series of subprograms which perform evaluation and computational functions. The subroutines include:

(1) A data read-in subroutine (READIN)

(2) A routine which solves the Riccati equation (POTTER)

(3) A routine which solves the state covariance equation (STCOV)

(4) Routines to form $\underline{D}(\underline{y})$, $\underline{G}_o(\underline{y})$ and their partial derivatives (GD, GPDP, and GPPDPP)

(5) A Fourier series evaluation routine (EVAL)

(6) Eignevalue and matrix inversion subroutines (ALLMAT, HSBG, ATEIG, TDINVR)

B.1 Main Program

The block diagram of the executive module (shown in Fig. 11) bears out the natural separation of the problem given in Section II.B, viz., estimation, control, and search. The estimation and control problems are well-known and need no further comment here, as the implementation follows precisely the equations in II.B. At the search stage, the manipulations in the actual program are slightly more complicated than shown in Fig. 11, since the matrix YFP(I, J), whose indices denote type and number, respectively of a given control surface, must be rearranged as a vector in computing the variations J_{1jk} and J_{2jk}.

The search procedure used is a modified Newton-Raphson scheme. If the second variation matrix is positive definite, the Newton-Raphson algorithm is used, but if J_{2jk} is not positive definite a gradient method is used. The sum of the absolute step sizes in each dimension is taken to be a constant (one which is just large enough to move rapidly into a region where J_{2jk} is positive definite), but the ratios of the step sizes in each dimension are in the same ratio as the respective components of the gradient, J_{1j}. More sophisticated techniques may be used.

Because of its generality the program as a whole requires a considerable amount of computer memory. The object program generated by the Fortran IV source deck, including dimensioned arrays, requires about 25,000 words of storage for a 14th order example; approximately 15,000 of which are required for the program itself and

Main Program Flow Chart

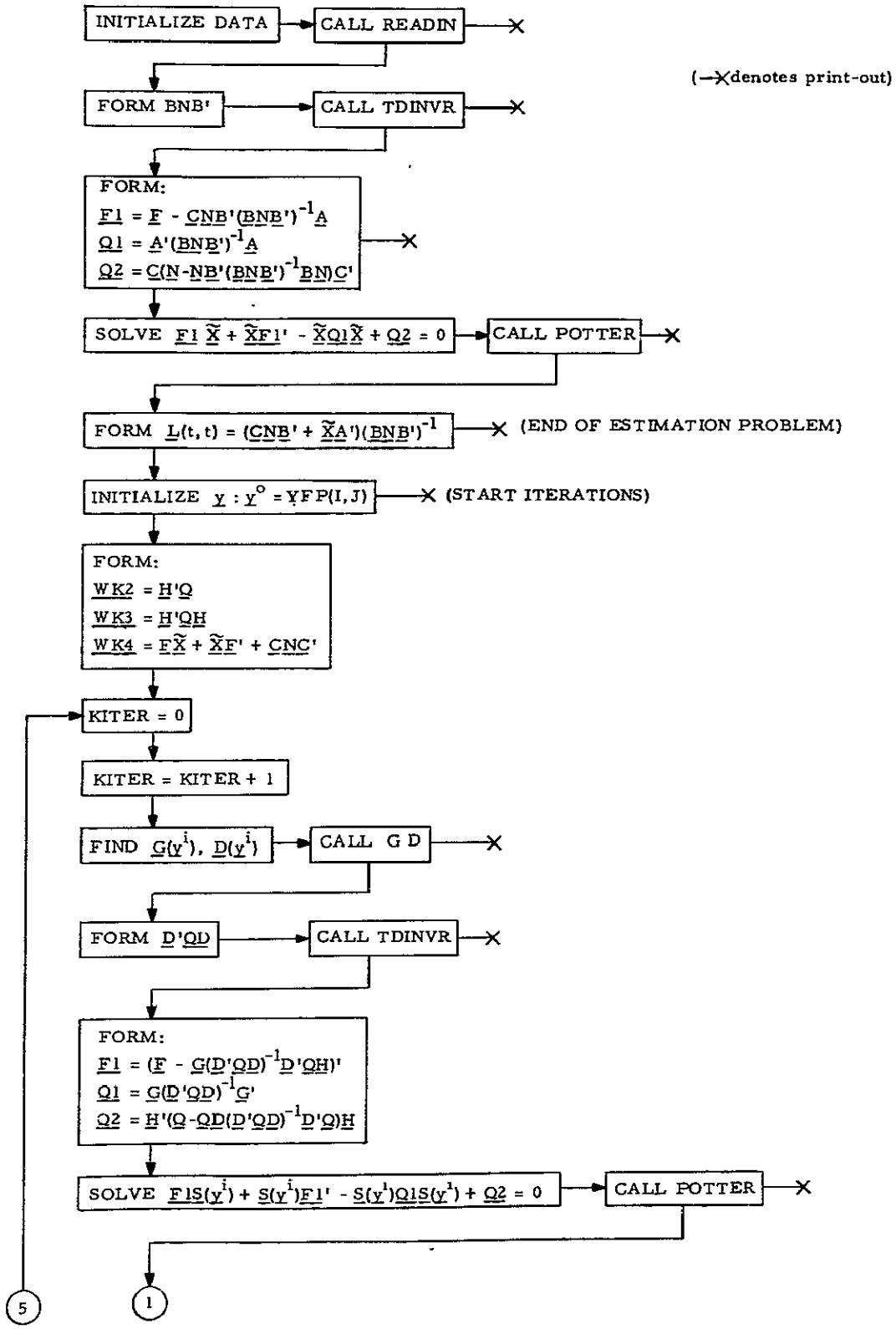

Figure 11

Main Program Flow Chart

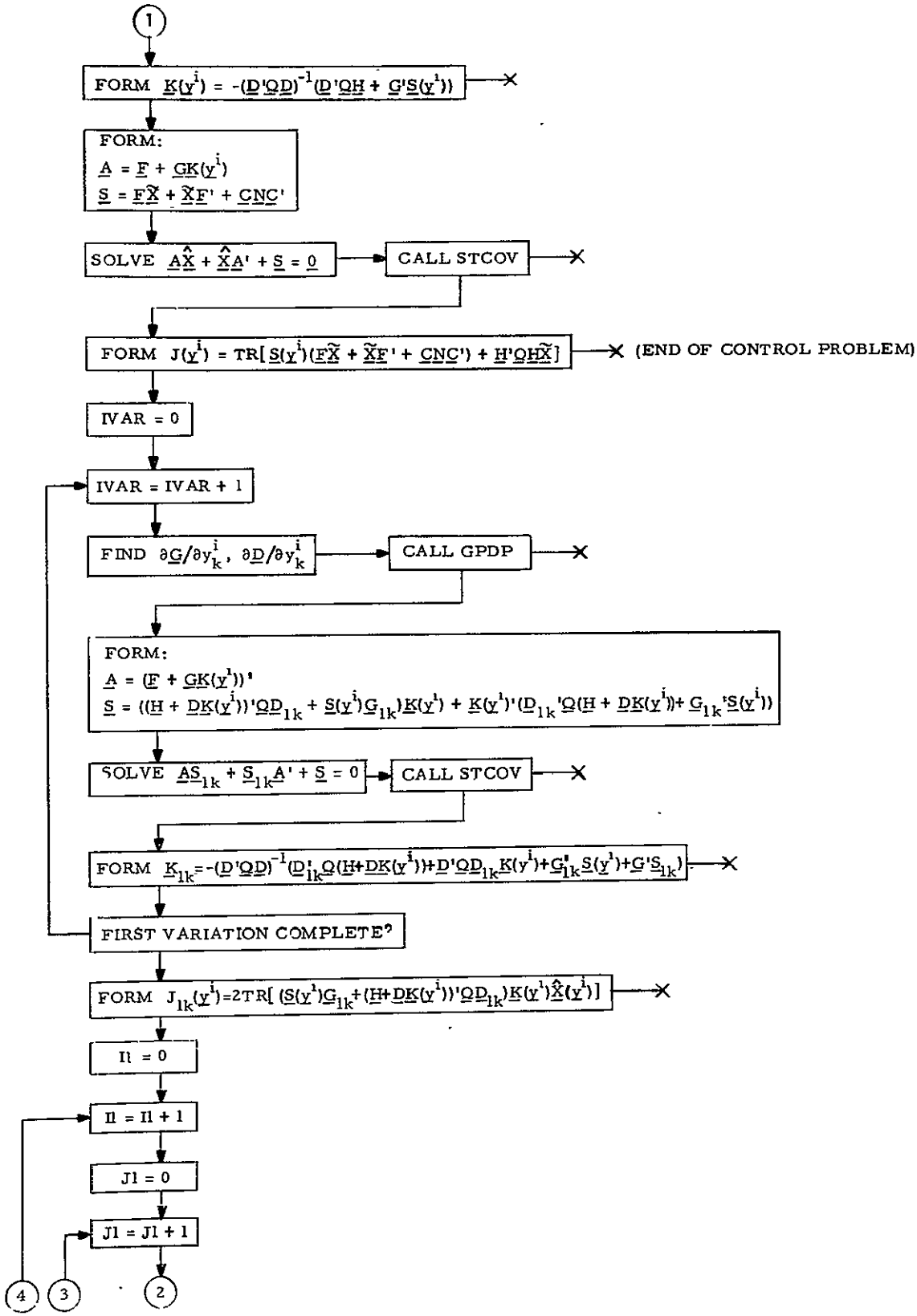

Figure 11 (Cont.)

Main Program Flow Chart

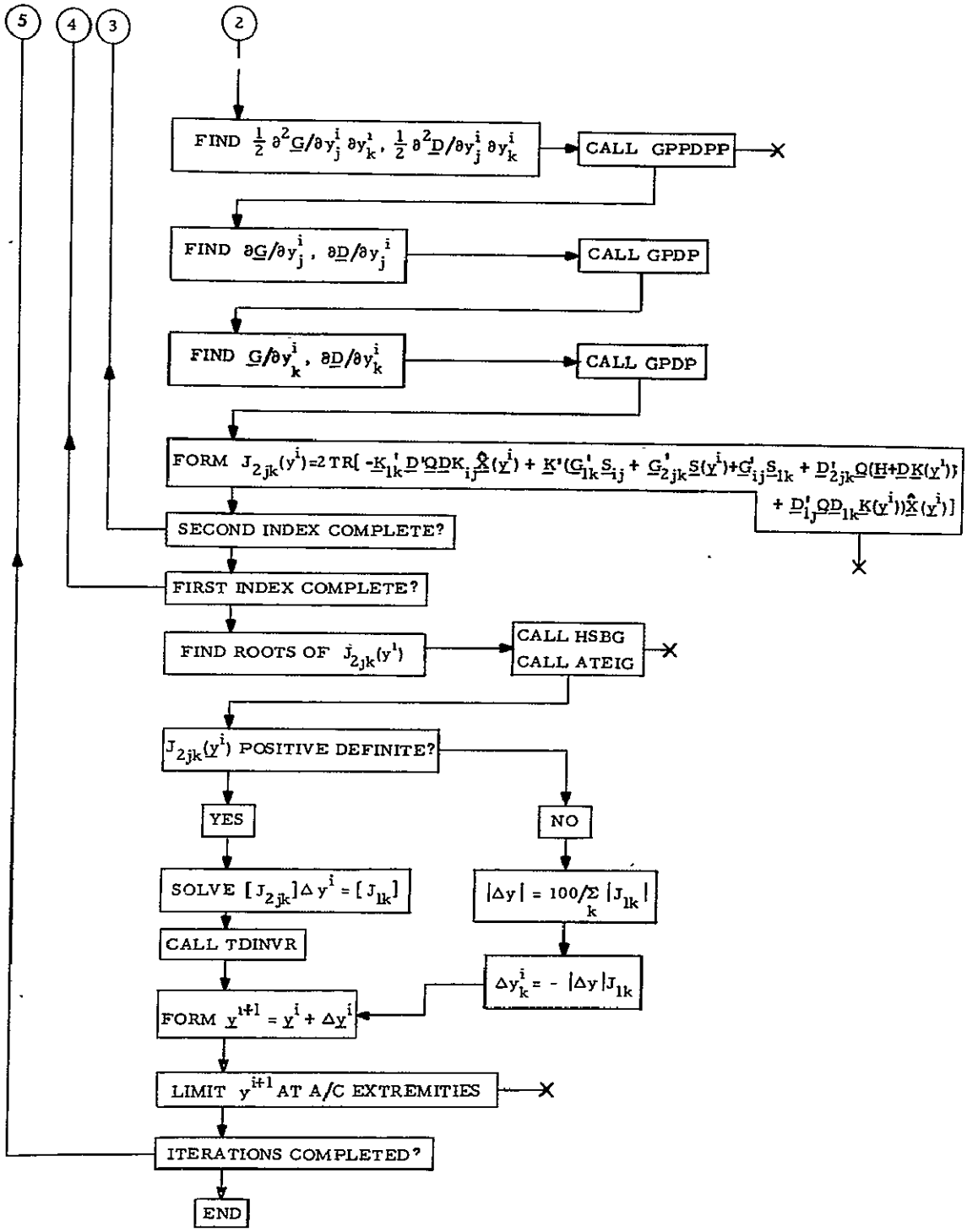

Note: The variational equations given above refer to the C-5A trial model of Section IV (see IV-A-8), although the program is readily modified to handle the general case of Section II.

Figure 11(Contd.)

for arrays of fixed dimension. With the availability of third-generation computers, computation time is a more significant economic consideration than storage requirements, however. The program does attempt to optimize on computation time. This is accomplished through fast single-product multiplications, elimination of needless loops and precomputations of certain matrix products, and (primarily) by great efficiency in the major computational subroutines. As an example, on the IBM 360/40 computer three iterations of a fourteenth order case took 2.75 minutes of main processor time; such a computation involves solution of four Riccati and 12 state covariance differential equations, all of order fourteen, plus the criterion computations of the search algorithm.

B.2 Major Subroutines

A significant portion of the time devoted to this thesis was used in writing and debugging computer programs; in addition, several standard subroutines were tried and compared on the practical C-5A example cited in Section IV, as well as on trial examples. As a by-product of this research, the author wishes to introduce three subroutines which significantly improve computation times over many existing schemes for solving commonly-occurring control problems. The subroutines are written so that they can be readily incorporated into programs of other users.

The first subroutine (called STCOV) computes solutions of state covariance differential equations with time-invariant parameters; the subroutine is written to compute steady-state solutions, but can be easily modified to give the solution at any given point in time, if desired. The iterative algorithm was developed by G. Stein of the

Honeywell Systems and Research Center* and has been used extensively there, but is not widely known. The author's subroutine, written primarily as an exercise, closely parallels those in use at Honeywell. Appendix G.3 contains a description of the algorithm and computer program.

The second subroutine (called POTTER) implements a method first described by Potter** for solving the steady-state time-invariant Riccati equation. It is well-known† that knowledge of the steady-state solution can be used to convert the differential equation to a state covariance form, which may be solved for the full time-varying solution via the above program or another scheme. For the time-invariant case where steady-state solutions are required, the subroutine described in Appendix G.1 has been demonstrated to be definitely more accurate and faster by a factor of approximately one system order than commonly available iterative methods. Such efficiencies result from the fact that Potter's method is algebraic rather than iterative.

The third subroutine (called EVAL) is used to evaluate Fourier series for flexure mode shapes, but can be used in more general applications. Given a set of n functions defined along r axes $(f^1(y_1 \ldots y_r), \ldots f^n(y_1 \ldots y_r))$ and the Fourier coefficients of the second derivatives of the functions along these axes the subroutine provides for evaluation of all functions, derivatives, or second derivatives at

---

*A still faster version of the algorithm has been developed for repeated solutions; the original results are given in Ref. 16.

**See Reference 12.

† See Reference 14.

any point specified by a co-ordinate value of one of the axes. The advantages of the program, which is outlined in Appendix G.4, are very compact storage of mode shape, slope and slope derivative data, as well as rapid access to these quantities at any point on the aircraft. A similar algorithm is available for obtaining the requisite Fourier coefficients, if these are not accessible to the engineer.

The remaining major subroutines are less generally applicable. They specify the dependence of control forces and responses on control surface position. These subroutines (GD, GPDP, GPPDPP) are documented in Appendix G.2.

SECTION IV

APPLICATION TO A TRIAL MODEL OF THE LOCKHEED C-5A TRANSPORT

In order to demonstrate the feasibility of the proposed computational scheme and to obtain insight into the significant factors of the surface placement problem, a mathematical trial model of the Lockheed C-5A transport aircraft was developed. The model illustrates the essential aspects of the problem by inclusion of three significant flexure modes and only two ailerons (per wing) for which optimal locations are to be determined.

The reader is cautioned regarding any interpretation he may make of the numerical data presented herein; the figures are expected to bear at most a casual resemblance to those which might be obtained in flight tests. First of all, the data used in developing the model was compiled during design of the aircraft--before the transport had ever been flown. It is well known among aeronautical engineers that preliminary mathematical model data such as this may differ quite significantly from models based on flight test data, especially with regard to flexure equations. Secondly, the trial model uses only a fraction of the full aircraft model--it does not correct for the effect of coupling to less significant structural modes, nor does it include lags for aerodynamic lift buildup due to control surface deflections, or for actuator dynamics. Finally, the author readily acknowledges that the trial model is a one-man effort and no doubt suffers certain deficiencies from the fact that he is not an aerodynamicist and could not have been perfectly infallible throughout the extensive hand calculations required to compile

the final trial model. Qualitative tests have been applied to verify the basic behavior characteristics of the model (e.g., sign tests, etc.), and the roots for the free-aircraft model do agree quite closely with those supplied in the original data base report. The author alone accepts full responsibility for the validity of the procedures described in this section and emphasizes that neither Lockheed nor Honeywell would use a model such as this for even trial design studies.

A. THE SIMPLIFIED VEHICLE MODEL

The essential features of this model follow closely those described in the Data Base Report* submitted by Honeywell, Inc. to the Lockheed-Georgia Company in its Load Alleviation and Mode Stabilization (LAMS) study of the C-5A. The report uses basic aircraft model data supplied by Lockheed in a simulation study of the significant structural modes and suggests lower-order models which accurately depict the behavior of the vehicle for a given flight condition. Beyond this information, the surface location program uses mode shape data computed by Lockheed (Case 110500, prepared on 4/7/67) for vertical and torsional deflections of the first, third, and sixth symmetric structural modes for the given flight condition.

A.1 Vehicle Geometry and Flight Configuration

In the notation of Section III.A.1, Figure 1, the vehicle geometry is specified by the values of y_o and y_{end}, plus the sweep angles and intersection points of wing and tail (AXANG and AXX) center of pressure axes and (EAXANG and EAXX) elastic axes. These values are as follows:

$$y_o' = [60,\ 277.5,\ 405.6,\ 20.3] \qquad \text{(inches)}$$

$$y_{end}' = [1300,\ 2841.3,\ 800.7,\ 385.5]$$

---

* Reference 6.

The center of gravity y_{CG} = 1369.315 inches on the y_2 axis and relative to this

AXX(1) = 220.55 (inches)

AXX(4) = -1469.51

EAXX(1) = 166.81

EAXX(4) = -1464.0

The angles are

AXANG(1) = 1.157 (radians)

AXANG(4) = 1.163

EAXANG(1) = 1.230

EAXANG(4) = 1.163

The variables for the y_3 body axis (vertical tail) have been omitted, since no rudder control is used in the trial model. In short, the wingspan and length are about 230 feet, with the wings at a sweep of about 25°, making the C-5A the largest aircraft aloft (see Fig. 1 of the Introduction). The true center of pressure and elastic axes actually bend back slightly about half-way out the wings, but they have been approximated as straight lines.

The flight condition is a low-altitude cruise with the following specifications:

Gross Weight:	593,154 lbs.
True Airspeed:	577 ft./sec. (M=.533)
Dynamic Pressure:	292 lbs./ft.^{2}
Altitude:	10,000 ft.

The moments of inertia (see Appendix E) are

I_{11} = 30.3 x 10^6 (slug-ft.^{2})

I_{22} = 28.8 x 10^6

$$I_{33} = 56.3 \times 10^6$$

$$I_{13} = 2.1 \times 10^6$$

All flaps are in an undeflected position.

A.2 Rigid Body Equations

For the given flight condition the equations of motion decouple into longitudinal (x, z, θ) and lateral (y, ψ, ϕ) triplets. By defining the angle of attack $\alpha = \dot{z} - V_o\theta$ where $V_o = 577$ ft./sec. and the pitch rate $\dot{\theta}$ and noting that all vertical aerodynamic forces and torques about the y axis may be expressed as functions of α and $\dot{\theta}$, one finds that Eqs. 13 and 15 of Appendix E further decouple from the forward acceleration equation, giving:

$$\dot{\alpha} = f_z(\alpha)/m \tag{1}$$

$$(\dot{\dot{\theta}}) = k_\theta(\alpha, \dot{\theta})/I_{22} \tag{2}$$

Thus if one is only interested in pitch and vertical acceleration he need only be concerned with two of the six equations of motion due to the decoupling of forces and accelerations. Since the most significant responses of the vehicle are vertical bending and torsion stresses of the wings, and vertical accelerations in the fuselage due to vertical gusts, it is sufficient to treat just these two equations in the trial model. Because these equations are coupled to the flexure mode acceleration equations, further manipulation of the rigid body equations (see Section I, Eq. 1) is postponed to the next section.

---

* A normalization constant ϕ_2 was used to convert $\dot{\theta}$ to units of inches so that numerical coefficient values are of uniform size.

A.3 Flexure Mode Equations

The original vehicle data includes 30 flexure modes, 15 of which are symmetric in y_2 and 15 of which are antisymmetric in y_2. Obviously, only the symmetric modes can give rise to vertical and pitch accelerations, so only 15 are relevant in light of the preceding section. For the trial model to be valuable in terms of insight, it was desired to cut the number of modes to a minimum consistent with a meaningful flexure control problem, namely three. Fortunately the LAMS study had identified the first, third, and sixth modes as the most significant contributors to RMS stresses and accelerations. Although this predominance was not overwhelming and although all modes exhibited fairly strong intercoupling these modes were seclected. The first mode is a pure wing bending mode, while modes three and six show coupled wing and fuselage bending, with fore and aft fuselage positive for positive wing bending in mode three and negative for positive wing bending in mode six. The normal co-ordinates for these modes will be denoted τ_1, τ_3, and τ_6 (corresponding to the $\eta_j(t)$ of Section III.A.3 (2)) to avoid confusion with the gust disturbances.

In correspondence to the system model of Section I.B, define

$$\underline{x}_1 = \begin{bmatrix} a \\ \dot{\theta}/\phi_2 \end{bmatrix} \quad \underline{x}_2 = \begin{bmatrix} \dot{\tau}_1 \\ \tau_1 \\ \dot{\tau}_3 \\ \tau_3 \\ \dot{\tau}_6 \\ \tau_6 \end{bmatrix} \quad \underline{q} = \begin{bmatrix} z \\ \theta \\ \tau_1 \\ \tau_2 \\ \tau_3 \end{bmatrix}$$

The LAMS report shows that the equations on motion may be written in the form

$$\underline{M}\ddot{q} + \underline{A}_o\dot{q} + \underline{K}q + \sum_n \underline{A}_{1n}\{\underline{K}_n * \dot{q}\} + \sum_n \underline{A}_{2n}\{\underline{K}_n * q\} \tag{3}$$

$$= \sum_n \underline{F}_{gn}\{\underline{\psi}_n * \ddot{Z}_g\} + \sum_i \underline{F}_{ci}\{\underline{K}_i * \dot{\delta}_i\}$$

where n = index corresponding to lifting surfaces

i = index corresponding to control surfaces

ψ_n = Kussner lift growth function for the n^{th} surface

K_n = Wagner lift growth function for n^{th} surface

$\ddot{Z}_g$ = vertical gust acceleration

δ_i = control surface deflections

and (*) denotes convolution. The precise details of this model are not relevant to the thesis, except to note that ψ_n and K_n correspond to unit-gain first order delays with time constants which represent the delay-time for build-up of aerodynamic forces on each lifting surface due to a change in attitude. These delays could be incorporated in the states $\underline{x}_1$ and $\underline{x}_2$ but they were approximated as zero in the trial model (this would never be done in practical design models) to simplify the system. The matrices may be roughly identified as follows:

$\underline{M}$ = mass-inertia matrix

$\underline{A}_o$ = matrix corresponding to terms such as $V_o\dot{\theta}$ which arise due to use of stability axes

$\underline{K}$ = structural restoring forces (elastic modes)

$\underline{A}_{1n}$ = aerodynamic damping forces

$\underline{A}_{2n}$ = aerodynamic linear restoring forces

$\underline{F}_{gn}$ = gust forces

$\underline{F}_{ci}$ = control forces

When the Kussner delays are ignored, the equations of motion may be written:

$$\underline{M}\,\ddot{\underline{q}} + (\underline{A}_o + \sum_n \underline{A}_{1n})\,\dot{\underline{q}} + (\underline{K} + \sum_n \underline{A}_{2n})\,\underline{q} \cong \sum_n \underline{F}_{gn}\{\underline{\psi}_n * \ddot{Z}_g\} + \underline{F}_c\underline{\delta} \qquad (4)$$

From this point it is a standard procedure to rearrange the equations into state-variable form in $\underline{x}_1$ and $\underline{x}_2$. Because the control surface aerodynamics and actuator dynamics (represented by the $\underline{K}_i$) have been ignored, however, the equations take a slightly different form than Eqs. 1 and 2 of Section I.B:

$$\begin{bmatrix} \dot{\underline{x}}_1 \\ \dot{\underline{x}}_2 \end{bmatrix} = \begin{bmatrix} \underline{F}_1 & \underline{L}_1 \\ \underline{L}_2 & \underline{F}_2 \end{bmatrix} \begin{bmatrix} \underline{x}_1 \\ \underline{x}_2 \end{bmatrix} + \begin{bmatrix} \underline{C}_1 \\ \underline{C}_2 \end{bmatrix} \begin{bmatrix} \underline{x}_4 \end{bmatrix} + \begin{bmatrix} \underline{G}_1(\underline{y}_o) \\ \underline{G}_2(\underline{y}_o) \end{bmatrix} [\underline{c}] \qquad (5)$$

In this case $\underline{y}_o$ corresponds to the (fixed) control surface locations specified in the available model and $\underline{x}_4$ corresponds to $\{\underline{\psi}_n * \ddot{Z}_g\}$.

A.4 Control Surfaces

The original model used the two large outboard ailerons (see Fig. 1, Introduction), combined inboard spoiler flaps, and combined elevator flaps for control. Spoilers are drag-creating flaps on the upper wing surface which are usually used for landing but are of some value in flexure control. For the trial model, it was decided to keep the elevators and spoilers fixed in position and to determine optimal locations for two sets of ailerons (in combined mode, of course).

Thus there is a "significant" location problem, since two ailerons, essentially, must be used to control three wing-bending modes. Estimating the various parameters for the variable-position ailerons is a fairly difficult task which may be resolved by either reference to handbooks (e.g., the U. S. Air Force Stability and Control Handbook) or by asking the question "If an aileron were located

at the wing-tip, what would the computer predict its force-coefficients to be in terms of the input parameters?" and then using the available data to "fit" parameter values. The parameters to be estimated are the appropriate elements of the GSTOCK matrix and the section lift curve scale factor CLC(1) (see Section III.A.3, paragraph 1(a)). The control vector $\underline{c}$ takes the form

$$\underline{c} = \begin{bmatrix} \delta_{sp} \\ \delta_{a_1} \\ \delta_{a_2} \\ \delta_e \end{bmatrix}$$

where δ_{sp}, δ_{a_1}, δ_{a_2}, and δ_e are combined spoiler, inboard aileron, outboard aileron, and elevator flap deflections (units were converted from inches to degrees to make the coefficients of uniform magnitude).

A.5 Wind Gust Filter and Gust Aerodynamics

The trial model uses the well-known Press-Meadows* wind filter and the same Kussner lift-buildup functions that were used in the LAMS optimization study of the C-5A.** The gust filter has a transfer function

$$\alpha_g(s)/\eta(s) = (\sqrt{3V_o/L})\,(s+V_o/\sqrt{3}\,L)/(s+V_o/L)^2 \qquad (6)$$

where α_g = gust "angle of attack"

η = white noise ($E\{\eta(t)\} = 0$)

---

*Press, H., Meadows, M.T., and Hadlock, I., "A Reevaluation of Data on Atmospheric Turbulence and Airplane Gust Loads for Application in Spectral Calculation," NACA Report 1272, 1956.

**Honeywell Interoffice Correspondence, April 19, 1968, W. A. Glasser to M. A. Bender, "LAMS Optimization Study of the C-5A."

V_o = forward velocity (577 ft./sec.)

L = gust correlation length (1000 ft.)

s = complex frequency

In state-vector form this is written as

$$\dot{a}_g(t) = (-2V_o/L)\ a_g(t) + p_5 + (\sqrt{3}\ V_o/L)\eta(t)$$

$$\dot{p}_5(t) = -(V_o/L)^2\ a_g(t) + (V_o/\sqrt{3}L)\eta(t)$$

The aerodynamic lift-buildup effect of a gust striking a surface is the sum of two first-order delays with different time constants; the delays are represented by p_1 and p_2 for the wing and p_3 and p_4 for the tail and are all driven by $a_g(t)$. Hence the gust filter and aerodynamics take the form:

$$\dot{\underline{x}}_3 = \underline{F}_3 \underline{x}_3 + \underline{C}_3 \underline{\eta}_1 \tag{7}$$

$$\dot{\underline{x}}_4 = \underline{F}_4 \underline{x}_4 + \underline{L}_4 \underline{x}_3 \tag{8}$$

where

$$\underline{x}_3 = \begin{bmatrix} p_5 \\ a_g \end{bmatrix} \qquad \underline{x}_4 = \begin{bmatrix} p_1 \\ p_2 \\ p_3 \\ p_4 \end{bmatrix} \qquad \underline{\eta}_1 = \eta$$

The mean square gust intensity was taken to be

$$E\{\eta(t)^2\} = 50 \ (\text{feet/sec})^2$$

representing a gust field of moderate intensity.

A.6 Sensor Equations

The sensor configuration chosen for the trial model does not correspond to that of the LAMS study but is motivated by the results of the optimization study, which indicated that the optimal controller required used as much "lead" as it could get in the filter networks.

In order to get this lead and provide some discrimination among the modes, the model uses wing tip accelerometers (averaged signal = m_1), an accelerometer on the nose (m_2), and a rate gyro at the center of gravity (m_3). Hence

$$m_1 = a_1\ddot{z} + (x_{CG}-x_{WT})b_1(\ddot{\theta}/\phi_2) + c_1(\xi_1(y_{WT})\ddot{\tau}_1 + \xi_3(y_{WT})\ddot{\tau}_3 + \xi_y(y_{WT})\ddot{\tau}_6) + \eta_2$$

$$m_2 = a_1\ddot{z} + (x_{CG}-x_N)b_1(\ddot{\theta}/\phi_2) + c_1(\xi_1(x_N)\ddot{\tau}_1 + \xi_3(x_N)\ddot{\tau}_3 + \xi_6(x_N)\ddot{\tau}_6) + \eta_3$$

$$m_3 = (\dot{\theta}/\phi_2) + \eta_4$$

where

a_1, b_1, c_1	=	conversion factors (such that m_1, m_2 are in g's)
x_{WT}	=	distance from nose to wing tip along the fuselage
x_{CG}	=	distance from nose to center of gravity along the fuselage
x_N	=	0 (position of nose on the fuselage)
ξ_1, ξ_3, ξ_6	=	mode shapes of first, third and sixth modes evaluated at sensor locations.
ϕ_2	=	conversion factor (see rigid body equations)
η_2, η_3, η_4	=	sensor noise for wing accelerometer, nose accelerometer, and rate gyro, respectively.

By means of the state equations (5) it is possible to express the sensor signals in terms of $\underline{x}_1$, $\underline{x}_2$, $\underline{x}_4$, the controls $\underline{c}$, and η_2, η_3, and η_4. In keeping with the comment on Eq. 6 of Section I-B, it is assumed that the measured signals have been modified by subtracting out the known contributions of the control $\underline{c}$. The variables η_2, η_3, and η_4 are obstensibly (white) sensor noise, but are usually magnified in

order to account for modelling uncertainty. For the trial model, η_2, η_3, and η_4 were assumed to have RMS values of .02, giving a signal/noise ratio very roughly on the order of unity. One could argue the merits of increasing these values still further. So the sensor equations may be summarized as:

$$\underline{m} = \underline{A}_1 \underline{x}_1 + \underline{A}_2 \underline{x}_2 + \underline{A}_4 \underline{x}_4 + \underline{B}_2 \underline{\eta}_2 \tag{9}$$

where $\underline{m} = \begin{bmatrix} m_1 \\ m_2 \\ m_3 \end{bmatrix}$ * and $\underline{\eta}_2 = \begin{bmatrix} \eta_2 \\ \eta_3 \\ \eta_4 \end{bmatrix}$

A.7 Response Equations

The locations of stress responses (s_i) and acceleration responses (A_i) are shown on Fig. 1 of the Introduction. There are two stress locations each on the wing and body and one on the horizontal tail root. The structural significance of these locations is readily understood from the diagram. There is one acceleration response at the pilot's station and two in the cargo bay; the fourth location is included to minimize flexing of the tail segment. These are the same responses used in the LAMS study. In the Data Base Report the bending moment equations are given as:

$$\underline{b} = \underline{I}\,\ddot{\underline{q}} + \sum_n \underline{N}_{1n}\{\underline{K}_n^* \ddot{\underline{q}}\} + \sum_n \underline{N}_{2n}\{\underline{K}_n^* \dot{\underline{q}}\} + \sum_n \underline{F}_{kn}\{\underline{\psi}_n^* \ddot{z}_g\} + \sum_i \underline{F}_{k_i}\{\underline{K}_i^* \ddot{\delta}_i\} \tag{10}$$

---

* Corrected to eliminate control signal contributions (see comments under the "Control Problem" paragraph of Section I.B).

The variables are defined as in Eq. 3, and

$$\underline{b} = [b_{v_1} \quad b_{v_2} \quad b_{c_1} \quad b_{c_2} \quad b_{v_3} \quad b_{v_4} \quad b_{v_5}]'$$

the numerical subscripts following those on the stress locations in Fig. 1, with "v" denoting the vertical and "c" the chordwise moment contributions. Using the approximations in Section IV.A.2 these equations may be rewritten as

$$\underline{b} = \underline{\tilde{I}}\,\ddot{\underline{q}} + (\sum_n \underline{N}_{1n})\,\dot{\underline{q}} + (\sum_n \underline{N}_{2n})\underline{q} + \underline{F}_{k_n}\,\underline{x}_4 + \underline{F}_{k_i}\,\underline{\delta} \qquad (11)$$

The stresses at each point are linear combinations of the bending moments, thus

$$\underline{s} = \underline{K}\underline{b} \quad , \quad \underline{s} = [s_1 \quad s_2 \quad s_3 \quad s_4 \quad s_5]' \qquad (12)$$

where $\underline{K}$ depends on structural parameters of the vehicle. The acceleration response equations are constructed in precisely the same way that accelerometer signals were constructed in the previous section, yielding

$$\underline{a} = [a_1 \quad a_2 \quad a_3 \quad a_4]'$$

as a function of $\underline{x}_1$, $\underline{x}_2$, $\underline{x}_4$ and $\underline{c}$. Hence the response equations may be written as

$$\underline{r} = \underline{H}_1\underline{x}_1 + \underline{H}_2\underline{x}_2 + \underline{H}_4\underline{x}_4 + \underline{D}(\underline{y}_o)\,\underline{c} \qquad (13)$$

corresponding to Eq. 7, Section I.B (with $\underline{F}_5 = \underline{0}$). Again, the parameters of $\underline{D}$ correspond to the fixed surface locations of the LAMS model and the parameters of the variable-location model must be computed by a technique similar to that outlined in Section IV.A.3.

A.8 Summary

Combining Eqs. 5, 7, 8, 9 and 13 the complete system can be written as:

$$\begin{bmatrix} \dot{\underline{x}}_1 \\ \dot{\underline{x}}_2 \\ \dot{\underline{x}}_4 \\ \dot{\underline{x}}_3 \end{bmatrix} = \begin{bmatrix} \underline{F}_1 & \underline{L}_1 & \underline{C}_1 & \underline{0} \\ \underline{L}_2 & \underline{F}_2 & \underline{C}_2 & \underline{0} \\ \underline{0} & \underline{0} & \underline{F}_4 & \underline{L}_4 \\ \underline{0} & \underline{0} & \underline{0} & \underline{F}_3 \end{bmatrix} \begin{bmatrix} \underline{x}_1 \\ \underline{x}_2 \\ \underline{x}_3 \\ \underline{x}_4 \end{bmatrix} + \begin{bmatrix} \underline{G}_1(\underline{y}) \\ \underline{G}_2(\underline{y}) \\ \underline{0} \\ \underline{0} \end{bmatrix} [\underline{c}] + \begin{bmatrix} \underline{0} & \underline{0} \\ \underline{0} & \underline{0} \\ \underline{0} & \underline{0} \\ \underline{C}_3 & \underline{0} \end{bmatrix} \begin{bmatrix} \underline{\eta}_1 \\ \underline{\eta}_2 \end{bmatrix}$$

or

$$\dot{\underline{x}} = \underline{F}\underline{x} + \underline{G}(\underline{y})\,\underline{u} + \underline{C}\,\underline{\eta} \tag{14}$$

with $$\underline{m} = [\underline{A}_1\ \underline{A}_2\ \underline{A}_4\ \underline{0}]\,\underline{x} + [\underline{0}\ \underline{B}_2]\,\underline{\eta} \equiv \underline{A}\underline{x} + \underline{B}\,\underline{\eta} \tag{15}$$

and $$\underline{r} = [\underline{H}_1\ \underline{H}_2\ \underline{H}_4\ \underline{0}]\,\underline{x} + \underline{D}(\underline{y})\underline{c} \equiv \underline{H}\underline{x} + \underline{D}(\underline{y})\,\underline{u} \tag{16}$$

The numerical values for the coefficient matrices are given in Appendix H. From the above discussion, the covariance matrix for the white noise disturbances is written as:

$$\underline{N} = \begin{bmatrix} 50. & 0 & 0 & 0 \\ 0 & 1. & 0 & 0 \\ 0 & 0 & 1. & 0 \\ 0 & 0 & 0 & 1. \end{bmatrix}$$

The weighting matrix, $\underline{Q}$, for the criterion function gives a weight of unity to all responses but s_2 (on the wing) and a_2 (near the center of gravity) which were weighted at ten. It was anticipated that, in view of the mode shape data, s_2 would be especially likely to pick up stresses due to bending modes, while a_2 would pick up primarily modal accelerations.

The mathematical model formulated in Section II, it should be noted, does not precisely correspond with this one, due to the neglect of actuator delays and control surface aerodynamics. In this model $\underline{F}$ and $\underline{H}$ are independent of $\underline{y}$, while $\underline{G}$ depends on $\underline{y}$. This fact does not affect the <u>form</u> of the answers for the estimation and control

problems, but it does change the variational equations. For this system the variational equations (corresponding to Eqs. 26-29 of Section II.D) become:

$$J_{1i} = -TR[\underline{S}_{1i}(\underline{F}\underline{\tilde{X}} + \underline{\tilde{X}}\underline{F}' + \underline{C}\underline{N}\underline{C}')] \tag{15}$$

$$J_{2ij} = 2TR[-\underline{K}'_{1j}\underline{D}'\underline{Q}\underline{D}\underline{K}_{1i}\underline{\hat{X}} + \underline{K}'(\underline{G}'_{1j}\underline{S}_{1i} + \underline{G}'_{2ij}\underline{S} + \underline{G}'_{1i}\underline{S}_{1j} + \underline{D}'_{2ij}\underline{Q}(\underline{H}+\underline{D}\underline{K}) + \underline{D}'_{1i}\underline{Q}\underline{D}_{1j}\underline{K})\underline{\hat{X}}] \tag{16}$$

$$(\underline{F}+\underline{G}\underline{K})'\underline{S}_{1i} + \underline{S}_{1i}(\underline{F}+\underline{G}\underline{K}) + \underline{K}'(\underline{G}'_{1i}\underline{S} + \underline{D}'_{1i}\underline{Q}(\underline{H}+\underline{D}\underline{K})) + (\underline{S}\underline{G}_{1i} + (\underline{H}+\underline{D}\underline{K})'\underline{Q}\underline{D}_{1i})\underline{K} = 0 \tag{17}$$

$$K_{1i} = -(\underline{D}'\underline{Q}\underline{D})^{-1}(\underline{D}'_{1i}\underline{Q}\underline{D}\underline{K} + \underline{D}'\underline{Q}\underline{D}_{1i}\underline{K} + \underline{D}'_{1i}\underline{Q}\underline{H} + \underline{G}'_{1i}\underline{S} + \underline{G}'\underline{S}_{1i}) \tag{18}$$

These were the equations implemented in solving the surface location problem for the trial model.

B. OPTIMIZATION RESULTS

The general purposes of this section are two-fold: (1) to answer the question posed in the introduction, i.e., how much performance improvement can be achieved by choosing surface locations optimally, and (2) to point out aspects of the results which will be useful in formulating the strategy of the next chapter. Of course all results are stated in terms of the behavior of the trial model of the C-5A described in the preceding section; to the extent that this aircraft is typical, the conclusions can be generalized. Because flexure contributions to responses are very significant, one may presume that flexure control and hence surface location become more important as the number of significant elastic modes increases--i.e., the more flexible the vehicle. Surface location could thus be considered a more important problem on very flexible aircraft such as the B-52 and less significant (except from the standpoint of passenger comfort) on most of the smaller commercial craft. Although a detailed analysis

of the assertion is beyond the scope of this thesis, one may also presume (to the extent that structure physics remain linear) that surface location becomes perhaps crucially important in extreme flight conditions, where flexure modes (if uncontrolled) may become critically unstable due to nonlinear aerodynamic effects.

B.1 Significance of the Control Surface Placement Problem

The first problem to be adressed is the evaluation of the significance of surface placement itself. In order to evaluate roughly the influence that location has on the performance criterion, the root mean square values of some of the state variables and the performance index $J(\underline{y})$ is given for some sample locations in Table 1. Figure 1 displays the positions graphically--the twelve cases span the possible domain of values for y_1 and y_2 fairly well.

The first case differs from the others in that it represents a nonoptimal control system for the given values of y_1 and y_2. The suboptimal controller was generated as a result of a programming error but happened to be a useful case for comparison. Note that this controller does far better than any of the flexure controllers insofar as it controls vertical velocity very tightly; it also happens to control the variables x_2 through x_6 as well as--if not better than--the optimal controllers. The nonoptimal controller does much worse than the others in controlling the sixth mode (x_7 and x_8). The weighting matrix given in the previous section, however, has been chosen to weight heavily those responses due primarily to mode six (from the mode shape diagrams of Appendix I, one sees that mode six is most significant at stress location two and acceleration station two). Indeed the value of $J(\underline{y})$ for Case I is 50 times as great as for the

Table 1

Significance of Flexure Control

CASE:	I	II	III	IV	V	VI	VII	VIII	IX	X	XI	XII
LOCATIONS:												
y_1	473.3	400.0	274.1	297.1	473.3	440.0	382.8	330.4	473.3	659.0	777.7	855.4
y_2	886.5	800.0	874.1	697.1	886.5	953.3	996.1	1044.0	886.5	1077.0	1163.0	1235.0
STANDARD DEVIATION OF:												
x_1	2.081	54.21	54.95	52.24	55.33	55.47	55.99	56.06	49.98	51.90	53.02	53.81
x_2	.1921	.2060	.1660	.2940	.1609	.1471	.1484	.1496	.2675	.2621	.2480	.2347
x_3	1.227	1.681	1.706	1.557	1.660	1.604	1.657	1.643	3.309	2.479	1.774	1.621
x_4	1.009	.2939	.3363	.2407	.3467	.4040	.4239	.4541	.4122	.2212	.2225	.2465
x_5	1.067	1.392	1.396	1.316	1.356	1.285	1.362	1.337	.7868	.8781	1.051	1.114
x_6	.9043	.2183	.2103	.2062	.2049	.1903	.2012	.1976	.0586	.1157	.1418	.1555
x_7	9.543	.8079	.8353	.7530	.8586	.8764	.8912	.9033	.7547	.8993	.8971	.8961
x_8	.4436	.04920	.05119	.04495	.05280	.03575	.05585	.05726	.05901	.06550	.06550	.06496
CRITERION VALUE:												
$J(\underline{y})$	971.4	27.369	28.110	25.861	28.469	28.949	29.621	30.065	N.A.	N.A.	N.A.	N.A.

DEFINITION OF STATES AND VARIABLES:

- y_1 = position of inboard aileron (inches)
- y_2 = position of outboard aileron (inches)
- x_1 = vertical velocity with respect to stability axes (inches/sec.)
- x_2 = pitch rate (degrees/sec.)
- x_3 = deflection of mode 1 (inches)
- x_4 = velocity of mode 1 (inches/sec.)
- x_5 = deflection of mode 3 (inches)
- x_6 = velocity of mode 3 (inches/sec.)
- x_7 = deflection of mode 6 (inches)
- x_8 = velocity of mode 6 (inches/sec.)
- $J(\underline{y})$ = $TR[\underline{S}(\underline{y})(\underline{F}\tilde{\underline{X}} + \tilde{\underline{X}}\underline{F}' + \underline{C}\underline{N}\underline{C}')]$

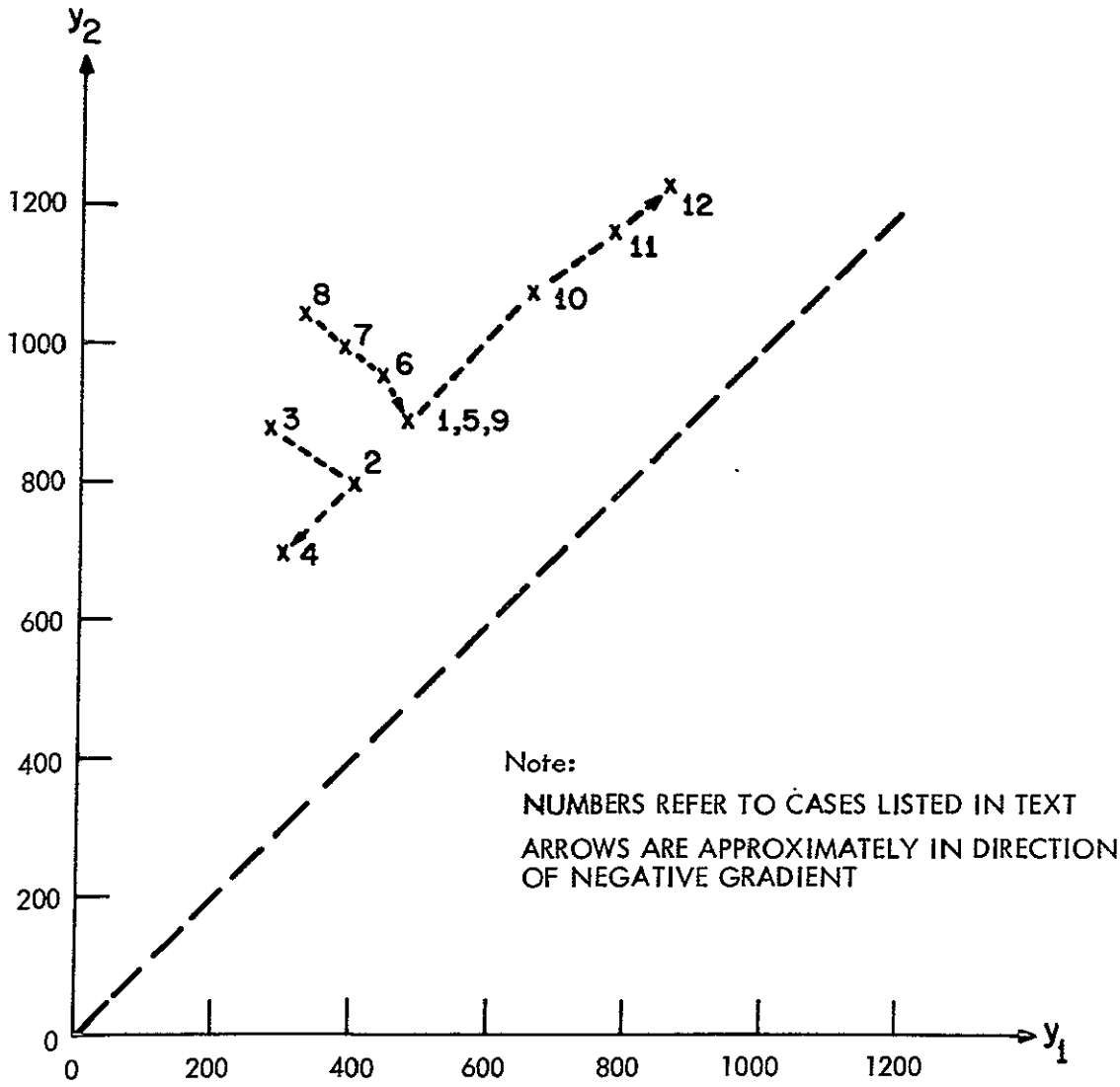

Surface Locations of Cases II-XII

Figure 1

optimal controllers, demonstrating the value of optimal flexure control *per se*'. Having demonstrated the merits of optimal control, it is worthwhile to ask how much optimal performance may be improved by paying attention to control surface locations. As a measure of the effect of surface locations on optimal performance, one can take the ratio of some variables from the worst case (VIII) to the best case (IV). The ratios are found in Table 2:

Table 2

Standard Deviation Ratios:
Worst and Best Cases

Variable	x_1	x_2	x_3	x_4	x_5	x_6	x_7	x_8	J
Ratio	1.072	.505	1.055	1.886	1.015	.958	1.200	1.274	1.162

Taken together, variables x_7, x_8 and the criterion J seem to indicate a potential improvement of about 20 percent in the performance of the optimal controller due to optimal positioning of the control surfaces.* There is, of course, no guarantee that surface positioning will be more or less successful than this estimate with respect to any other criteron. On the basis of intuition, it seems likely that optimal surface location will yield a significant performance improvement in cases where the criterion emphasizes a number of modes not too much greater than the number of control surfaces. A comparison of cases I, IV and VIII, for example, indicates that if $\underline{Q}$ were chosen to weight x_1 and x_2 more heavily (say by letting $Q(6,6) = 10.$,

---

* Note that the "worst" locations of Case VIII do not appear at all unreasonable upon cursory surveillance of the aircraft.

weighting the pilot's acelleration) control surface positioning might be less effective than in the above instance. Pitch rate (x_2) control, especially, seems to experience a trade-off with control of the sixth mode. The trade-off in pitch rate appears to involve the last few "ounces" of improvement for the original criterion, whereas the trade-off between vertical velocity and control of mode six seems to occur on a large scale (compare I and IV), except for the last degree of improvement, when the goals become complementary.

In the interest of practical application, a detailed discussion of the philosophy of choosing quadratic weights would be very valuable at this point, but the subject is far too large and intricate to be treated in this document. Two general conclusions, however, may be drawn from the C-5A results. First, there exist some applications and some reasonable performance criteria for which optimal surface locations yield a significant performance improvement. Secondly, such performance criteria will tend to emphasize responses (especially stresses) which are closely related to a limited number of flexure modes (i.e., a number not too much greater than the number of control surfaces). This second point is utilized in Section V.

B.2 Analysis of Results for the C-5A Trial Model

The analysis of this subsection is directed toward the identification of significant trends which emerge from the computer results rather than a precise description of the detailed performance of the optimally-controlled aircraft. Publication of detailed results serves no purpose because neither the vehicle model, the criterion, nor the performance accurately represents the true aircraft. Instead, there

is an attempt to evaluate the search procedure and to find indications of the "strategy" of the optimal controller.

The Newton-Raphson search procedure did not prove to be very effective, since the "neighborhood" of the minimum appeared to be too small for the positive semidefiniteness of the second criterion variation to be attained. Although some of the locations approached this condition quite closely, both roots of $\underline{J}_2$ never actually entered the right half plane together, so a gradient method had to be used. The failure of $\underline{J}_2$ to become positive definite could indicate (1) very sharply localized minima, (2) a very "bumpy" criterion with many local minima, (3) a saddle point, and/or (4) boundary extrema. A detailed analysis of the results seems to indicate (3) in one region and (4) in a second region (see Fig. 1). If one visualizes $J(y_1, y_2)$ as a surface over Fig. 1, cases II-IV tend to indicate a "valley" leading to a (inverted) saddle point, while cases IX-XII point to a boundary extremum. These results are not inconsistent, as both give local minima.

Search results indeed demonstrate this trend, as depicted in Fig. 2. Contrast runs one and three. The first run starts at (400, 800) and the inboard aileron moves further toward the fuselage, causing a decrease in the criterion. The third run begins at (473, 886) and both ailerons move outboard until the outermost one reaches the end of the wing.

Although the two runs were made with slightly different computer programs (run three, from a Honeywell computer, uses longer Fourier series for the mode shapes than run one, from the IBM system at M.I.T.), they accurately demonstrate the initialization

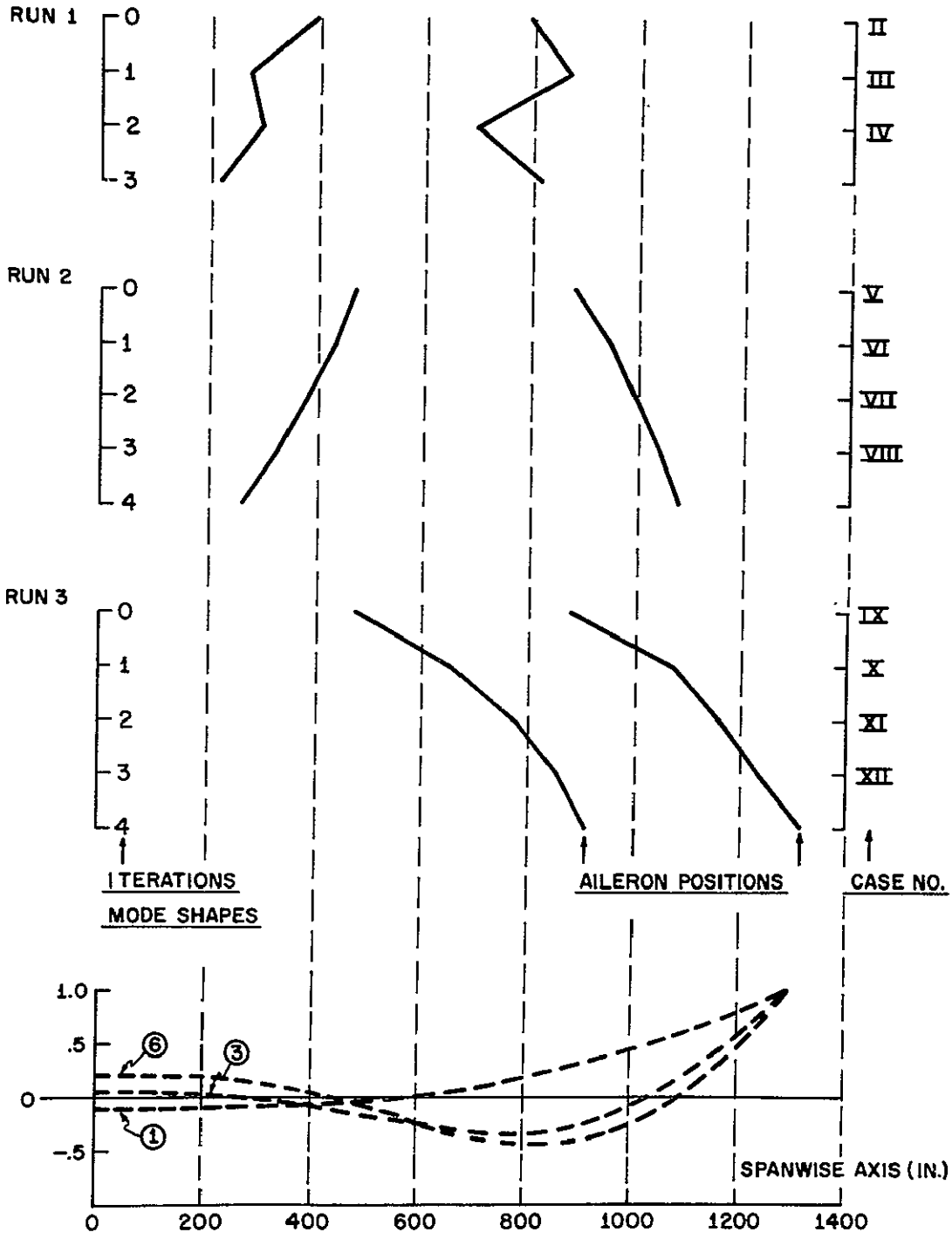

Fig. 2 Aileron Locations Generated by Computer Program

problem involved. The initialization points happened to lie near a local maximum of the criterion and hence the ailerons could "slide down" either side of the hill, which they did. Reference to Table 1, incidentally, indicates that the minimum of run 1 is probably lower than the boundary extremum of run 3.*

Thus the initialization problem can cause severe consequences. The only way to avoid this problem is to develop some effective strategy for making a good estimate of initial locations. Not only should such a strategy help to locate global minima, but is should also bring the program into a region of positive definite J_2 much more rapidly than a random search.

If one recognizes that the objective of the optimal controller is primarily control of the sixth mode, the surface placement strategies for the trial model should be fairly evident from the mode shapes, which are also shown in Fig. 2. Evidently, the two options are (1) use the ailerons to exert a force couple at locations 200 and 800 or else (2) exert the couple of forces at about 800 and 1300. One might even be led to suspect the superiority of locations 200 and 800, since forces at these locations are less likely to excite the other modes of vibration than a force couple at the end of the wing. In general, however, as the number of significant modes and the number of control surfaces increases, the optimal strategy will become less and less evident on intuitive grounds. The different frequencies of the various modes and the varying degrees to which the gusts excite each mode will confound any simple theory based on mode shapes alone.

---

* Due to a programming error, run 2 had a reversed sign on the gradient search and should be read backwards to indicate proper behavior of the program. Viewing this run as a lead-in to run 3, one sees the strange (but reasonable) search patterns which can develop.

If one were designing a suboptimal controller to "do the job" within loose constraints, it might be possible to form some crude generalizations about the manner in which various modes might be controlled and to go on to invent a "pure" strategy based only on evident principles (e.g., location of surfaces near mode shape maxima in a way such as to achieve an ability to discriminate in control of various modes). When one is designing optimal controllers, however, the considerations can be quite different from those involved in a rough guess. Note, for instance, how the rigid body variables x_1 and x_2 radically changed roles between the "rough guess" and "final ounce" in the C-5A example. At the "rough guess" stage behavior of x_1 was very loosely constrained, while control of pitch rate, x_2 was more tightly constrained; at the "final ounce" stage, better control of x_1 tended to closely coincide with reductions in J, while control of x_2 was in actual conflict with the reduction of J. Because flexure control itself is a rather "fine tuning" sort of problem (as opposed to rigid body control), the optimal strategy must depend heavily on the exact nature of the criterion, or at very least on the effect of the gains generated by the criterion. There is still hope, however, of devising a strategy based on one (or a very few) solution(s) of the optimal control problem for a given criterion--a strategy which avoids the costly and difficult search procedure. The remainder of the thesis is directed toward development of such a strategy.

In order for a placement strategy to be applicable, consideration must be limited to a reasonable number of flexure modes, since the analysis must obviously have something to do with the mode shapes. A diagram of the migration of the roots for the optimally-controlled C-5A model indicates why this is likely (see Fig. 3). The optimal control system damped the free aircraft rigid body response

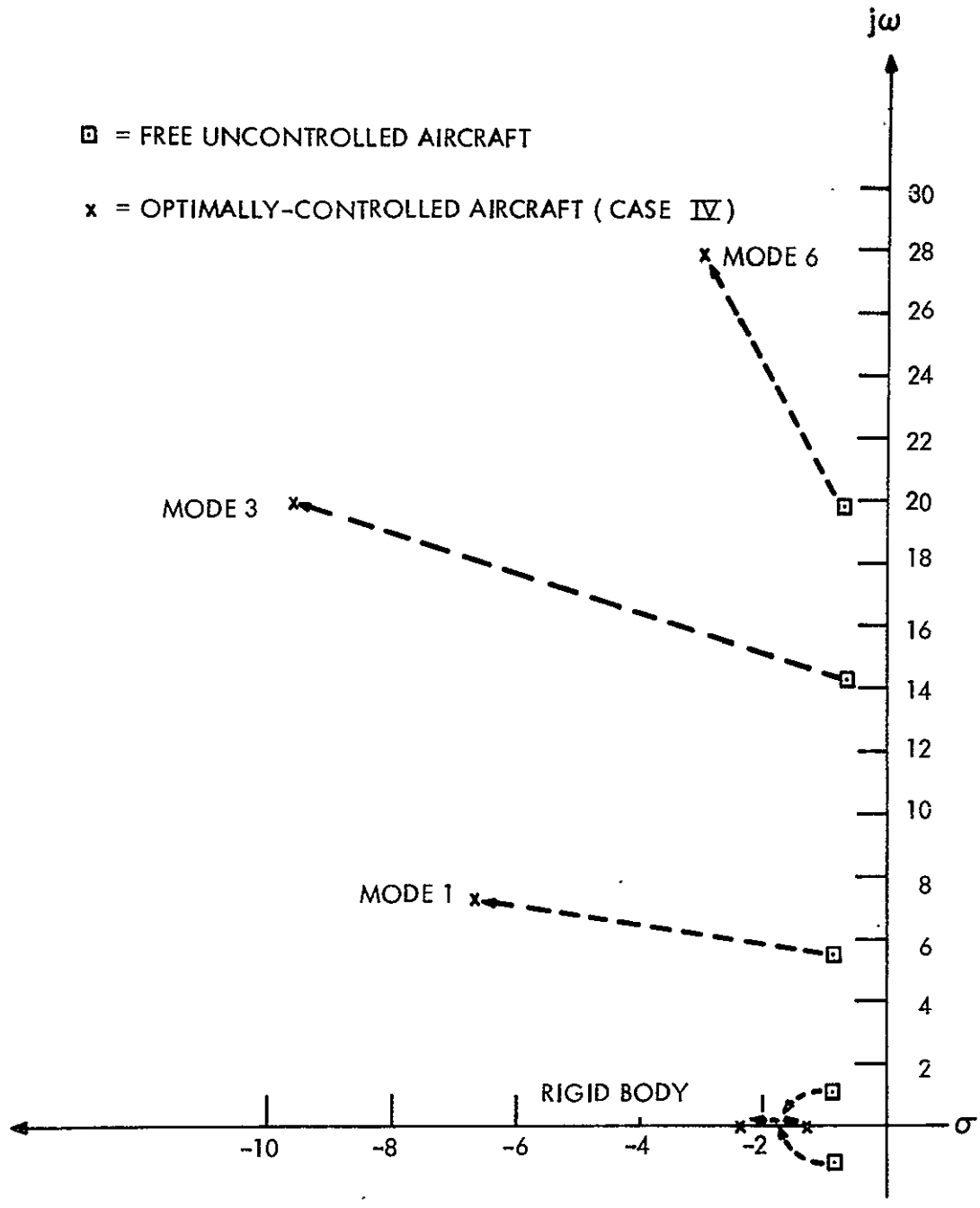

Fig. 3 Closed vs. Open-Loop Poles

considerably and also modes one and three. The important reduction of mode six responses, however, was accomplished almost as much by a frequency shift as by simple damping. At the higher frequency, less energy is put directly into the mode since both the gust correlation filter and the Kussner delays act as low-pass filters. Assuming that structural coupling of the modes is not dominant in the aircraft physics or aerodynamics, the effect of higher frequency modes cannot be strong, because a limited amount of energy is coupled into them by the wind gusts.

As evidenced by the discussion above, most of the behavior of the search program for the C-5A trial model can be explained by direct reference to the flexure physics, so no note has been made of the actual values of the criterion variations. For reference purposes, the first variations for cases two through twelve are given in Table 3.

Minimization of the first variation of the criterion (provided that second variation conditions are satisfied) is the true mathematical goal of the solution technique. In higher order problems, one is forced to rely increasingly on mode slopes rather than the mode shapes themselves, because mode slopes (upon which $\underline{J}_1$ depends) give a better picture of the trade-offs between different locations. Because it yields equations (i.e., $\underline{J}_1 = \underline{0}$) rather than the inequalities of global investigations, the strategy of driving $\underline{J}_1$ to zero seems a good one to pursue. This approach also gives rise to a well-defined surface location procedure for the general case, as shown in Section V.

One final trend in the results of the C-5A study is worthy of note. Once one of the two basic control strategies had been chosen, the optimal costate matrix $\underline{S}$ and the optimal gains changed relatively

Table 3

First Variations of the Criterion

CASE NUMBER:	II	III	IV	V	VI	VII	VIII	IX	X	XI	XII
AILERON LOCATIONS:											
y_1	400.0	274.1	297.1	473.3	440.0	382.8	330.4	473.3	659.0	777.7	855.4
y_2	800.0	874.1	697.1	886.5	953.3	996.1	1044.0	886.5	1077.0	1163.0	1235.
CRITERION VARIATIONS:											
$\partial J/\partial y_1$	.006458	-.001432	.09866	.002623	.003841	.005062	.006771	.04541	-.009937	-.02761	-.03457
$\partial J/\partial y_2$	-.003802	.01101	-.1642	-.005271	-.002873	-.00460	-.002615	-.1606	-.06712	-.03337	-.01583

little as the search procedure progressed. The greatest variations appeared in the $\underline{G}_o(\underline{y})$ matrix and in the state covariance, although (see Table 1) even the state covariance did not change radically. These results of the C-5A example are perhaps the most important facts to note in developing a surface placement strategy.

SECTION V

A CONTROL SURFACE LOCATION STRATEGY

The apparent complexity of the surface placement problem is the basic impediment to its solution. A wind gust strikes the aircraft, exciting both the rigid body and its elastic modes. The energy imparted to the vehicle is dissipated through aerodynamic damping, structural damping, and transfer (via mode coupling) to high frequency modes. The relationship between these forms of excitation and dissipation is very complex. The object of flexure control, generally, is to minimize the amount of energy dissipated in structural damping (since structural damping is ultimately a result of the heating and friction which occurs when the vehicle is deformed), especially at certain critical points on the aircraft, as this energy dissipation eventually gives rise to dangerous elastic fatigue. The optimal controller must disperse the gust energy in a way such as to avoid dissipation at these critical points. It can accomplish this (1) by "anticipating" the gusts and keeping the aircraft in such a position that it absorbs the least gust energy, (2) by dissipating the energy in the viscous air flow (e.g., spoilers or rigid body motion), or (3) by forcing the energy into elastic modes giving rise to noncritical responses. The C-5A flexure controller does all of these. The trade-offs involved in these forms of dissipation are very difficult to quantify.

In order to solve the surface placement problem by a process involving less work (and more insight) than an iterative computer simulation of the aircraft, one must simplify the problem so that the

fundamentals are bared. The physics are simplified in Section V.A. Secondly, one must simplify the mathematics, since some ability to evaluate solutions globally is desirable, while it is impossible to carry the explicit $\underline{y}$-dependence of all matrices through the entire problem. This is accomplished in Section V.B. Finally, it is necessary to display the alternatives in such a way that they are easy to evaluate, a task carried through in Section V.C. A demonstration of the strategy for the C-5A is given in the concluding subsection.

A. SIMPLIFICATION OF STRUCTURE PHYSICS

The following simplifications of the problem are introduced at this point:*

(1) Assume point forces with magnitude independent of location, i.e., use section lift curves $C_{L_i}(y_i)$ = CONSTANT. (See curve (a), Fig. 5, of Section III.A.3).

(2) Linearize expressions for all rigid body moment arms.

(3) Assume only stress (or stress rate) responses are to be used, so that the $\underline{D}$ matrix becomes independent of $\underline{y}$, and $\underline{D}_{1i}=\underline{0}$, $\underline{D}_{2ij}=\underline{0}$ for all $i,j = 1 \ldots \eta_y$. Actually any responses depending on the state $\underline{x}$ and not on $\dot{\underline{x}}$ are permissible.

(4) Neglect actuator dynamics and use the equations presented for the trial model (Section IV.A.8, Eqs. 14-18). This assumption is not essential, but merely simplifies many of the variational equations.

Now consider the effects embodied in the $\underline{G}(\underline{y})$ matrix. First, there are the forcing functions for the mode accelerations. Using

---

* Assumptions (3) and (4) are readily discarded, while assumption (1) may be relaxed by multiplying all mode shapes by $C_L(\underline{y})$ and adding some other minor modifications

assumption (1) these may be written (see Eq. 15, Section III.A.3):

$$\ddot{\eta}_{i_y} = \sum_{i=1}^{9} c_{ij}[\xi_i(y_j) + d(y_j)\phi_i(y_i)]\ \delta_j \tag{1}$$

where $c_{ij} = C_{L_j}/(M_i/M)$ is independent of y_i. In the spirit of the summary of Section III, a shorthand notation for the elements of the $\underline{G}$ matrix is now introduced. Each element is denoted by $G(EQ; s)$, where EQ is a symbol describing the force equation and s is a symbol denoting the type of control surface. Using this notation, the coefficients corresponding to (1) may be written as

$$G(\ddot{\eta}_i, j) = c_{ij}(\xi_i(y_j) + d(y_j)\phi_i(y_j))^* \tag{2}$$

It is also advantageous (in light of assumption (3)) to define the modified mode shapes, $\beta_i(y)$, as follows:

$$\beta_i(y) \doteq \xi_i(y) + d(y)\phi_i(y) \tag{3}$$

With the convention that

$$\beta_o(y) = y \tag{4}$$

Thus (2) becomes

$$G(\ddot{\eta}_i, j) = c_{ij}\beta_i(y_j) \tag{5}$$

One can similarly write the rigid body forcing terms as

$$G(\ddot{x}_k, j) \tilde{=} g_{kj} + c_{koj}\beta_o(y_j) + \sum_{i=1}^{NI} c_{kij}\beta_i(y_j) \tag{6}$$

$$\tilde{=} g_{kj} + \sum_{i=0}^{NI} c_{kij}\,\beta_i(y_j)$$

---

* Multiplication by δ_i, the i^{th} surface deflection, occurs when $\underline{G}(\underline{y})$ is multiplied by $\underline{u}$, the vector of control settings.

where $\ddot{x}_k$ = k^{th} rigid body acceleration (e.g., $\ddot{z}, \ddot{x}, \ddot{\psi}, \ddot{\phi}, \ddot{\theta}$)

g_{kj} = constant terms (e.g., $C_{L_j}(y_j) = C_{L_k}$ in the $\ddot{z}$ equation)

c_{kij} = coefficient of i^{th} mode acceleration due to j^{th} control surface in mode acceleration pick-up of k^{th} rigid body equation

c_{koj} = moment arm coefficent of j^{th} control surface

The evident course is now to define a matrix $\underline{B}(\underline{y})$, to be distinguished from the constant $\underline{B}$ matrix of the sensor equations, whose $(i,j)^{th}$ entry is

$$[\underline{B}(\underline{y})]_{ij} = \beta_i(y_j) \tag{7}$$

where

$$i = 0, \ldots, NI$$

$$j = 1, \ldots, n_y$$

Finally, the $\underline{G}(\underline{y})$ matrix may be written as

$$\underline{G}(\underline{y}) = \underline{G}_o + \underline{G}_1\underline{B}(\underline{y}) \tag{8}$$

$\underline{G}_o$ is a constant matrix containing terms such as g_{kj} of Eq. 6 and also force coefficients for surfaces which are fixed in position. The $\underline{G}_1$ matrix contains the coefficients c_{ij} of (5) and c_{kij} of (6).

With this notation it is also easy to represent the derivatives of $\underline{G}$ with respect to y_j, $\underline{G}_{1j}$:

$$\underline{G}_{1j} \triangleq \frac{\partial \underline{G}(\underline{y})}{\partial y_j} = \underline{G}_1 \frac{\partial \underline{B}(\underline{y})}{\partial y_j} \tag{9}$$

Note, however, that only the j^{th} column, $\underline{b}_j$, of $\underline{B}(\underline{y})$ depends on y_j, so $\underline{B}_{1j}$ has only the j^{th} column, $\partial \underline{b}_j / \partial y_j$, nonzero. This fact motivates the shorthand notation:

$$\underline{G}_1(\underline{y}) = \underline{G}_1 \underline{B}_1(y) \tag{10}$$

where the i^{th} column of $\underline{G}_1(\underline{y})$ contains the nonzero entries of $\underline{G}_{1i}$, and the j^{th} column of $\underline{B}_1(\underline{y})$ contains the nonzero entries of $\underline{B}_{1j}$, i.e.,

$$[(\underline{B}_1(\underline{y})]_{ij} = \frac{\partial \beta_i}{\partial y_j}(y_j) \tag{11}$$

where $\frac{\partial \beta_i}{\partial y_j}(y_j) = \xi_i'(y_j) + d'(y_j)\phi_i(y_j) + d(y_j)\phi_i'(y_j) \qquad i \neq 0$

and $\frac{\partial \beta_o}{\partial y_j}(y_j) = 1 \qquad i=0$

$\underline{B}_1$ is simply a matrix of the modified mode slopes evaluated at the various surface locations.

Thus there exists s relatively simple expression for both the explicit $\underline{y}$-dependence of $\underline{G}(\underline{y})$ and the $\underline{y}$-dependence of its first derivatives $\underline{G}_{1j}(\underline{y})$. Furthermore, due to assumption (3), this comprises the entire $\underline{y}$-dependence of the problem.

B. SIMPLIFICATION OF MATHEMATICS

In the best possible situation, one would hope to be able to obtain an explicit expression for $J(\underline{y})$ in terms of $\underline{y}$ itself, or in terms, say, of the mode shapes. It will be shown that this is not feasible. The next best situation would be to obtain the first variations of $J(\underline{y})$ as explicit functions of the normal modes. Provided that one is willing to make a few approximations, it will be shown that this is possible (although the optimal control problem must be solved at least once). Furthermore, the requisite expressions for $\underline{J}_{1i}(\underline{y})$, $i=1 \ldots \eta_y$, are readily evaluated and put into a form where near-optimal locations become evident.

First consider the problem of obtaining an explicit expression for $J(\underline{y})$. The most promising expression for $J(\underline{y})$ is given in Appendix D:

$$J(\underline{y}) = \mathrm{TR}[\underline{S}(\underline{y})(\underline{F}\tilde{\underline{X}} + \tilde{\underline{X}}\underline{F}' + \underline{C}\underline{N}\underline{C}')] \tag{12}$$

This expression is promising because the matrix $(\underline{F}\tilde{\underline{X}}+\tilde{\underline{X}}\underline{F}'+\underline{C}\underline{N}\underline{C}')$ is independent of $\underline{y}$ and depends only on the results of the state estimation problem, which can be solved independently of $\underline{y}$. The costate matrix $\underline{S}(\underline{y})$, in addition, is the best one could hope for, in that $\underline{K}(\underline{y})$ and $\hat{\underline{X}}(\underline{y})$ are derived from it, and would necessarily be more complicated functions of $\underline{y}$ (i.e., $\underline{K}(\underline{y})$ involves $\underline{G}'(\underline{y})\underline{S}(\underline{y})$ and $\hat{\underline{X}}(\underline{y})$ involves $\underline{G}(\underline{y})\underline{K}(\underline{y})$). Unfortunately, however, $\underline{S}(\underline{y})$ is a solution of the Riccati equation

$$\begin{aligned}(\underline{F}-\underline{G}(\underline{y})(\underline{D}'\underline{Q}\underline{D})^{-1}\underline{D}'\underline{Q}\underline{H})'\underline{S}(\underline{y}) + \underline{S}(\underline{y})(\underline{F}-\underline{G}(\underline{y})(\underline{D}'\underline{Q}\underline{D})^{-1}\underline{D}'\underline{Q}\underline{H}) \\ -\underline{S}(\underline{y})\underline{G}(\underline{y})(\underline{D}'\underline{Q}\underline{D})^{-1}\underline{G}'(\underline{y})\underline{S}(\underline{y}) + \underline{H}'(\underline{Q}-\underline{Q}\underline{D}(\underline{D}'\underline{Q}\underline{D})^{-1}\underline{D}'\underline{Q})\underline{H} = \underline{0}\end{aligned} \tag{13}$$

The third term of this equation involves, effectively, the product $\underline{G}(\underline{y})G'(\underline{y})$, which is a thorough mixture of mode shapes, moment arms, constants, and every combination of these three multiplied together. There is virtually no hope of carrying any "bookkeeping" procedure on the mode shapes through the solution of the Riccati equation. The linear equations which give bounds on the solution of the Riccati equation might yield relatively simple expressions in the mode shapes, but the bounding solutions are known to be very poor. Thus there appears to be very little hope of finding the criterion as an explicit function of $\underline{y}$, other than mapping it tediously, point by point.

The next alternative is to seek the variations of the criterion as functions of $\underline{y}$. One might well ask why this should offer any more hope than the evaluation of the criterion itself, as the first variations

have been seen to involve at least the solution of the control problem at each location, which is just the task that led to difficulties above, due to the squared terms in $\underline{G}(\underline{y})\underline{G}'(\underline{y})$. Some justification for using the first variation of the criterion can be derived from this very fact. Differentiation of the product terms can yield only:

(1) zero

(2) mode shapes

(3) mode slopes

(4) products of mode shapes and mode slopes

But if the mode slopes are sufficiently strong functions of $\underline{y}$ as opposed to the mode shapes, one may well be able to justify using some nominal values in place of the mode shapes, and thinking of the first variations as nearly valid in a relatively large neighborhood of these nominal values. This argument, admittedly, is heuristic; nevertheless, it does motivate an avenue of approach.

The most obvious expressions for the first variations are derived directly from (12) above, i.e.,

$$J_{1i}(\underline{y}) = TR[\underline{S}_{1i}(\underline{y})(\underline{F}\,\underline{\tilde{X}} + \underline{\tilde{X}}\,\underline{F}' + \underline{C}\,\underline{N}\,\underline{C}')], \qquad i=1\ldots\eta_y \tag{14}$$

The difficulty with these expressions, however, is that the matrices $\underline{S}_{1i}(\underline{y})$ are solutions of the state covariance type of equation given in Section IV, Eq. 17. Although the functions $\underline{S}_{1i}(\underline{y})$ do have a linear dependence on the mode slopes, as can be seen by examining the row operations used in an algebraic solution of the system of equations, a great deal of "bookkeeping" is involved, and this motivates one to look for a more useful representation of $\underline{J}_1(\underline{y})$. Such an expression actually exists:

$$\begin{aligned} J(\underline{y}) &= TR[\underline{S}(\underline{y})(\underline{F}\,\underline{\tilde{X}} + \underline{\tilde{X}}\,\underline{F}' + \underline{C}\,\underline{N}\,\underline{C}')] \\ &= -2TR[\underline{S}(\underline{y})(\underline{F} + \underline{G}(\underline{y})\,\underline{K}(\underline{y}))\,\underline{\hat{X}}(\underline{y})] \end{aligned} \tag{15}$$

Using the equations of Appendices B and C, modified for the $\underline{y}$-dependence in the trial model equations, one finds that (for $\underline{D}_{1i}=\underline{0}$), it is possible to write

$$J_{1i}(\underline{y}) = 2TR[\underline{S}(\underline{y})\,\underline{G}_{1i}(\underline{y})\,\underline{K}(\underline{y})\hat{\underline{X}}(\underline{y})] \tag{16}$$

C. THE SURFACE LOCATION STRATEGY

In the spirit of the preceding discussion, one expects that the approximation

$$\tilde{J}_{1i}(\underline{y}) = 2TR[\underline{S}(\underline{y}_o)\,\underline{G}_{1i}(\underline{y})\,\underline{K}(\underline{y}_o)\,\hat{\underline{X}}(\underline{y}_o)] \tag{17}$$

will be nearly valid in a relatively large region around $\underline{y}_o$. The optimal control results of Section IV.B indeed indicate what sort of a region this will be. The C-5A study indicated two distinct control strategies, one using a force couple near the fuselage and another using a couple near the wing tips. In the y_1, y_2 plane, these strategies yielded optimal locations which were widely separated, and control laws which differed significantly between but not within the region of each strategy. Thus in the general case, one is prompted to think in terms of "regions" where different basic strategies prevail, the boundaries of these regions being (essentially) determined by the character of the weighting matrix, $\underline{Q}$. As the number of modes or the number of control surfaces becomes greater, and/or the weighting of the modes implicit in $\underline{Q}$ becomes more evenhanded, the number of "regions" is likely to increase. One anticipates that an expression such as (17) will be nearly valid within the "region" of $\underline{y}_o$, and perhaps somewhat beyond, with luck.

Within each region, however, $\underline{J}_1(\underline{y})$ has become fairly easy to evaluate explicitly, since, according to (9), $\underline{G}_{1i}$ contains simple

linear terms in the modified mode slopes. It is a very easy matter to write a computer program which does the bookkeeping involved in evaluating (17). The expressions for the $\tilde{J}_{1i}(\underline{y})$ will be of the form:

$$\tilde{J}_{1i}(\underline{y}) = J_{1i}(y_i) = \sum_{j=0}^{NI} a_{ij}(\partial\beta_j(y)/\partial y_i); a_{ij} = a_{ij}(\underline{y}_o) \tag{18}$$

Following the heuristic notation of (10), one may write

$$\tilde{\underline{J}}_1(\underline{y}) = 2TR[\underline{S}(\underline{y}_o)\underline{G}_1\underline{B}_1(\underline{y})\,\underline{K}(\underline{y}_o)\hat{\underline{X}}(\underline{y}_o)]^* \tag{19}$$

In summary, the following search strategy promises considerably more insight and more rapid convergence on a globally optimal set of control surface locations than a "blind" gradient (or Newton-Raphson) search:

(1) Choose a reasonable initial set of surface locations, $\underline{y}_o$, based, if possible, on a best guess of what the optimal controller will attempt to accomplish in view of the weighting matrix $\underline{Q}$.

(2) Solve the optimal control problem for $\underline{S}(\underline{y}_o)$, $\underline{K}(\underline{y}_o)$ and $\hat{\underline{X}}(\underline{y}_o)$, as given in Appendix B.

(3) Evaluate $\tilde{J}_{1i}(\underline{y})$ according to (17) above.

(4) Using these functions, determine if y_o appears to lie in a large region where $\underline{J}_1$ can be nearly driven to zero; if so

(a) Choose a new set of locations $\underline{y}^1$ and proceed with a modified Newton-Raphson search (or call $\underline{y}^1$ the answer); if not

(b) Determine the boundaries of the region near $\underline{y}_o$ and make an educated guess at $\underline{y}^1$ on the basis of $\tilde{\underline{J}}_1(\underline{y}_o)$.

---

* A similar expression for $\tilde{\underline{J}}_2(\underline{y})$ can be derived if desired.

(5) If 4(a) is true, return to (2) and proceed with a more exact local search; if 4(b) is true, repeat (2)-(4) in order to identify a better "region."

D. DEMONSTRATION OF THE SURFACE LOCATION STRATEGY

The above steps have been carried out for the locations $\underline{y}_o = [297.1, 697.1]'$ of Case IV, Section IV.B. For the $\underline{G}(\underline{y})$ matrix:

$$G(\ddot{\alpha}, j) = \sum_{i=1,3,6} (-3.25\,\xi_i(y_{CG})/Z2M(i))\beta_i(y_j)$$

$$G(\ddot{\theta}/\phi_2, j) = \sum_{i=1,3,6} (-3.25\xi_i'(y_{CG})/\phi_2 \cdot Z2M(i))\beta_i(y_j) + (.791 \times 10^{-4}/\phi_2)y_j$$

$$G(\ddot{\tau}_i, j) = (-3.25/Z2M(i))\beta_i(y_j) \quad , \quad i=1,3,6$$

Inserting the relevant constants and taking the partial derivatives with respect to y_1 and y_2 $(j=1,2)$, one obtains $\underline{G}_1(\underline{y})$:

$$G_1(\ddot{\alpha}, j) = 11.153\beta_1'(y_j) - .96123\beta_3'(y_j) - 1.691\beta_6'(y_j)$$

$$G_1(\ddot{\theta}, j) = +.1304 + 16.085\beta_1'(y_j) + 6.2554\beta_3'(y_j) - 4.3894\beta_6'(y_j)$$

$$G_1(\ddot{\tau}, j) = -103.27\beta_1'(y_j)$$

$$G_1(\ddot{\tau}_3, j) = -38.449\beta_3'(y_j)$$

$$G_1(\ddot{\tau}_6, j) = -6.9592\beta_6'(y_j)$$

These equations are readily cast into the form of Eq. 10. Using the computer results for $\underline{S}(\underline{y}_o)$, $\underline{K}(\underline{y}_o)$ and $\underline{X}(\underline{y}_o)$ and evaluating the expressions (17), one obtains

$$(\tilde{J}_1)_1 \tilde{=} 2.1065\,\beta_1'(y_1) + .06489\beta_3'(y_1) + .4337\,\beta_6'(y_1) + .02826$$

$$(\tilde{J}_1)_2 \tilde{=} -4.1398\,\beta_1'(y_2) + 1.5120\beta_3'(y_2) + .79705\beta_6'(y_2) - .03849$$

These functions are sketched in Fig. 1.

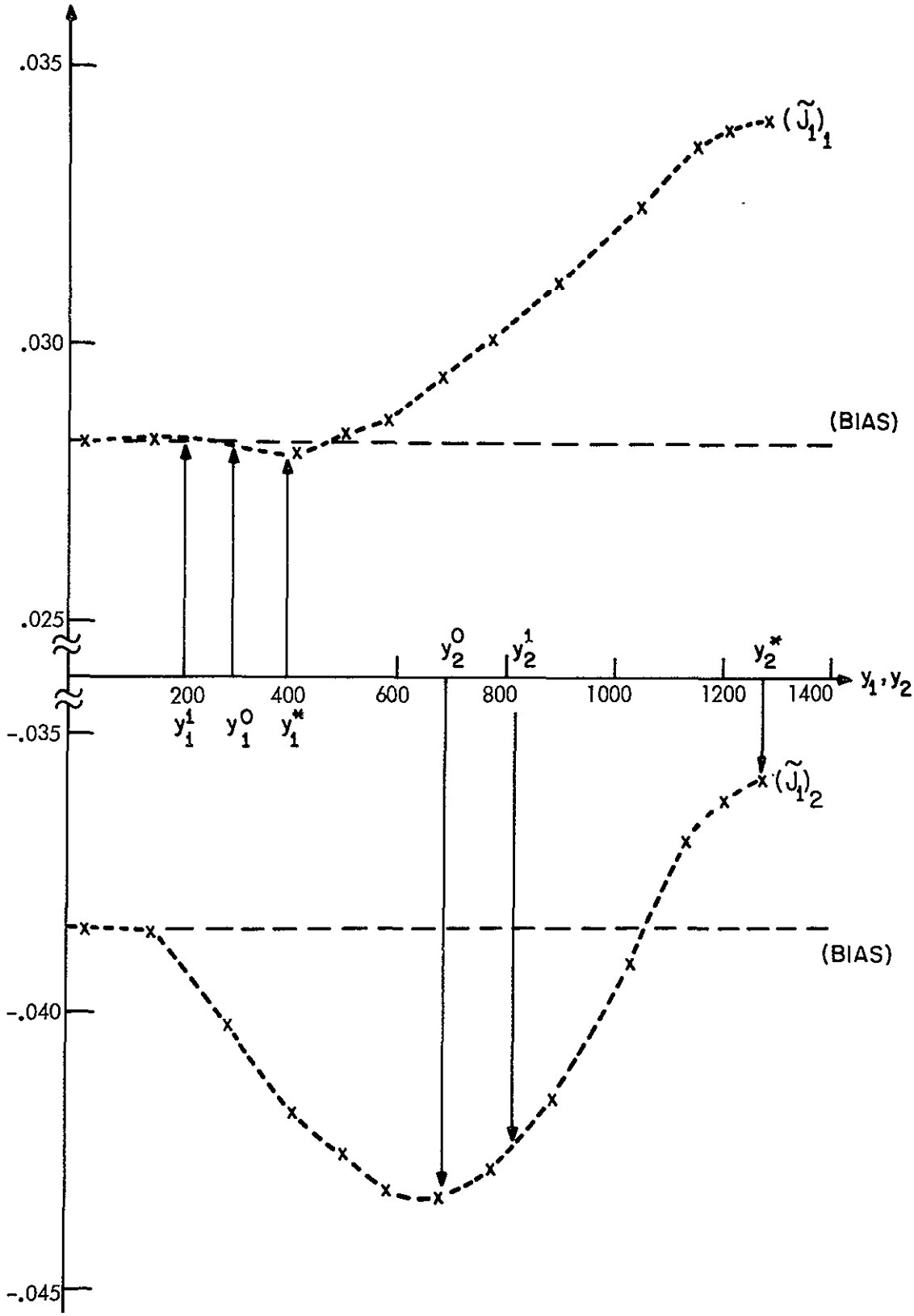

Fig. 1 First Variations of the Criterion

The actual locations for case IV are denoted by (y_1^o, y_2^o); the gradient method generated a new set of locations (y_1^1, y_2^2) which are shown in Fig. 2. According to the proposed surface location strategy, the optimal locations should be (y_1^*, y_2^*) of Fig. 3, although some comments on these locations are in order. The first fact of note is that the bias terms (due to rigid body effects) are too large to allow the condition $\underline{J}_1=\underline{0}$ to be met for any $\underline{y}$. This possibly indicates a modelling error in one of the force coefficients, a problem which would have otherwise been very difficult to identify. Note that if one were to assume for the minute that rigid body torque are in effects were negligible, these biases would become zero, yielding optimal locations $y_1^* \tilde{=} 280$ or 480 and $y_2^* \tilde{=} 1060$, which appear quite reasonable. Secondly, note the indication of the "regions". Beyond $y_1 \approx 600$, $(\tilde{J}_1)_1$ blows up, indicating a likelihood that $(\tilde{J}_1)$ has passed out of its region of validity (indeed, for the other strategy, the optimization results indicate $y_1 > 600$ as in case XII). Similarly, one observes that in the region of validity $(y_2 \approx y_2^o)$ for y_2, $(\tilde{J}_1)_2$ experiences a maximum. This clearly indicates that y_2^o is near a barrier between regions and that the behavior of the criterion may change considerably as y_2 is varied. These notions indicate the sort of global insight one might anticipate from the proposed scheme. Evidently, human cleverness has a considerable role to play here.

SECTION VI

SUGGESTIONS FOR FUTURE RESEARCH

Many possibilities for future research into both mathematics and physics have been indicated throughout this work. Promising computational methods give some hope of making formerly intractable problems mere exercises in linear algebra.

First, some basic investigations for distributed systems are in order. Some general convergence proofs must be developed in order that consideration of a limited number of flexure modes has rigorous justification. The energy considerations mentioned in the introduction to Section V, plus a bound on the amount of coupling between flexure modes should (with difficulty) establish this result.

Next, a formalism must be developed in order to enable one to optimize on number as well as location of control surfaces. In this thesis, the number of surfaces is tacitly assumed to be prespecified.

The form of the system might be generalized to allow sensor locations as free variables, in addition to control surface locations. In this event, decoupling of the estimation problem from the other phases of solution can no longer be accomplished, although use of optimal estimators may simplify the variational problem as it did in Section II.

More application-oriented research is definitely needed in the area of search techniques. The proposed search strategy should be fully investigated, as it offers some hope of being useful in obtaining global solutions. The current data is too scanty to allow adequate evaluation of how generally applicable the proposed strategy is.

Finally, there is the problem of simplifying the physics. Because a great number of physical systems can be put into the form of the elasticity equations for the aircraft, a vigorous attempt should be made, in the spirit of Section V.A to obtain explicit general solutions for the distributed-force control problem and sensor location problem.* Tensor notation, plus use of the close analogy between equations in space and time appear to be essential ingredients in the solution of these problems.

---

* Research along these lines has recently been carried out. See Greenberg, S., Optimal Pointwise Feedback Control of Distributed Parameter Systems, Doctoral Dissertation, Massachusetts Institute of Technology, June, 1969.

SECTION VII

SUMMARY

The basic physical relationships involved in control of a flexible aircraft disturbed by random wind gusts were used in formulating the surface location problem as one in optimal control of a distributed system, using a limited number of point-force controllers. The three phases of this problem--estimation, control, and surface placement--were then solved by means of the matrix minimum principle and the calculus of variations. The variational equations were greatly simplified and the order of the problem considerably reduced by the use of optimal controllers at each stage in the search for optimal surface locations. These simplifications, plus advanced computational techniques made the general solution of the problem practically feasible.

Aircraft physics had to be investigated in great detail in order to obtain general equations expressing the distributed nature of the system exactly. A computer program was written which stored these equations and used them in solving the surface location problem for a general aircraft.

This program was tested on a fourteenth order model of the Lockheed C-5A transport aircraft. As a guide for future applications, the derivation of the model parameters was carried through explicitly. The results of the optimization study were then analyzed in an attempt to recognize and develop a "strategy" for control surface placement.

A simple practical strategy was developed for systems with stress and stress rate responses and slightly simplified physics. This strategy, which was also verified for the C-5A model, has the two major advantages of (1) insight into the tradeoffs involved in surface location, and (2) partial insight into global solutions.

The major contributions of this thesis are (1) a computationally feasible general solution to the surface placement problem, (2) a practical application of optimal flexure control to a trial model of the C-5A transport, (3) implementation of efficient computational techniques for solving state covariance and Riccati equations, and (4) recognition of the nature of the optimal solutions and presentation of a search strategy which makes use of the basic aircraft flexure physics.

APPENDIX A

DETERMINISTIC FORMULATION OF THE PLACEMENT PROBLEM

The state and state estimate differential equations are:

$$\dot{\underline{x}} = \underline{F}\,\underline{x} + \underline{G}\,\underline{K}\hat{\underline{x}} + \underline{C}\underline{\eta}$$

$$\dot{\hat{\underline{x}}} = (\underline{F} + \underline{G}\,\underline{K})\hat{\underline{x}} + \underline{L}(\underline{m} - \underline{A}\hat{\underline{x}})$$

$$= (\underline{F} + \underline{G}\,\underline{K} - \underline{A})\hat{\underline{x}} + \underline{L}\,\underline{A}\,\underline{x} + \underline{L}\,\underline{B}\,\underline{\eta}$$

Defining $\underline{z} = [\underline{x}\ ,\ \hat{\underline{x}}]'$, write

$$\underline{\dot{z}} = \begin{bmatrix} \underline{F} & \underline{G}\,\underline{K} \\ \underline{L}\,\underline{H} & \underline{F}+\underline{G}\,\underline{K}-\underline{A} \end{bmatrix} \underline{z} + \begin{bmatrix} \underline{C} \\ \underline{L}\,\underline{B} \end{bmatrix} \underline{\eta} \doteq \underline{F}_2\underline{z} + \underline{C}_2\underline{\eta}$$

The associated covariance differential equation is:

$$\dot{\underline{Z}} = \underline{F}_2\underline{Z} + \underline{Z}\,\underline{F}_2' + \underline{C}_2\underline{N}\,\underline{C}_2' \ , \text{ where}$$

$$\underline{Z} = E\{\underline{z}\,\underline{z}'\} = \begin{bmatrix} E\{\underline{x}\underline{x}'\} & E\{\underline{x}\hat{\underline{x}}'\} \\ E\{\hat{\underline{x}}\underline{x}'\} & E\{\hat{\underline{x}}\hat{\underline{x}}'\} \end{bmatrix} = \begin{bmatrix} \underline{X} & \hat{\underline{X}} \\ \hat{\underline{X}} & \hat{\underline{X}} \end{bmatrix}$$

using the orthogonal projection lemma of Kalman. Extracting the $\dot{\underline{X}}$ equation,

$$\dot{\underline{X}} = \underline{F}\,\underline{X} + \underline{G}\underline{K}\hat{\underline{X}} + \underline{X}\,\underline{F}' + \hat{\underline{X}}(\underline{G}\underline{K})' + \underline{C}\,\underline{N}\underline{C}' \qquad (1)$$

$$= (\underline{F} + \underline{G}\underline{K})\underline{X} + \underline{X}(\underline{F} + \underline{G}\underline{K})' + \underline{C}\underline{N}\underline{C}' - \underline{G}\underline{K}\tilde{\underline{X}} - \tilde{\underline{X}}\,\underline{K}'\underline{G}' \qquad (2)$$

$$= (\underline{F} + \underline{G}\underline{K})\hat{\underline{X}} + \hat{\underline{X}}(\underline{F} + \underline{G}\underline{K})' + \underline{F}\tilde{\underline{X}} + \tilde{\underline{X}}\underline{F}' + \underline{C}\underline{N}\underline{C}' \qquad (3)$$

since $\underline{X} = E\{\underline{x}\underline{x}'\} = E\{(\hat{\underline{x}} + \tilde{\underline{x}})(\hat{\underline{x}}' + \tilde{\underline{x}}')\} = E\{\hat{\underline{x}}\,\hat{\underline{x}}'\} + E\{\tilde{\underline{x}}\,\tilde{\underline{x}}'\} = \hat{\underline{X}} + \tilde{\underline{X}}$

Similarly, $\dot{\underline{X}} = \dot{\tilde{\underline{X}}} + \dot{\hat{\underline{X}}}$, so

$$\dot{\hat{\underline{X}}} = (\underline{F} + \underline{G}\underline{K})\hat{\underline{X}} + \hat{\underline{X}}(\underline{F} + \underline{G}\underline{K})' + \underline{C}\underline{N}\underline{B}'(\underline{B}\underline{N}\underline{B}')^{-1}\underline{A}\tilde{\underline{X}} \qquad (4)$$

$$+ \tilde{\underline{X}}(\underline{C}\underline{N}\underline{B}'(\underline{B}\underline{N}\underline{B}')^{-1}\underline{A})' + \tilde{\underline{X}}\,\underline{A}'(\underline{B}\underline{N}\underline{B}')^{-1}\underline{A}\tilde{\underline{X}} + \underline{C}\underline{N}\underline{B}'(\underline{B}\underline{N}\underline{B}')^{-1}\underline{B}\underline{N}\underline{C}'$$

Of these four formulations of the problem, expression 3 is most convenient. The last three terms of this equation have no $\underline{y}$-dependence and thus disappear in the variational equations. Similarly, the criterion function may be separated so that $J(\underline{X}) = J_1(\hat{\underline{X}}, y) + J_2(\tilde{\underline{X}})$ Thus J_2 also disappears from the variational equations.

APPENDIX B

DERIVATION OF THE OPTIMAL CONTROL (FIXED LOCATIONS) VIA THE MATRIX MINIMUM PRINCIPLE

Form the Hamiltonian for the problem using the LaGrange multiplier, $\underline{S}$

$$J = TR[\underline{Q}\underline{R} + \underline{S}\dot{\underline{X}}]$$

$$= TR\{\underline{Q}[\underline{H} + \underline{D}\underline{K})\hat{\underline{X}}(\underline{H} + \underline{D}\underline{K})' + \underline{H}\tilde{\underline{X}}\underline{H}']$$

$$+\underline{S}[(\underline{F} + \underline{G}\underline{K})\hat{\underline{X}} + \hat{\underline{X}}(\underline{F} + \underline{G}\underline{K})' + \underline{F}\tilde{\underline{X}} + \tilde{\underline{X}}\underline{F}' + \underline{C}\underline{N}\underline{C}']\}$$

Taking $\underline{y}$ as fixed, choose $\underline{K}$, $\underline{S}$ and $\hat{\underline{X}}$ to minimize J:

$$\partial J/\partial \underline{X} = (\underline{H} + \underline{D}\hat{\underline{K}})'\underline{Q}(\underline{H} + \underline{D}\hat{\underline{K}}) + (\underline{F} + \underline{G}\hat{\underline{K}})'\underline{S} + \underline{S}(\underline{F} + \underline{G}\hat{\underline{K}}) = \underline{0} \qquad (1)$$

$$\partial J/\partial \underline{K} = 2\underline{D}'\underline{Q}(\underline{H} + \underline{D}\hat{\underline{K}})\hat{\underline{X}} + 2\underline{G}'\underline{S}\hat{\underline{X}} = \underline{0}\ ;\ \hat{\underline{K}} = -(\underline{D}'\underline{Q}\underline{D})^{-1}(\underline{D}'\underline{Q}\underline{H} + \underline{G}'\underline{S}) \qquad (2)$$

$$\partial J/\partial \underline{S} = \dot{\underline{X}} = (\underline{F} + \underline{G}\hat{\underline{K}})\hat{\underline{X}} + \hat{\underline{X}}(\underline{F} + \underline{G}\hat{\underline{K}})' + \underline{F}\tilde{\underline{X}} + \tilde{\underline{X}}\underline{F}' + \underline{C}\underline{N}\underline{C}' = \underline{0} \qquad (3)$$

Inserting $\hat{\underline{K}}$ from (2) into (1)

$$(\underline{F} - \underline{G}(\underline{D}'\underline{Q}\underline{D})^{-1}\underline{D}'\underline{Q}\underline{H})'\underline{S} + \underline{S}(\underline{F} - \underline{G}(\underline{D}'\underline{Q}\underline{D})^{-1}\underline{D}'\underline{Q}\underline{H}) - \underline{S}\underline{G}(\underline{D}'\underline{Q}\underline{D})^{-1}\underline{G}'\underline{S}$$

$$+ \underline{H}'(\underline{Q} - \underline{Q}\underline{D}(\underline{D}'\underline{Q}\underline{D})^{-1}\underline{D}'\underline{Q})\underline{H} = \underline{0}$$

With $\underline{y}$ given, this equation may be solved for $\underline{S}$. Then $\hat{\underline{K}}$ is formed using (2) and $\hat{\underline{X}}$ is found from (3).

APPENDIX C

VARIATIONS OF THE CRITERION FUNCTIONAL

Consider a small change in $\underline{y}$ -- call it $\Delta\underline{y}$. Demand that Eqs. 1-3 of Appendix B be satisfied at all $\underline{y}$, i.e., at $\underline{y}$ and $\underline{y}+\Delta\underline{y}$. This means that the first and second order variations of the above equations must be zero for all $\Delta\underline{y}$, yielding variational equations in $\underline{S}$, $\underline{K}$, and $\hat{\underline{X}}$.

First variations of Eqs. 1 and 2, Appendix B:

$$(\underline{F}+\underline{G}\underline{K})'\underline{S}_{1i}+\underline{S}_{1i}(\underline{F}+\underline{G}\underline{K})+\underline{F}_{1i}'\underline{S}+\underline{S}\underline{F}_{1i}+(\underline{H}_{1i}+\underline{D}_{1i}\underline{K})'\underline{Q}(\underline{H}+\underline{D}\underline{K}) \tag{1}$$

$$+(\underline{H}+\underline{D}\underline{K})'\underline{Q}(\underline{H}_{1i}+\underline{D}_{1i}\underline{K})=\underline{0}$$

$$\underline{D}'\underline{Q}\underline{D}\underline{K}_{1i}+\underline{D}_{1i}'\underline{Q}(\underline{H}+\underline{D}\underline{K})+\underline{D}'\underline{Q}(\underline{H}_{1i}+\underline{D}_{1i}\underline{K})+\underline{G}'\underline{S}_{1i}=\underline{0} \tag{2}$$

Equation 2, Appendix C has been used to eliminate $\underline{X}_{1i}$ and $\underline{K}_{1i}$ terms which are not shown above.

The second variation of Eq. 1, Appendix B is:

$$(\underline{F}+\underline{G}\underline{K})'\underline{S}_{2ij}+\underline{S}_{2ij}(\underline{F}+\underline{G}\underline{K})+(\underline{F}_{1i}+\underline{G}\underline{K}_{1i})'\underline{S}_{1j}+\underline{S}_{1j}(\underline{F}_{1i}+\underline{G}\underline{K}_{1i})$$

$$+(\underline{F}_{1j}+\underline{G}\underline{K}_{1j})'\underline{S}_{1i}+\underline{S}_{1i}(\underline{F}_{1j}+\underline{G}\underline{K}_{1j})+(\underline{H}_{1i}+\underline{D}_{1i}\underline{K}+\underline{D}\underline{K}_{1i})'\underline{Q}(\underline{H}_{1j}+\underline{D}_{1j}\underline{K}+\underline{D}\underline{K}_{1j})$$

$$+(\underline{H}_{1j}+\underline{D}_{1j}\underline{K}+\underline{D}\underline{K}_{1j})'\underline{Q}(\underline{H}_{1i}+\underline{D}_{1i}\underline{K}+\underline{D}\underline{K}_{1i})+(\underline{F}_{2ij}+\underline{G}\underline{K}_{2ij})'\underline{S}$$

$$+(\underline{H}_{2ij}+\underline{D}_{2ij}\underline{K}+\underline{D}\underline{K}_{2ij}+\underline{D}_{1i}\underline{K}_{1j}+\underline{D}_{1j}\underline{K}_{1i})'\underline{Q}(\underline{H}+\underline{D}\underline{K})+\underline{S}(\underline{F}_{2ij}+\underline{G}\underline{K}_{2ij})$$

$$+(\underline{H}+\underline{D}\underline{K})'\underline{Q}(\underline{H}_{2ij}+\underline{D}_{2ij}\underline{K}+\underline{D}\underline{K}_{2ij}+\underline{D}_{1i}\underline{K}_{1j}+\underline{D}_{1j}\underline{K}_{1i})=\underline{0} \tag{3}$$

Using the preceding equations, this can be manipulated into the following form:

$$(\underline{F}+\underline{G}\underline{K})'\underline{S}_{2ij}+\underline{S}_{2ij}(\underline{F}+\underline{G}\underline{K})+\underline{F}'_{2ij}\underline{S}+\underline{S}\underline{F}_{2ij}+\underline{F}'_{1i}\underline{S}_{1j}+\underline{S}_{1j}\underline{F}_{1i}+\underline{F}'_{1j}\underline{S}_{1i}+\underline{S}_{1i}\underline{F}_{1j}$$

$$+(\underline{H}_{2ij}+\underline{D}_{2ij}\underline{K})'\underline{Q}(\underline{H}+\underline{D}\underline{K})+(\underline{H}+\underline{D}\underline{K})'\underline{Q}(\underline{H}_{2ij}+\underline{D}_{2ij}\underline{K})$$

$$+(\underline{H}_{1i}+\underline{D}_{1i}\underline{K})'\underline{Q}(\underline{H}_{1j}+\underline{D}_{1j}\underline{K})+(\underline{H}_{1j}+\underline{D}_{1j}\underline{K})'\underline{Q}(\underline{H}_{1i}+\underline{D}_{1i}\underline{K})$$

$$-\underline{K}'_{1i}\underline{D}'\underline{Q}\underline{D}\underline{K}_{1j}-\underline{K}'_{1j}\underline{D}'\underline{Q}\underline{D}\underline{K}_{1i}=\underline{0} \qquad (4)$$

In the general case, one takes two variations of Eqs. 1, 2, and 3 from Appendix B, yielding six equations in $\underline{S}$, $\underline{K}$, $\hat{\underline{X}}$, $\underline{S}_{1i}$, $\underline{K}_{1i}$, $\hat{\underline{X}}_{1i}$, $\underline{S}_{2ij}$, $\underline{K}_{2ij}$ and $\hat{\underline{X}}_{2ij}$. This is a total of $3(1+n_y+n_y^2)$ equations which may be solved for all of the variables above. Closer investigation reveals that the solution procedure for the variational sets of equations is the same as for the $\underline{S}$, $\underline{K}$, and $\hat{\underline{X}}$ equations, except that the $\underline{S}$ variational equations are of state covariance rather than Riccati form. The $n_y^2+2n_y+3$ equations given above (Appendix B and (1), (2) and (4)), however, are all that are needed in the remaining derivations.

APPENDIX D

CONDENSATION OF THE SECOND VARIATION EQUATIONS

In order to carry out the Newton-Raphson search it is necessary to compute the first and second variations of the criterion; this appendix contains a series of manipulations which reduces the number of equations needed to compute these variations from a potential $3(1 + n_y + n_y^2)$ to $3 + 2n_y$, minimizing computational effort.

Using Eq. 1 of Appendix B, rewrite Eq. 15 of Section II as follows:

$$J(\underline{y}) = TR[\underline{S}(\underline{F}\,\underline{\tilde{X}} + \underline{\tilde{X}}\,\underline{F}' + \underline{C}\underline{N}\underline{C}') + \underline{H}'\underline{Q}\underline{H}\underline{\tilde{X}}] \tag{1}$$

Because of the form of $\underline{\tilde{X}}$ (Section II, Eq. 13), $\underline{S}$ is the only term of the criterion having a $\underline{y}$ dependence. Hence the first variations of $J(\underline{y})$ are:

$$J_{1i} = TR[\underline{S}_{1i}(\underline{F}\,\underline{\tilde{X}} + \underline{\tilde{X}}\,\underline{F}' + \underline{C}\underline{N}\underline{C}')] = -2TR[\underline{S}_{1i}(\underline{F}+\underline{G}\underline{K})\underline{\hat{X}}] \tag{2}$$

by Eq. 1, Appendix B. Similarly, the second variations may be written

$$J_{2ij} = -2TR[\underline{S}_{2ij}(\underline{F}+\underline{G}\underline{K})\underline{\hat{X}}] = TR[(-\underline{S}_{2ij}(\underline{F}+\underline{G}\underline{K}) - (\underline{F}+\underline{G}\underline{K})'\underline{S}_{2ij})\underline{\hat{X}}] \tag{3}$$

But by Eq. 4 of Appendix C, these are

$$J_{2ij} = 2TR\{[(\underline{S}\underline{F}_{2ij} + \underline{S}_{ij}\underline{F}_{1i} + \underline{S}_{1i}\underline{F}_{ij} + (\underline{H}+\underline{D}\underline{K})'\underline{Q}(\underline{H}_{2ij} + \underline{D}_{2ij}\underline{K})$$

$$+ (\underline{H}_{1j} + \underline{D}_{1j}\underline{K})'\underline{Q}(\underline{H}_{1i}+\underline{D}_{1i}\underline{K}) - \underline{K}'_{1j}\underline{D}'\underline{Q}\underline{D}\underline{K}_{1i})]\underline{\hat{X}}\} \tag{4}$$

Thus computation of the variations requires solution of the $\underline{S}$, $\underline{K}$, $\underline{\hat{X}}$, $\underline{S}_{1i}$ and $\underline{K}_{1i}$ equations, or one Riccati equation, n_y+1 state covariance

equations and n_y+1 direct evaluations. (Note: $\underline{K}_{1i}$ and $\underline{K}_{ij}$ may be eliminated from the J_{2ij} equations, but no essential simplification results.)

APPENDIX E

EQUATIONS OF RIGID BODY MOTION AS LINEARIZED EULER'S EQUATIONS

The following derivation is a synthesis of Landau and Lifshitz' treatment of "Motion of a Rigid Body," and Etkin's "General Equations of Unsteady Motion,"(Refs. 1 and 2). Mechanics provides the basis for the notational conventions (with 1,2,3 corresponding to Cartesian coordinates x, y, z and angular momenta being referred to the axes about which rotation occurs), while Dynamics of Flight is used to phrase the problem in aerodynamicists' terminology. The derivation attempts to provide motivation for the linearized equations of motion on the basis of first principles well-known in classical physics and to put the flexure problem in proper perspective to the over-all control problem. Since this appendix is intended only as a link between physics and aerodynamics for the control engineer, details in the derivation of aerodynamic and propulsion force terms are not given.

It is well known that the motion of a rigid body can be described by (1) the motion of its center of gravity with respect to a fixed coordinate system (e.g., fixed to the earth or fixed with respect to a mean wind), and (2) the change in orientation of the body with respect to its center of mass. Newton's second law governs the three translational and three rotational degrees of freedom:

Ref. 1. Etkin, Bernard, Dynamics of Flight, John Wiley and Sons., Inc., New York, N. Y., 1959, Ch. 4.

Ref. 2. Landau, L. D., and Lifshitz, E. M., Mechanics, Addison-Wesley Publishing Co., Inc., Reading, Mass., 1960, Pergamon Press, Ch. VI.

$$d'\underline{P}/dt' = \underline{F} \qquad (1)$$

$$d'\underline{M}/dt' = \underline{K} \qquad (2)$$

$\underline{P}$ = linear momentum of the aircraft (time derivative with respect to fixed axis system)

= $m\underline{V}$, where m is the mass of the body and $\underline{V}$ is the velocity of the center of mass

$\underline{F}$ = sum of forces on the body

$\underline{M}$ = angular momentum of the body (time derivative with respect to fixed axis system)

= $\overline{\overline{I}} \cdot \underline{\Omega}$, where $\overline{\overline{I}}$ is the inertia tensor and $\underline{\Omega}$ is the angular velocity of the body about its center of mass. (Note: $\overline{\overline{I}}$ becomes diagonal when the principal axes of the body are used).

$\underline{K}$ = sum of torques on the body

Because $\underline{M}$ bears a simple relation to the angular momentum with respect to the center of mass of the body, it is desirable to express the time derivatives above with respect to the body co-ordinates rather than the fixed co-ordinates; letting (d/dt) denote differentiation with respect to the body co-ordinates, one writes for any vector $\underline{A}$, $d'\underline{A}/dt' = d\underline{A}/dt + \underline{\Omega} \times \underline{A}$ (Note: this convention does not follow Mechanics). Thus (1) and (2) become:

$$d\underline{P}/dt + \underline{\Omega} \times \underline{P} = \underline{F} \qquad (3)$$

$$d\underline{M}/dt + \underline{\Omega} \times \underline{M} = \underline{K} \qquad (4)$$

If the body axes are chosen as principal axes, these six equations may be written out in component form as follows:

$$dV_1/dt + \Omega_2 V_3 - \Omega_3 V_2 = F_1/m \qquad (5)$$

$$dV_2/dt + \Omega_3 V_1 - \Omega_1 V_3 = F_2/m \tag{6}$$

$$dV_3/dt + \Omega_1 V_2 - \Omega_2 V_1 = F_3/m \tag{7}$$

$$I_1 d\Omega_1/dt + (I_3 - I_2)\Omega_2\Omega_3 = K_1 \tag{8}$$

$$I_2 d\Omega_2/dt + (I_1 - I_3)\Omega_3\Omega_1 = K_2 \tag{9}$$

$$I_3 d\Omega_3/dt + (I_2 - I_1)\Omega_1\Omega_2 = K_3 \tag{10}$$

These are Euler's equations. (Note $I_j \doteq (\bar{\bar{I}})_{jj}$)

The next problem is to choose a convention for expressing the rotation of the body co-ordinate system (x, y, z) with respect to the fixed co-ordinate system (X, Y, Z) and to express the components of the angular velocity of the body $(\Omega_1, \Omega_2, \Omega_3)$ in terms of the change in rotational position. Euler's angles define the convention to be used.

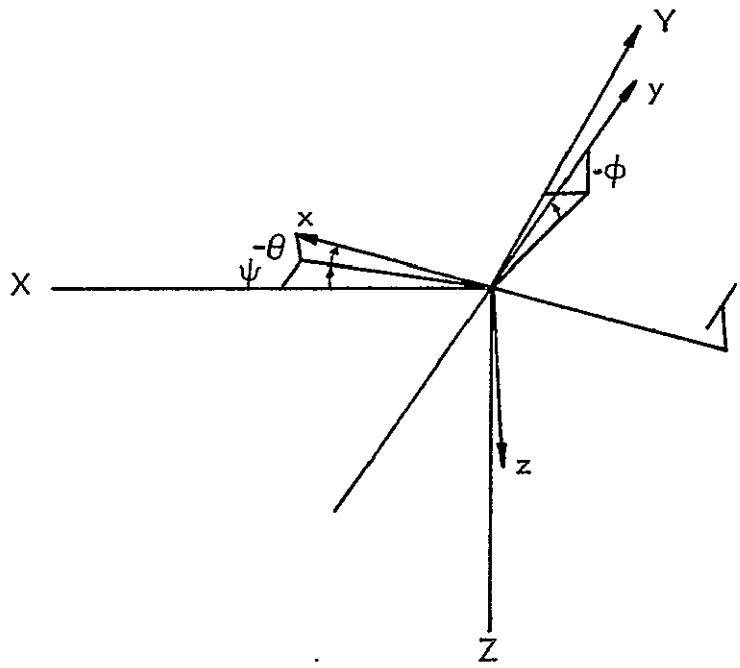

Fig. 1 Euler Angles

To rotate the xyz axes from a position of alignment with the XYZ system to a position of alignment with the principal vehicle axes, one carries out three rotations, in the following order:

(1) A rotation ψ about the Z axis

(2) A rotation θ about the position of the y axis resulting from rotation (1), and then

(3) A rotation ϕ about the position of the x axis resulting from rotation (2).

For clarity of presentation, the final position of the aircraft above was chosen in such a way that θ and ϕ as shown happen to be negative. Aerodynamicists usually define the z axis "down"; note that the signs of the angles follow the right-hand rule.

By considering the directions of $\dot{\psi}$, $\dot{\theta}$, and $\dot{\phi}$ relative to the final position of the xyz system along the principal axes of the vehicle, one obtains the following expression for the components of Ω:

$$\Omega_1 = \dot{\phi} - \dot{\psi} \sin \theta$$

$$\Omega_2 = \dot{\theta} \cos \phi + \dot{\psi} \cos \theta \sin \phi$$

$$\Omega_3 = \dot{\psi} \cos \theta \cos \phi - \dot{\theta} \sin \phi$$

If the principal axes were to be used in a linearized analysis, one would simply proceed to linearize Euler's equations as given above; this is sometimes done. More often, however, one uses a set of "stability axes." First, a condition of steady forward flight is specified about which to linearize; the flight condition cannot be chosen arbitrarily, but corresponds to a detailed balance of the aerodynamic and thrusting forces on the vehicle for a given "mean wind." In order to achieve a constant altitude at a specified speed, the nose of the aircraft must be tilted slightly upward (or downward) by an angle, say α_o (Etkin uses ϵ). Hence, in a given flight condition the velocity

vector of the center of mass and the principal axes don't coincide; one is thus motivated to use a set of "stability axes" aligned with the forward velocity vector of the aircraft, rather than the principal axes.

In the following derivations the most commonly encountered flight condition is used as an example, viz., steady forward speed, V_1, constant altitude and small α_o, with no mean wind. With stability axes, the inertia tensor has nonzero components:

$$I_{11} = I_1 \cos^2 \alpha_o + I_3 \sin^2 \alpha_o \simeq I_1$$

$$I_{22} = I_2$$

$$I_{33} = I_1 \sin^2 \alpha_o + I_3 \cos^2 \alpha_o \simeq I_3$$

and $$I_{13} = I_{31} = -\frac{1}{2}(I_1 - I_3) \sin 2\alpha_o \simeq \alpha_o (I_3 - I_1)$$

where single subscripts refer to the principal moments of inertia. The reference values of V_2, V_3, ψ, θ, and ϕ are zero.

Carrying out the linearization of Eqs. 5-10 (as modified by the presence of I_{13}), using small letters for the perturbed values, one obtains:

$$dv_1/dt = f_1/m \tag{11}$$

$$dv_2/dt + V_1 \dot{\psi} = f_2/m \tag{12}$$

$$dv_3/dt - V_1 \dot{\theta} = f_3/m \tag{13}$$

$$I_1 \ddot{\phi} + \alpha_o (I_2 - I_1) \ddot{\psi} = k_1 \tag{14}$$

$$I_2 \ddot{\theta} = k_2 \tag{15}$$

$$\alpha_o (I_3 - I_1) \ddot{\phi} + I_3 \ddot{\psi} = k_3 \tag{16}$$

The basic equations of motion for a general linearized rigid body problem are thus six in number: horizontal, lateral, and vertical

acceleration equations; and roll (ϕ), pitch(θ), and yaw (ψ) acceleration equations. The role of the aerodynamicist in such linearized control problems is to specify the linearized forces, f_i, and torques, k_i, $i=1,2,3$ which excite the vehicle. The forces fall into several categories:

(1) aerodynamic forces

(2) gravitational forces

(3) thrust and propulsion forces

(4) gust forces

(5) control forces

Gravitational forces (usually negligable in the incremental model) and aerodynamic forces are usually specified in terms of forward velocity, v_1, angle of attack ($\alpha=(v_3-V_1\theta)/V_1$) and sideslip angle ($\beta=(v_2+V_1\psi)/V_1$), and the roll, pitch and yaw angles and their derivatives. Thrust and propulsion forces are usually related to throttle position. Gust forces depend on side, head-on and vertical gust strengths, which are usually stochastic inputs. Control forces are generated as functions of the aerodynamic surface deflections.

Generally, the control engineer is given the coefficients of the linearized equations of motion and hence need not be concerned with the detailed physics of their derivation; the control surface location problem, however, poses an exception to this rule. It is necessary here to estimate all types of forces which depend on control surface location. For the rigid body equations, the only effect of surface location is to change the torque arms of the control force contributions to k_1, k_2 and k_3. The other effects of surface placement arise from the flexible nature of the aircraft.

The relation of the rigid body equations of motion to the flexure equations is not as clear-cut in practice as it is in theory. Certainly the deflection of a mode gives rise to aerodynamic force and torque terms in Eqs. 11-16. The issue is whether, when and how to include inertial coupling between rigid body motions and motions of the flexible vehicle. Most theoretical treatments claim there is no inertial coupling of rigid body and flexure motions; this is because the normal modes are defined as the responses with distributed force and moment terms of the flexure equations set to zero. Such modes, however, are non-physical. Because mode excitation must give rise to aerodynamic forces, which in turn feed back to excite the modes, it is unreasonable to set such terms to zero; rather, only applied forces (such as those arising from control surface deflections) must be set to zero. This procedure yields the true mode shapes for a given flight condition, but there is still the problem of normalization of the mode shapes. Fortunately, Stilley and Pollack (Ref. 17) have shown that (at least for vertical deflection modes) it is always possible to define mode shapes in such a way that inertial coupling to rigid body motion can be eliminated. Because normalization conventions vary widely, it is necessary to decide for each application whether or not the rigid body equations of motion do or do not contain acceleration due to flexure modes. The computer programs assume that flexure accelerations are included by definition in the model variables $\dot{v}_3$, $\ddot{\phi}$ and $\ddot{\theta}$.

Comment: The equations of motion used in the C-5A model correspond to Eqs. 13 and 15. Since vertical gusts are the only inputs to the system and since the angle of attack is defined as above, these two equations decouple from the others, allowing one to treat the longitudinal axis separately. Decoupling of longitudinal and lateral equations

of motion is a general property of the equations of motion for the standard flight condition described above. For the C-5A equations, the $\ddot{z}$ equation of the original data was purged of flexure contributions, but $\ddot{\theta}$ was not.

APPENDIX F

ORTHOGONALIZATION OF FLEXURE MODES

Mode Acceleration Equations:

$$m\sum_{i=1}^{\infty}(\xi_i - s\phi_i)\ddot{\eta}_i + \sum_{i=1}^{\infty}(EI\xi_i'')''\eta_i = F_z(y,t) \tag{1}$$

$$\sum_{i=1}^{\infty}(I\phi_i - ms\xi_i)\ddot{\eta}_i + \sum_{i=1}^{\infty}(GJ\phi_i')'\eta_i = \tau(y,t) \tag{2}$$

The Normal Modes ξ_i, ϕ_i satisfy the equations:

$$m(\xi_i - s\phi_i)\omega_i^2 + (EI\xi_i'')'' = 0 \qquad (' = d/d_y) \tag{3}$$

$$(I\phi_i - ms\xi_i)\omega_i^2 + (GJ\phi_i')' = 0 \tag{4}$$

or

$$\omega_i^2 I\phi_i = \omega_i^2 ms\xi_i - (GJ\phi_i')' \tag{5}$$

$$\omega_i^2 m\xi_i = \omega_i^2 ms\phi_i - (EI\xi_i'')'' \tag{6}$$

So $$\omega_i^2\int_0^{y_{end}} I(\phi_i\phi_j)dy = \omega_i^2\int_0^{y_{end}} ms\,\xi_i\phi_j dy - \int_0^{y_{end}} (GJ\phi_i')\phi_j' dy$$

$$\omega_j^2\int_0^{y_{end}} I(\phi_i\phi_j)dy = \omega_j^2\int_0^{y_{end}} ms\xi_j\phi_i dy - \int_0^{y_{end}} (GJ\phi_j')'\phi_i dy$$

$$\therefore\ (\omega_i^2 - \omega_j^2)\int_0^{y_{end}} I(\phi_i\phi_j)dy = \int_0^{y_{end}} (\omega_i^2\xi_i\phi_j - \omega_j^2\xi_j\phi_i)ms\,dy$$

$$- \int_0^{y_{end}} [(GJ\phi_i')'\phi_j - (GJ\phi_j')'\phi_i]\ dy$$

But as a boundary condition

$$\left.\begin{aligned} GJ\phi_j'(y_{end}) &= 0 \quad \text{(free end at } y_{end}\text{)} \\ \phi_j(0) &= 0 \quad \text{(fixed end at } y=0\text{)} \end{aligned}\right\} \quad \text{for all } j$$

On integration by parts, the last term is:

$$[(GJ\phi_i')\phi_j - (GJ\phi_j')\phi_i]_0^{y_{end}} = 0$$

$$\therefore (\omega_i^2-\omega_j^2)\int_0^{y_{end}} I(\phi_i\phi_j)dy = \int_0^{y_{end}} (\omega_i^2\xi_i\phi_j - \omega_j^2\xi_j\phi_i)ms\ dy \qquad (7)$$

By precisely analogous manipulations on the Eq. 3, one establishes that:

$$(\omega_i^2 - \omega_j^2)\int_0^{y_{end}} m\xi_i\xi_j\,dy = \int_0^{\ell} (\omega_i^2\phi_i\xi_j - \omega_j^2\xi_j\phi_i)ms\ dy \qquad (8)$$

Adding, one obtains:

$$M_{ij} = \int_0^{y_{end}} [m\xi_i\xi_j - ms(\phi_i\xi_j + \phi_j\xi_i) + I\phi_i\phi_j]\,dy = 0 \qquad i \neq j$$

This is the orthogonality condition in the case of structurally coupled bending and torsional modes.

When $i=j$

$$M_{jj} \doteq M_j = \int_0^{y_{end}} [m\xi_j^2 - 2ms\phi_j\xi_j + I\phi_j^2]\,dy \neq 0$$

Since $I = I_{CG} + ms^2$

$$M_j = \int_0^{y_{end}} m[\xi_j - s\phi_j]^2 dy + \int_0^{y_{end}} I_{CG}\phi_j^2\,dy$$

Now, multiplying (1) by ξ_j and (2) by ϕ_j, integrating over the length and adding, one finds:

$$\sum_i \ddot{\eta}_i \int_0^{y_{end}} [m\xi_i\xi_j - ms(\phi_i\xi_j + \phi_j\xi_i) + I\phi_i\phi_j]\,dy$$

$$+\eta_i \int_0^{y_{end}} [(EI\xi_i'')''\xi_j + (GJ\phi_i')'\phi_j]\,dy = \int_0^{y_{end}} (F_z(y,t)\xi_j + \tau(y,t)\phi_j)\,dy$$

Referring to Eqs. 5 and 6, there results

$$\sum_i M_{ij}(\ddot{\eta}_i + \omega_i^2\eta_i) = \int_0^{y_{end}} (F_z(y,t)\xi_j + \tau(y,t)\phi_j)\,dy$$

Or since $M_{ij} = M_j\delta_{ij}$

$$M_j\ddot{\eta}_j(t) + M_j\omega_j^2\eta_j(t) = \int_0^{y_{end}} (F_z(y,t)\xi_j(y) + \tau(y,t)\phi_j(y)\,dy$$

as claimed in the text.

APPENDIX G

DESCRIPTIONS OF THE MAJOR SUBPROGRAMS

G.1 SUBROUTINE POTTER

This subroutine solves the steady-state Riccati equation using an algebraic algorithm discovered by J. E. Potter. In order to solve the equation $\underline{F}_1\underline{X} + \underline{X}\,\underline{F}_1' - \underline{X}\underline{Q}_1\underline{X} + \underline{Q}_2 = \underline{0}$ one first forms Potter's matrix $\underline{ZP}$, where

$$\underline{ZP} = \begin{bmatrix} \underline{F}_1 & \underline{Q}_2 \\ \underline{Q}_1 & -\underline{F}_1' \end{bmatrix}$$

If the equation is of n^{th} order, $\underline{ZP}$ is a $2n \times 2n$ matrix. Next the eigenvalues and the eigenvectors corresponding to eigenvalues with positive real parts are found; the roots of $\underline{ZP}$ can be shown to be the poles of the closed loop control system and their negatives, so there will be exactly n roots with positive real parts, assuming no zero roots. The n eigenvectors corresponding to these roots (real and imaginary parts of eigenvectors for complex roots) are then arranged column-wise and the resulting $n \times 2n$ matrix is partitioned, so that:

$\begin{bmatrix} \underline{F}_1 & \underline{Q}_2 \\ \underline{Q}_1 & -\underline{F}_1' \end{bmatrix} \begin{bmatrix} \underline{Y}_1 \\ \underline{Y}_2 \end{bmatrix} = \begin{bmatrix} \underline{Y}_1 \\ \underline{Y}_2 \end{bmatrix} \underline{\Lambda}$, where $\underline{\Lambda}$ is the Jordan real form for for the eigenvalues of $\underline{ZP}$ with positive real parts.

Then the solution may be written $\underline{X} = \underline{Y}_1\underline{Y}_2^{-1}$. Proof:

$$\underline{F}_1\underline{Y}_1 + \underline{Q}_2\underline{Y}_2 = \underline{Y}_1\underline{\Lambda} \qquad (1)$$

$$\underline{Q}_1\underline{Y}_1 - \underline{F}_1'\underline{Y}_2 = \underline{Y}_2\underline{\Lambda} \qquad (2)$$

Right-multiply (1) by $\underline{Y}_2^{-1}$; left-multiply (2) by $\underline{Y}_1\underline{Y}_2^{-1}$ and right-multiply by $\underline{Y}_2^{-1}$, gives:

$$\underline{F}_1(\underline{Y}_1\underline{Y}_2^{-1}) + \underline{Q}_2 = \underline{Y}_1\underline{\Lambda}\underline{Y}_2^{-1} \tag{3}$$

$$(\underline{Y}_1\underline{Y}_2^{-1})\underline{Q}_1(\underline{Y}_1\underline{Y}_2^{-1}) - (\underline{Y}_1\underline{Y}_2^{-1})\underline{F}_1' = \underline{Y}_1\underline{\Lambda}\underline{Y}_2^{-1} \tag{4}$$

Subtracting (4) from (3) and letting $\underline{X} = \underline{Y}_1\underline{Y}_2^{-1}$,

$$\underline{F}_1\underline{X} + \underline{X}\underline{F}_1' - \underline{X}\underline{Q}_1\underline{X} + \underline{Q}_2 = \underline{0}, \text{ as desired.}$$

Potter has shown that $\underline{X}$ will be the positive definite solution of the problem, providing $\underline{Q}_2$ is positive definite.

The program forms $\underline{Z}\underline{P}$ and then uses an eigenvalue-eigenvector routine, ALLMAT,* which utilizes the double QR iteration of Francis[4] to find $\underline{Y}_1$ and $\underline{Y}_2$. $\underline{X}$ is found directly by solving the system $\underline{Y}_2'\underline{X} = \underline{Y}_1$ using the Gauss-Jordan method.

The primary appeals of Potter's method as compared to iterative schemes are (1) speed and (2) accuracy. The savings in speed goes roughly as the system order (e.g., a 10 to 1 saving for a tenth order system), and the accuracy appears to be considerably better due to far more moderate error propagation. Note also that no free parameters (such as step size) are involved. To the author's knowledge this method is the most efficient technique available for solution of the steady-state Riccati equation; the computer program is available on request.

G.2 SUBROUTINE STCOV

This subroutine solves the state covariance equation $\underline{A}\underline{X} + \underline{X}\underline{A}' + \underline{S} = \underline{0}$ for $\underline{X}$, where $\underline{A}$, $\underline{X}$, and $\underline{S}$ are N x N and $\underline{S}$ and $\underline{X}$ are symmetric.

* Courtesy of Union Carbide Corp. (Nuclear Division), Oak Ridge, Tenn. (Authors: John Rinzel and R. E. Funderlic).

The condition for convergence of the iterative algorithm (i.e., for existence of a steady-state solution to the associated differential equation) is that the eigenvalues of $\underline{A}$ have negative real parts; the program assumes this to be true. Certain convergence checks are provided, however. First, one may specify the maximum number of iterations via the parameter ITMAX appearing in the subroutine CALL (if the first time increment is $\sim 1/30$ of the system settling time, ITMAX - 15 has been found sufficient for good convergence). Secondly, one may demand that the fractional change of all diagonal elements of $\underline{X}$ at the final iteration be below the constant CTMAX appearing (currently as .001) in the program listing. The vector TRX is used to store the values of diagonal elements from the previous iteration and may be printed out as an exact check on convergence if desired. The remaining parameter, FR, is set to be the fraction of system settling time taken for the first iteration; settling time is approximated as TSET = $1/\text{MAX}(A_i)$. Stein* has shown that the error in the initial iteration is always propagated as a constant in the answer and will never lead to a "fictitious" instability in the algorithm itself. The input matrices $\underline{A}$ and $\underline{S}$ are not preserved. Computation time is well under a second for a tenth order example (using the IBM 360-40 computer).

---

*Honeywell Interoffice Correspondence (MR10033), G. Stein to V. Levapi, "A Note on High-Speed Computation of Steady State Solutions to Linear Differential Equations," Systems and Research Center, July 14, 1967.

The method is an iterative algorithm for integrating the differential equation associated with the system above; the computational speed of the algorithm is due to the fact that step size is doubled with each iteration. The initialization and generation sequence are as follows:

Define $\underline{Z}(1) = e^{\underline{A}\Delta t} \cong (\underline{I} + \underline{A}\Delta t)$, where Δt is chosen to be some fraction of the settling time of the system, approximated by $(1/\max_{i,j}(A_{ij}))$.

Define $$\underline{X}(1) = \int_0^{\Delta t} \underline{Z}(t-\tau)\underline{S}\,\underline{Z}^t(t-\tau)dt$$

$$\cong (\Delta t/2)((\underline{I} + \underline{A}\Delta t) + (\underline{I} + \underline{A}^t\Delta t))$$

Then iterate using the algorithm:

$$\underline{Z}(2i) = (\underline{Z}(i))^2$$

$$\underline{X}(2i) = \underline{X}(i) + \underline{Z}(i)\underline{X}(i)\underline{Z}^t(i)$$

$$i = 1, 2, 4, 8, 16, \ldots$$

The process ends when the desired convergence (via one of the criteria above) is attained.

G.3 SUBROUTINES GD, GPDP AND GPPDPP

Subroutine GD directly computes all elements of $\underline{G}_o(\underline{y})$ and $\underline{D}(\underline{y})$ given $\underline{y}$ and the parameters of the equations in Sections III.A.3 and III.A.4. The basic pattern is to identify the equation, identify the matrix elements which it contributes, and then proceed to compute these elements. The forcing terms of the mode acceleration equations are computed first and then added into the rigid body equations (those which are not orthogonalized to the flexure modes) as the other $\underline{y}$-dependent terms are computed. As shown in Section III, the modal forcing functions and the rigid body forcing terms can then be used to compute the terms of the response matrix $\underline{D}(\underline{y})$.

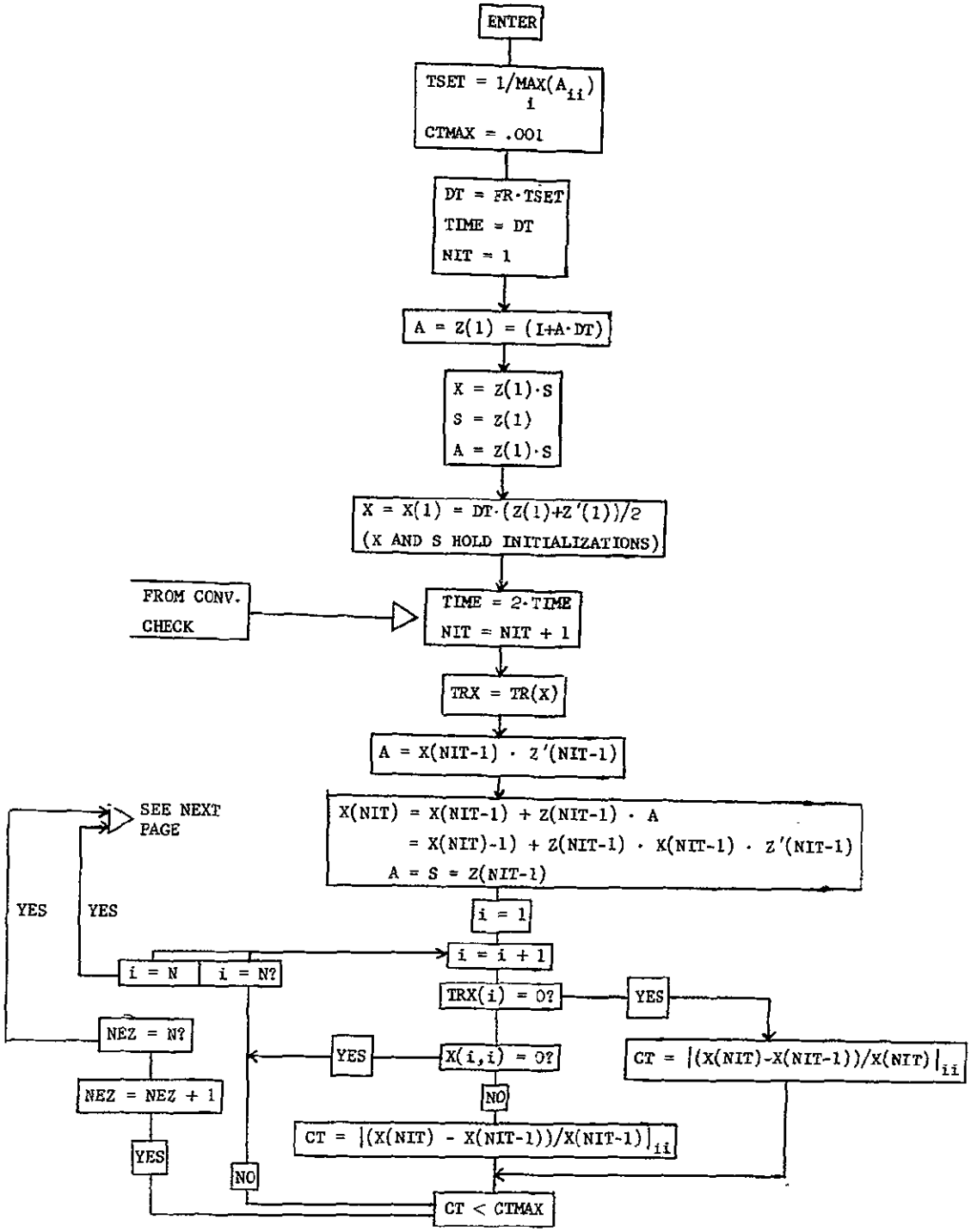

Fig. 1 Subroutine STCOV

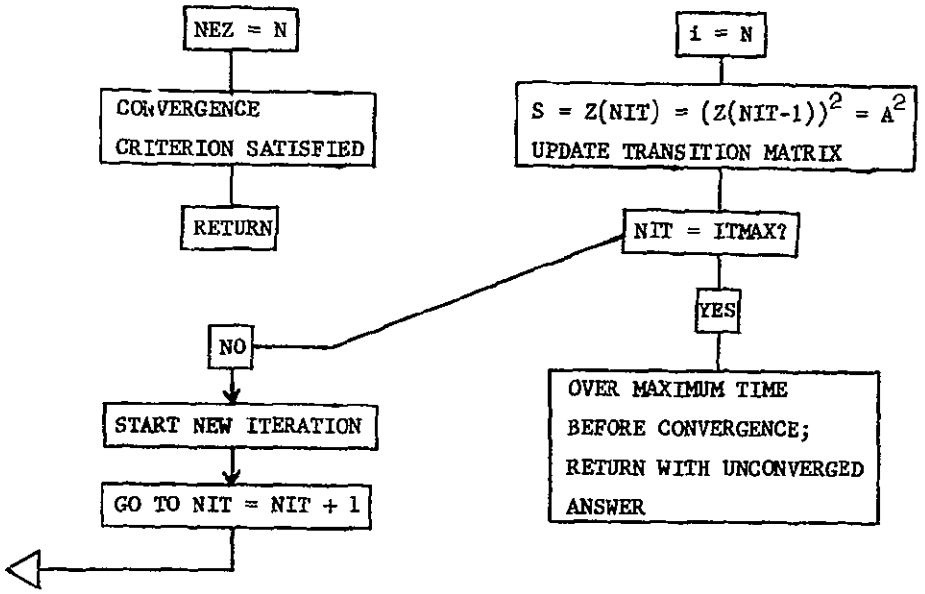

Definition of variables:

TSET = conservative approximation of system settling time

CTMAX = maximum allowable fractional error between estimates for satisfactory convergence

DT = Δt for first iteration

FR = fraction of settling time for first iteration

TIME = time to which equation has been integrated

NIT = current number of iterations

Z = transition matrix corresponding to the system $\dot{X} = AX$ (Z is not a matrix in the program itself but is used as an identifier in the flow chart to show which storage locations contain the current transition matrix; this is the same as the Z used in the thesis proposal write-up).

X = current value of solution matrix

TRX = trace of previous solution matrix

CT = fractional change of diagonal element for current iteration

NEZ = number of diagonal elements converged so that CT < CTMAX

ITMAX = maximum number of iterations (run time) allowed for convergence

N = system order

Fig. 1 Subroutine STCOV (Contd.)

NOTE: The left-hand side of an equation represents the storage locations in which the right-hand side is stored. For example, $\underline{A} = \underline{Z}(1)$ means that the storage locations originally assigned to the $\underline{A}$ matrix contain the elements of the initial transition matrix, $\underline{Z}(1)$. Considerable shuffling occurs in order to save storage space.

The variables used by the subroutine may be broken up as follows: (1) $\underline{G}_o$ and $\underline{D}$ matrices, their dimensions and constant terms; (2) descriptors of state, response, and control vectors; (3) variables specifying force producer position; (4) aircraft geometry parameters; (5) mode shape variables; and (6) lift curve parameters. A list of variables follows.

(1) $\underline{G}_o$ and $\underline{D}$ matrices, their dimensions, and constant terms:

G(NX, NU) = $\underline{G}_o(\underline{y})$ matrix

DY(NR, NU) = $\underline{D}(\underline{y})$ matrix

NX = dimension of state vector

NR = dimension of response vector

NU = dimension of control vector

GSTOCK(NX, NU) = constant terms for $\underline{y}$-independent part of $\underline{G}_o(\underline{y})$; positions of $\underline{y}$-dependent elements contain coefficients of these elements

DSTOCK(NR, NU) = constant terms for y-independent part of $\underline{D}(\underline{y})$; positions of $\underline{y}$-dependent elements contain coefficients of these elements

(2) Descriptors of state, response and control vectors:

IXPOS(NX)

IXPOS(1) = position of $\ddot{z}$ equation in state vector

IXPOS(2) = position of $\ddot{\theta}$ equation in state vector

IXPOS(3) = position of $\ddot{y}$ equation in state vector

IXPOS(4) = position of $\ddot{\psi}$ equation in state vector

IXPOS(5) = position of $\ddot{\phi}$ equation in state vector

IXPOS(6) = position of $\ddot{x}$ equation in state vector

IXPOS(K+6), K=1, NI = position of $\dot{\eta}_k$ in state vector; NI = number of flexure modes considered

IUPOS(I,J) = position of force producer J of type I in the control vector; I=1, NT; J=1, NMAX, where NT(=9)= number of force producer types and NMAX = maximum number of force producers of any type

IRPOS(I,J) = position of J^{th} response of type I in the response vector

I = 1 - acceleration responses

I = 2 - stress responses

I = 3 - stress rate responses

IRT = 3 = maximum value of I

NRT = maximum number of responses of any type (maximum value of J).

YR(IRT=NRT) = response station location on airplane

IRSEG(IRT=NRT) = axis upon which response station is located (i.e., $y_1 = 1$, $y_2 = 2$, $y_3 = 3$, $y_4 = 4$)

NRI(I), I = 1, IRT = number of responses of type I

(3) Variables specifying force producer position

LOC(I), I = 1, NT - number of axis upon which I^{th} type of force producer is located

NFP(I), I = 1, NT - number of surfaces of type I (see Section III for definition of types)

YFP(I, J), I = 1, NT, J = 1, NMAX - location of J^{th} force producer of type I, referred to axis system described in Section III

AXANG(I), I = 1, NT - angle between center of pressure axis for control surface type I and fuselage

AXX(I), I = 1, NT - distance of root of center of pressure axis of I^{th} type control surface fore of center of gravity

(4) Aircraft geometry parameters

YO(I), I = 1, 4 - start of I^{th} aircraft (flexure model) axis

YEND(I), I = 1, 4 - end of I^{th} aircraft (flexure model) axis

YCG = position of center of gravity on y_2 axis

EAXX(I), I = 1, 4 - AXX for I^{th} segment of elastic axis system

EAXANG(I), I = 1, 4 - AXANG for I^{th} segment of elastic axis system

(5) Mode shape variables

AK, AKK(I, J, K); I = 1, NI, J = 1, 4, K = 1, NFIN - cosine coefficients in Fourier series for mode slope derivative of vertical (AK) and torsional (AKK) displacements for I^{th} mode, J^{th} axis, K^{th} component in the series (NFIN = maximum number of terms in series).

BK, BKK(I, J, K); I = 1, NI, J = 1, 4, K = 1, NFIN - sine coefficients in Fourier series for vertical (BK) and torsional (BKK) mode slope derivatives for I^{th} mode.

PERIOD(I), I = 1, 4 - period of fundamental in the the Fourier series for axis I.

LAST (I), I = 1, 4 - number of last term in Fourier series for axis I

ZO(I, J), ZPO(I, J), I = 1, NI, J = 1, 4 - mode shape (ZO) and mode slope (ZPO) for vertical displacement of I^{th} mode evaluated at YO of axis J.

TO(I, J), TPO(I, J), I = 1, NI, J = 1, 4 - mode shape (TO) and mode slope (TPO) for torsional displacement of I^{th} mode evaluated at YO of axis J.

Z2M(I), I = 1, NI - normalization constant for I^{th} mode generalized force (see Appendix I)

(6) Lift Curve parameters

CLAK(1, 4, NFIN) - coefficients of cosine terms in Fourier series for section lift curve (second index = axis number, third index = term number, first index always unity)

CLBK(1, 4, NFIN) - coefficients of sine terms in Fourier series for section lift curve

CLO, CLPO(1, J), J = 1, 4 - value of section lift curve and lift curve slope at YO for axis J.

CLC(I, J) I = 1, NT; J = 1, NMAX - coefficient by which lift curve is multiplied for I^{th} type surface -

e.g., the wing section lift curve will be multiplied by one constant for ailerons, another constant for spoilers, etc., the constants depending on size and position of the surface type.

Working arrays in GD

COSS, SINS(NFIN) - used to store values of sine and cosine series terms

RROW, RCOL, ZEV(NI) - used to store vector of NI modes evaluated at a given point

CL(NT,NMAX) - used to store lift coefficients for each control surface

Evaluation of the $\underline{y}$-dependent portion of a plant equation (say the K^{th} equation) follows a pattern similar to the example below:

NROW = IXPOS(K) = row of $\underline{G}_o(\underline{y})$ under consideration

NCOL = IUPOS(I, J) = column of $\underline{G}_o(\underline{y})$ under consideration corresponds to position of control surface (I, J) in control vector, $\underline{u}$.

G(NROW, NCOL) = F(YFP(I,J)), F being the appropriate function of $\underline{y}$

$$G(NROW, NCOL) = F(YFP) + C_L(YFP) \cdot \sum_{k=1}^{NI} C_j(YFP)\xi_j(YFP)$$

where $C_j(YFP)$ is the appropriate constant (e.g., $\frac{\partial \xi_j}{\partial y_2}(y_{CG})$ for $\ddot{\theta}$, etc.) for the modal acceleration terms.

Generally there are three nested DO loops - one on I (type of control surface), one on J (number of force producers of type I), and

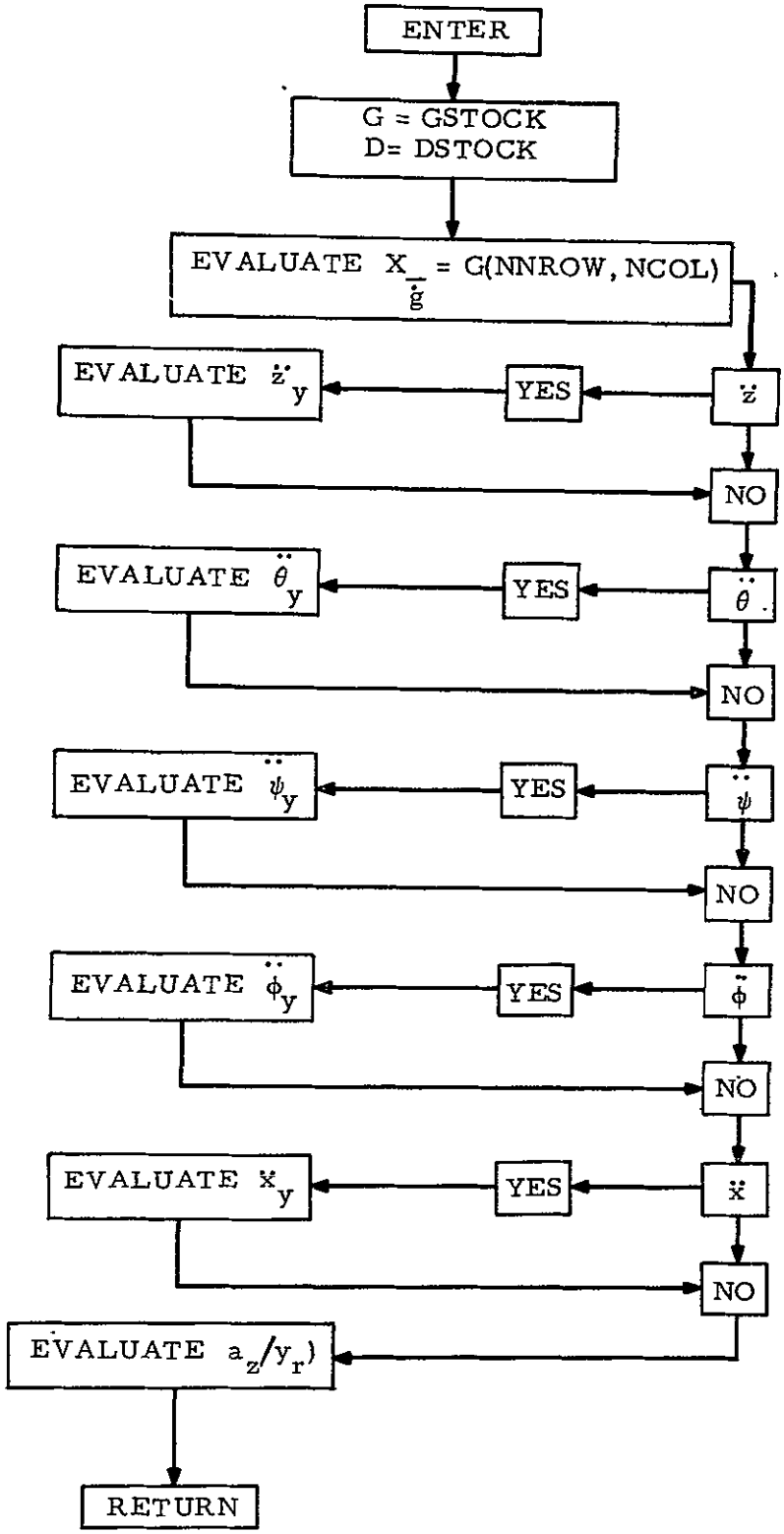

Fig. 2 Subroutine GD

one on K (for mode acceleration pickup in the rigid body equations). The DO loop on I usually skips terms to pick up either collective deflection contributions to pitch equations or differential deflection contributions to lateral equations. The subroutine EVAL is called several times to evaluate

(1) C_{L_i}, if these are functions of y_k

(2) $\xi_j(y_k)$ and $\theta_j(y_k)$, J = 1, NI

(3) $\xi_j(y_{CG})$, $\frac{\partial \xi_j}{\partial y_2}(y_{CG})$, etc. used for the coefficients $C_j(y_i)$

Subroutine GPDP

This subroutine evaluates the first partials $\frac{\partial \underline{G}(\underline{y})}{\partial y_i}$ and $\frac{\partial \underline{D}(\underline{y})}{\partial y_i}$ where y_i=YFP(ID, JD) is specified by ID and JD in the subroutine CALL. The derivatives are evaluated directly by differentiating the expressions given in Section III.A.3:

$$\partial \ddot{z}_y/\partial y_i=(\partial C_{L_i}/\partial y_i)\delta_i + \sum_{j=1}^{NI} (\xi_j(y_{CG})(\partial X_j/\partial y_i)/Z2M(j) \quad i=1,3,5,7$$

$$\partial \ddot{\theta}_y/\partial y_i = \left[\frac{\partial C_{L_i}}{\partial y_i}[\,AXX(i)-y_i/TAN(AXANG(i))\,] - C_{L_i}/TAN(AXANG(i)\right]\delta_i \quad (1)$$

$$+\sum_{j=1}^{NI} \frac{\partial \xi_j}{\partial y_2}(y_{CG})\,\frac{\partial X_i}{\partial y_i}\,Z2M(j) \quad (2)$$

$$i = 1,3,5,7$$

$$\partial \ddot{Y}_y/\partial y_i = 0 \quad (3)$$

$$\partial \ddot{x}_y/\partial y_i = C_{D_i} \frac{\partial C_{L_i}}{\partial y_i} [\, AXX^2(i) + y_i^2(1+COT^2(AXANG(i)) - 2y_i AXX(i) COT(AXANG(i))\,]^{1/2} \delta_i \qquad (4)$$

$$+ C_{D_i} C_{L_{i-1}}(y_i) \frac{[\, y_i(1+COT^2(AXANG(i))) - AXX(i) COT(AXANG(i))\,]\delta_i}{[\, AXX^2(i) + y_i^2(1+COT^2(AXANG(i))) - 2y_i AXX(i) COT(AXANG(i))\,]^{1/2}}$$

$$i = 2, 4, 6$$

$$\partial \ddot{\psi}_y/\partial y_9 = C_{D_9} COT(AXANG(9))\ \delta_9$$

$$\partial \ddot{\phi}_y/\partial y_i = C_{P_i}(y_i \partial C_{L_{i-1}}(y_i)/\partial y_i + C_{L_{i-1}}(y_i))\delta_i \qquad (5)$$

$$+ \sum_{j=1}^{NI} \frac{\partial \xi_i}{\partial y_1}(y_{CG})(\partial X_j/\partial y_i)/Z2M(j)$$

$$i = 2, 4, 6, 9$$

$$\partial \dot{\phi}_y/\partial y_8 = C_{P_8} \left[\partial C_{L_7}(y_8)/\partial y_8 (y_{VT}^2 + y_8^2)^{1/2} + C_{L_7}(y_8) y_8/(y_{VT}^2+y_8)^{1/2} \right] \delta_8$$

$$+ \sum_{j=1}^{NI} \frac{\partial \xi_j}{\partial y_1}(y_{CG}) \frac{\partial X_i}{\partial y_8}(y_8)\ Z2M(j)$$

$$\partial X_y/\partial y_i = C_{D_i} \partial C_{L_i}/\partial y_i \qquad i = 1, 3, 5, 7 \qquad (6)$$

$$= C_{D_i}\ \partial C_{L_{i-1}}/\partial y_i \qquad k = 2, 4, 6, 8$$

$$= 0 \qquad i = 9$$

The term

$$\frac{\partial X_j}{\partial y_i} = \partial C_{L_i}/\partial y_i [\, \xi_j(y_i) + d(y_i)\, \phi_j(y_i)]\delta_i \qquad (7)$$

$$+ C_{L_i}(y_i)[\, \partial \xi_j/\partial y_i + d(y_i) \partial \phi_j/\partial y_i + \partial d/\partial y_i \phi_j(y_i)]\ \delta_i$$

In the computer program $d(y_i)$ = DIS and $\partial d/\partial y_i$ = DISP. Here ξ_j is the vertical deflection of the j^{th} mode (see above) and ϕ_j is the torsional deflection of the j^{th} mode. The subroutine EVAL evaluates mode shapes (ξ_j, ϕ_j), mode slopes $(\partial\xi_j/\partial y_i, \partial\phi_j/\partial y_i)$, and lift curve shape and slope $(C_{L_i}, \partial C_{L_i}/\partial y_i)$.

The structure of this subroutine is basically the same as in GD and the variable names are unchanged. The major differences are that the first variation matrices GP = $\partial\underline{G}_o/\partial y_i$ and DP = $\partial\underline{D}/\partial y_i$ have only one nonzero column corresponding to control surface i (note that a single index i has been used on $\underline{y}$ throughout this description, whereas in the program, y_i = YFP(ID, JD), is identified by two indices -- one for the type of surface and one for the number of surfaces of that type). In GPDP, the constants CLIFT = C_{L_i} and CLIFTP = $\partial C_{L_i}/\partial y_i$ are used in place of the matrix CL = C_{L_i} which stored lift coefficients in subroutine GD. As in GD, the constants of $\underline{y}$-dependent terms (e.g., C_{D_i}, C_{P_i}, etc.) are stored in GSTOCK and DSTOCK. A flow chart for the program is shown in Fig. 3.

The acceleration terms of $\partial D/\partial y_i$ are proportional to:

$$\partial a_z/\partial y_i = \partial \dot{z}_y/\partial y_i - x_r \cdot \partial \ddot{\theta}_y/\partial y_i + y_r\, \partial \ddot{\phi}_y/\partial y_i + \sum_{j=1}^{NI} (\partial X_j/\partial y_i)\xi_j(y_r) \tag{8}$$

The proportionality constant, again, is stored in GSTOCK. Note that the $\partial \ddot{\theta}_y/\partial y_i$ terms apply to the pitch axis control surfaces (i=1, 3, 5, 7) and the $\partial \ddot{\phi}_y/\partial y_i$ terms apply to lateral axis control surfaces (i=2, 4, 6, 8, 9). The moment arms x_r = XR and y_r = YR(1, K), and the $\xi_j(y_r)$ are computed first; remaining terms have been computed for GP.

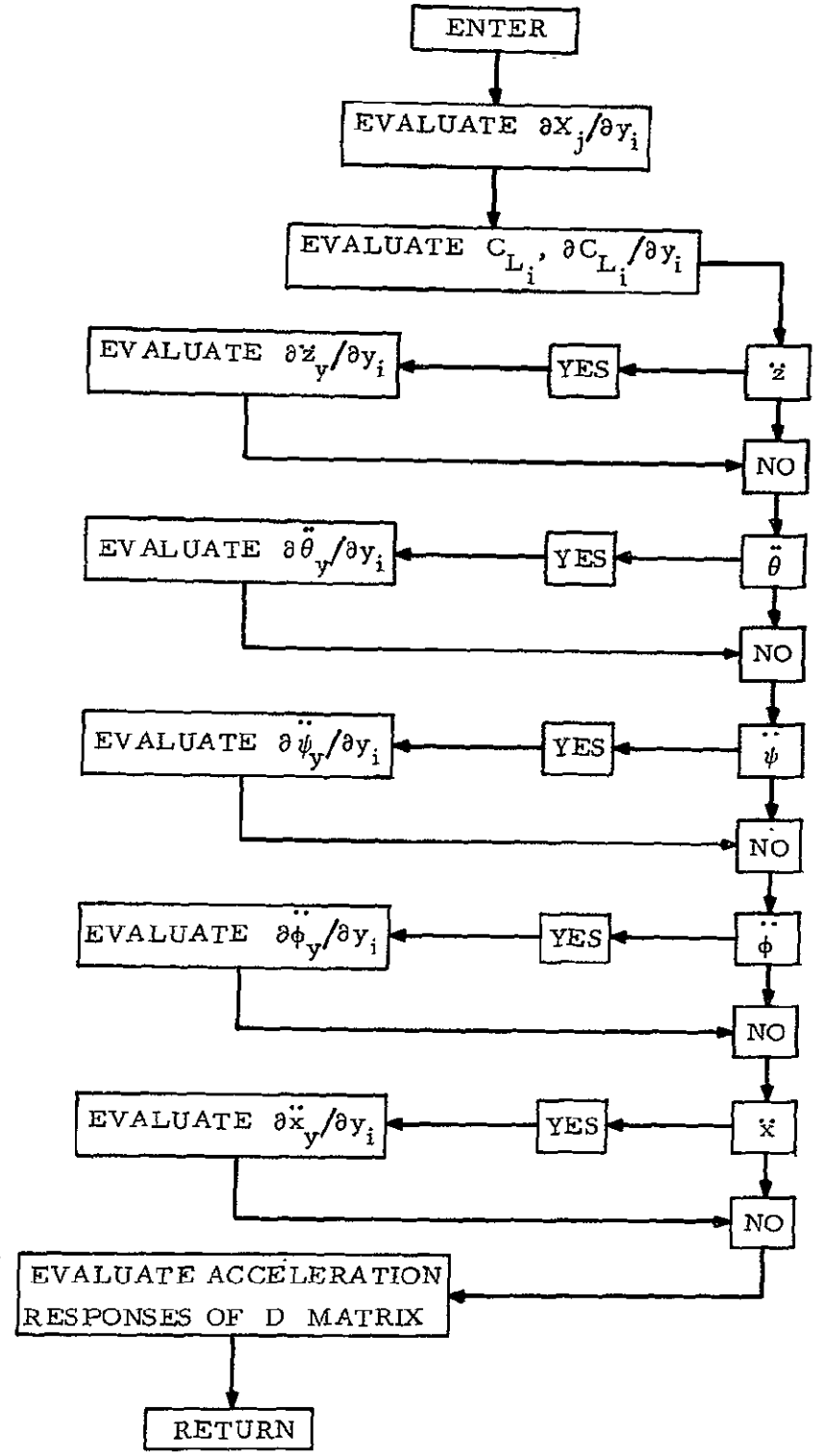

Fig. 3 Subroutine GPDP

Subroutine GPPDPP

This subroutine computes the second variations $\underline{GPP} = \partial^2 \underline{G}_o / \partial y_i \partial y_j$ and $\underline{DPP} = \partial^2 \underline{D} / \partial y_i \partial y_j$ of $\underline{G}_o(\underline{y})$ and $\underline{D}(\underline{y})$. Note that the equations given in the GD description contain no cross-product terms in y_i and y_j, and that force producer locations are varied independently so that y_i and y_j are unrelated unless i=j. Hence $\underline{GPP} = \underline{0}$ and $\underline{DPP} = \underline{0}$ for $i \neq j$. For $i = j$, $\underline{GPP}$ and $\underline{DPP}$ each have one nonzero column (as in GPDP) which contains second partial derivatives of the rigid body acceleration equations, mode aceleration equations and response acceleration equations. These are written out as:

$$\partial^2 \ddot{z}_y / \partial y_i^2 = \partial^2 C_{L_i} / \partial y_i^2 \, \delta_i + \sum_{k=1}^{NI} \xi_k(y_{CG})(\partial^2 X_k / \partial y_i^2)/Z2M(j) \qquad (1)$$

$$i = 1,3,5,7$$

$$\partial^2 \ddot{\theta}_y / \partial y_i^2 = [\partial^2 C_{L_i} / \partial y_i^2 [AXX(i) - y_i COT(AXANG(i))]$$

$$- 2(\partial C_{L_i} / \partial y_i) COT(AXANG(i))] \delta_i \qquad (2)$$

$$+ \sum_{k=1}^{NI} \frac{\partial \xi_k}{\partial y_2}(y_{CG})(\partial^2 X_k / \partial y_i^2)/Z2M(j)$$

$$i = 1,3,5,7$$

$$\partial^2 \ddot{y}_y / \partial^2 y_i = 0 \qquad (3)$$

$$\partial^2 \ddot{\psi}_y / \partial y_i^2 = C_{D_i} \partial^2 C_{L_{i-1}} / \partial y_i^2 [AXX(i)^2 + y_i^2(1+COT^2(AXANG(i)))$$

$$-2y_i AXX(i) COT(AXANG(i))]^{1/2}$$

$$+2\partial C_{L_i} / \partial y_i \frac{(y_i(1+COT^2(AXANG(i)) - AXX(i) COT(AXANG(i)))}{(AXX(i)^2 + y_i^2(1+COT^2(AXANG(i))) - 2y_i AXX(i) COT(AXANG(i))^{1/2}} \qquad (4)$$

$$+C_{L_{i-1}} \frac{(1+COT^2(AXANG(i)))}{(AXX(i)^2+y_i^2(1+COT^2(AXANG(i)))-2y_i AXX(i)COT(AXANG(i))^{1/2}}$$

$$- \frac{y_i^2(1-AXX(i)COT(AXANG(i))+COT^2(AXANG(i))^2}{(AXX(i)^2+y_i^2(1+COT^2(AXANG(i)))-2y_i AXX(i)COT(AXANG(i)))^{3/2}}$$

$i = 2,4,6$

$$\partial^2\ddot{\phi}_y/\partial^2 y_i = C_{P_i}(2\cdot\partial C_{L_{i-1}}(y_i)/\partial y_i + y_i\partial^2 C_{L_{i-1}}(y_i)/\partial y_i^2)\,\delta_i \qquad (5)$$

$$+\sum_{k=1}^{NI}\frac{\partial\xi_k}{\partial y_1}(y_{CG})(\partial^2 X_k/\partial y_i^2)/Z2M(j)$$

$i = 2,4,6,9$

$$\partial^2\ddot{\phi}_y/\partial y_8^2 = C_{P_8}(\partial^2 C_{L_7}(y_8)/\partial y_8^2)(y_{VT}^2+y_8^2)^{1/2}$$

$$+2(\partial C_{L_7}(y_8)/\partial y_8)/(y_{VT}^2+y_8^2)^{1/2}$$

$$+ C_{L_7}(y_8)[1/(y_{VT}^2+y_8^2)^{1/2} - y_8^2/(y_{VT}^2+y_8^2)^{3/2}]$$

$$+\sum_{k=1}^{NI}\frac{\partial\xi_j}{\partial y_1}(y_{CG})\,\partial^2 X_j(y_8)/\partial y_8^2)/Z2M(j)$$

$$\partial\ddot{x}_y/\partial y_i = C_{D_i}\partial^2 C_{L_i}/\partial y_i^2 \qquad i = 1,3,5,7 \qquad (6)$$

$$= C_{D_i}\partial^2 C_{L_{i-1}}/\partial y_i^2 \qquad i = 2,4,6,8$$

$$= 0 \qquad i = 9$$

The mode forcing terms are

$$\partial^2 X_j/\partial y_i^2 = \{\partial^2 C_{L_i}/\partial y_i^2[\xi_j(y_i) + d(y_i)\phi_j(y_i)] \qquad (7)$$

$$+ 2\partial C_{L_i}/\partial y_i[\partial\xi_j/\partial y_i + d(y_i)\partial\phi_j/\partial y_i + \partial d/\partial y_i\phi_j(y_i)]$$

$$+ C_{L_i}(y_i)[\partial^2\xi_j/\partial y_i^2 + 2\partial d/\partial y_i\partial\phi_j/\partial y_i]\}\,\delta_i$$

(NOTE: $\partial^2 d/\partial y_i^2 = 0$)

The response accelerations are

$$\partial^2 a_z/\partial y_i^2 = \partial^2 \ddot{z}_y/\partial y_i^2 - x_r \partial^2 \ddot{\theta}_y/\partial y_i^2 + y_r \partial \ddot{\theta}_y/\partial y_i \qquad (8)$$

$$+ \sum_{j=1}^{NI} \partial^2 X_j/\partial y_i^2 \xi_j(y_r)$$

The organization of GPPDPP is precisely that of GPDP, and variables retain their definitions. The subroutine EVAL is also used to compute second derivatives of mode shapes and section lift curves C_{L_i}.

G.4 EVAL

Equations Solved:

$$z(y) = z_o + z_o' y + (a_o/4)y^2 - \sum_{k=1}^{N} a_k (L/2\pi k)^2 \cos(2\pi k y/L) \qquad (1)$$

$$\sum_{k=1}^{N} b_k (L/2\pi k)^2 \sin(2\pi k y/L)$$

$$z'(y) = z_o' + (a_0/2)y + \sum_{k=1}^{N} a_k (L/2\pi k)\sin(2\pi k y/L) - \sum_{k=1}^{N} b_k (L/2\pi k)\cos(2\pi k y/L) \qquad (2)$$

$$z''(y) = a_o/2 + \sum_{k=1}^{N} a_k \cos(2\pi k y/L) + \sum_{k=1}^{N} b_k \sin(2\pi k y/L) \qquad (3)$$

Here a_k and b_k are the sequences of Fourier coefficients in the Fourier series for $z''(y)$, N is the length of the series, L is the period of the fundamental, and y is the point at which z is to be evaluated. The program simultaneously evaluates any number of modes (z), mode slopes, or slope derivatives at the desired evaluation point y. The point y may be anywhere on the aircraft.

Note on computation method:

The sine and cosine terms in the series are rapidly evaluated via the trigonometric identities

$$\sin(n+1)x = \cos(x)\cos(nx) - \sin(x)\sin(nx) \quad (4)$$

$$\cos(n+1)x = \cos(x)\sin(nx) + \sin(x)\cos(nx) \quad (5)$$

The program may also be used for evaluation of other y-dependent parameters such as section lift coefficient, bending stiffness, and torsional rigidity.

G.4 SUBROUTINE EVAL

This compact, fast little program is the reason that mode shapes, slopes and slope derivatives are conveniently stored as coefficients of Fourier series. Given any point on the aircraft, EVAL will return a vector of mode shapes, slopes, or slope derivatives for all flexure modes evaluated at that point. Hundreds of mode shapes may be evaluated in a single second. The subroutine has a counterpart, SEFOUR which has been used in the Fourier decomposition of mode shape data. The subroutine itself is amply annotated so as to be easily "lifted" for other applications. A description of variables follows.

AK = "tensor" of Fourier cosine coefficients for mode slope derivatives; first index is number of the mode, second index is segment of aircraft (1-wing, 2-fuselage, 3-vertical tail, 4-horizontal tail) and the third index is the term in the series (with a_o as the first element).

BK = "tensor" of Fourier sine coefficients. Series generally tend to have only the first cosine term and odd sine terms nonzero, though the program doesn't require this.

NI = total number of modes

NFIN = maximum length of series for any segment of the aircraft

PERIOD = vector containing the period of the series for each aircraft segment (4 elements). The fundamental period should be about four times the length of the segment.

LAST = vector containing number of last term of series for each aircraft segment. The number of terms for a given segment should be such that the shortest period in the series is approximately the length of a panel used to compute the mode shapes. Inclusion of higher order terms introduces extraneous "noise" due to the lumped modeling of the aircraft.

ZO = matrix of initial values of mode shapes for each segment. First index is mode number; second index is segment number (1-4).

ZPO = matrix of initial values of mode slopes for each segment. ZO and ZPO correspond to z(0) and z'(0) of Eqs. 1 and 2 and are used to obtain constants of integration for the series.

NSEG = number of aircraft segment where modes are to be evaluated (1-4)

YON = value of coordinate variable where axis (corresponding to NSEG) begins

YEV = value of coordinate variable where modes are to be evaluated.

NFN = 1 for mode shapes

2 for mode slopes

3 for mode slope derivatives

ZEV = vector of NI mode shapes, slopes, or slope derivatives, depending on NFN (output)

COSS = vector of evaluated cosine terms (storage)

SINS = vector of evaluated sine terms (storage)

PI = π

PIOL = 2π/PERIOD = "frequency" of fundamental

YE = equivalent point at which series is evaluated (since Fourier coefficients are evaluated for $y_o = 0$, it is necessary to shift the axis by YON in evaluating the series).

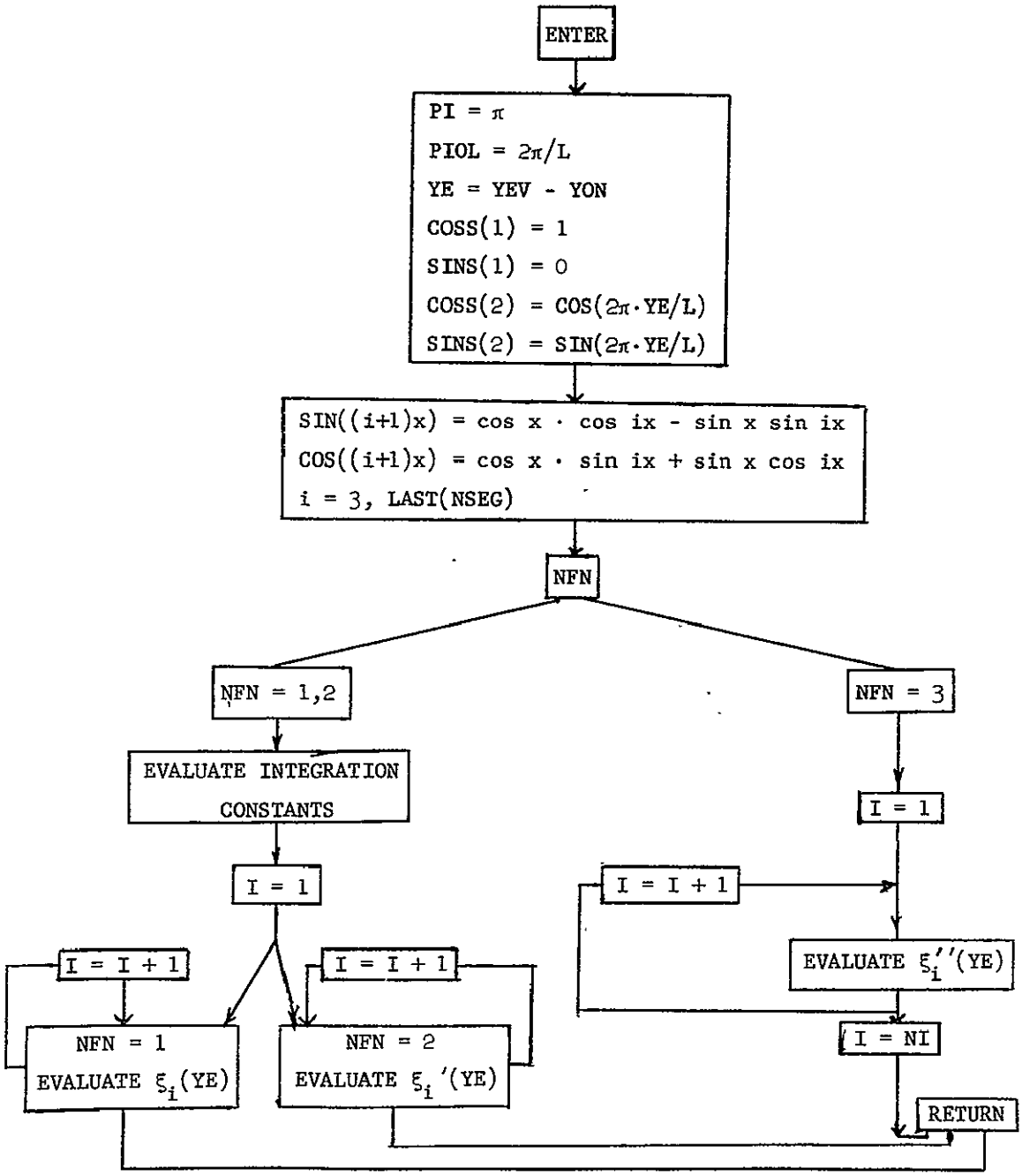

Fig. 4 Subroutine EVAL

APPENDIX H

TRIAL MODEL COEFFICIENT DATA

The parameters and coefficient data for the three-mode trial model of the C-5A described in Section IV is presented on Tables 1-4. Charts 1-4 show the mode shapes of the first, third and sixth modes used in the trial model. The dimensions of the model variables are as follows:

Variable	Dimension	Name
$\alpha = w$	(inches/sec.)	angle of attack
$\dot{\theta}/\phi_2$	(inches/sec.)	pitch rate
$\dot{\tau}_i$, i=1, 3, 6	(inches/sec.)	normal mode velocities
τ_i, i=1, 3, 6	(inches)	normal mode deflections
p_i, i=1, 2, 3, 4, 5	(dimensionless)	Kussner gust delays
α_g	(ft./sec.)	gust angle of incidence
δ_{sp}	(degrees)	spoiler deflection
δa_1, δa_2	(degrees)	aileron deflections
δ_e	(degrees)	elevator deflections
m_1, m_2	(g's)	accelerometer signals
m_3	(inches/sec.)	rate gyro signal
s_i, i=1, 2, 3, 4, 5	((1/(12)(32.2))lb./in.^{2}	stress responses
a_i, i=1, 2, 3, 4	(g's)	acceleration responses
ξ_i, i=1, 3, 6	(inches)	mode shapes (vertical)
y_i, i=1, 2, 3, 4	(inches)	orthogonal body coordinates
ϕ_i, i=1, 3, 6	(dimensionless)	mode shapes (torsional)

Sign conventions for trial model are positive for:

(a) Trailing edge down for all control surfaces (Note: the "zero" deflection position for spoiler flaps corresponds to the flaps deflected 30^{o}, or half their full range, to permit a valid linearization).

(b) Wing tips down and aft for bending modes.

(c) Trailing edge of wings down for torsion modes.

(d) Pitch nose-up for θ.

(e) Decreasing altitude for z.

Table 1

Plant Model

	w	$\dot{\theta}/\Phi_2$	$\dot{\tau}_1$	τ_1	$\dot{\tau}_3$	τ_3	$\dot{\tau}_6$	τ_6	P_1	P_2	P_3	P_4	P_5	a_g	δ_e	δ_{a_1}	δ_{a_2}	δ_{ep}	η_1
$\dot{w}$	-.90693	3.7519	-.058079	-.87283	-.12556	-6.4331	.21854	-2.0946	-8.7948	-8.7948	-1.7381	-1.7381	0	-.35055	-11.449	-7.3159	-7.3159	-10.166	0
$\dot{\theta}/\Phi_2$	-.33171	-.92625	.08650	-.020925	-.37688	-8.1329	.88275	13.965	-.39799	-.39799	-5.6862	-5.6862	0	2.1038	-37.786	-7.8105	-7.8105	-5.5767	0
$\dot{Y}_1$	-1.2472	-.0020083	-1.7430	-31.246	1.1387	-37.464	-1.3756	-63.141	-20.401	-20.401	4.7342	4.7342	0	.70142	31.241	-72.180	-72.180	-36.308	0
$\dot{\tau}_1$	0	0	1.0	0	0	0	0	0	0	0	0	0	0	0	0	0	0	0	0
$\dot{\tau}_3$	.62623	-.38234	.13214	2.4256	-1.4351	-212.96	.24775	18.999	14.599	14.599	-5.1462	-5.1462	0	-1.9377	-34.025	-26.855	-26.855	24.337	0
$\dot{\tau}_3$	0	0	0	0	1.0	0	0	0	0	0	0	0	0	0	0	0	0	0	0
$\dot{\tau}_6$	.58550	.57199	-.07345	.43421	.088236	6.1284	-1.4044	-377.34	3.2838	3.2838	3.4289	3.4289	0	.31323	22.585	-4.8639	-4.8639	7.8744	0
$\dot{\tau}_6$	0	0	0	0	0	0	1.0	0	0	0	0	0	0	0	0	0	0	0	0
$\dot{p}_1$	0	0	0	0	0	0	0	0	-2.2	0	0	0	0	.8578	0	0	0	0	0
$\dot{p}_2$	0	0	0	0	0	0	0	0	0	-26.36	0	0	0	16.062	0	0	0	0	0
$\dot{p}_3$	0	0	0	0	0	0	0	0	0	0	-4.44	0	0	1.643	0	0	0	0	0
$\dot{p}_4$	0	0	0	0	0	0	0	0	0	0	0	-53.24	0	33.544	0	0	0	0	0
$\dot{p}_5$	0	0	0	0	0	0	0	0	0	0	0	0	0	-.33293	0	0	0	0	.43843
$\dot{a}_g$	0	0	0	0	0	0	0	0	0	0	0	0	1.0	-1.154	0	0	0	0	1.31567

$\underline{\dot{x}} = \underline{F}\underline{x} + \underline{G}\underline{\zeta} + \underline{C}\underline{\eta}$

Table 2
Sensor Signals

$$\underline{m} = \begin{bmatrix} m_1 \\ m_2 \\ m_3 \end{bmatrix} = \begin{bmatrix} -.0034441 & -.0014509 & -.0036953 & -.06417 & -.00015241 & -.41392 & -.0033636 & -.59212 & -.039828 & -.039828 & -.00057125 & -.00057125 & 0 & -.026303 \\ -.0017543 & -.00040394 & -.00002408 & .0010934 & -.00095952 & -.17437 & .00062801 & .33870 & -.012414 & -.012414 & -.0022638 & -.0022638 & 0 & -.0063736 \\ 0 & 1.0 & 0 & 0 & 0 & 0 & 0 & 0 & 0 & 0 & 0 & 0 & 0 & 0 \end{bmatrix}$$

$\underline{A}\,\underline{x}$

$$+ \begin{bmatrix} 0 & .02 & 0 & 0 \\ 0 & 0 & .02 & 0 \\ 0 & 0 & 0 & .02 \end{bmatrix} \begin{bmatrix} \eta_1 \\ \eta_2 \\ \eta_3 \\ \eta_4 \end{bmatrix}$$

$+ \quad \underline{B}\,\underline{n}$

Table 3

Response Equations

	$\dot{w}$	$\dot{\theta}/\phi_2$	τ_1	τ_1	τ_3	τ_3	τ_6	τ_6	p_1	p_2	p_3	p_4	p_5	a_g	δ_e	δ_{a_1}	δ_{a_2}	δ_{sp}
s_1	-.002259	016123	004345	.61545	-.040193	-1 9026	-.018744	-2 6249	- 09278	-.09278	10836	.10836	0	-.046017	71742	.15419	15419	-.025543
s_2	-.00494	.010717	.002208	.90554	-.056853	3.6342	-.005142	4 2301	- 12055	- 12055	085468	.085468	0	-.024255	.57011	.25621	.25621	14172
s_3	-.009193	-.011387	.000546	.020272	-.007464	-1.2465	005044	1 7633	-.88974	-.88974	-.044539	-.044539	0	.82391	-3.5580	-1.2710	-1 2710	-1 2953
s_4	.011624	020647	-.003803	12533	-.003639	-1 3265	.052461	4.2468	-.02778	-.02778	.14917	.14917	0	.017830	.014234	-.016017	- 016017	-.068960
s_5	-.032271	- 056583	.015456	020311	- 022388	22195	.071748	-1.1886	.001542	.001542	087109	.087109	0	- 002485	-1.1601	-.000249 (.092033)	- 000249 (.092033)	.020248
a_1	-.060422	-.02609	.000993	048292	-.033856	-5 0565	.028502	8 8001	-.41993	-.41993	-.14794	-.14794	0	-.157222	-.96555	-.63825 (.25722)	-.63825 (25722)	-.19986
a_2	-.05541	-.03890	.010905	22427	-.027222	- 65968	014487	-7.0216	-.45400	-.45400	-.2053	-.2053	0	-.005648	-1.3576	- 21854 (.23887)	- 21854 (23887)	-.37799
a_3	-.05369	-.05469	.01881	34491	-.038589	- 56536	028181	-9 3949	- 36562	-.36562	-.31980	-.31980	0	041112	-2.1192	-.14305 (020241)	- 14305 (020241)	-.31141
a_4	- 063589	- 09943	035119	55015	- 072403	-2 6920	.097791	.17274	-.19103	-.19103	-.64786	- 64786	0	.075801	-4 2917	-.072513	- 072513	- 21035

$\underline{\dot{r}} = \underline{H}\underline{\Delta} + \underline{D}\underline{\delta}$

Stresses in $1/(12)(32\ 2)$ $lb/in.^2$

Accelerations in g's

Control Displacements in Degrees

Table 4

Auxiliary Matrices

$$ZO = \begin{bmatrix} -.0973 & -.0223 & -.1663 & -.2865 \\ .0349 & .3051 & .1687 & .3215 \\ .2012 & -.3578 & -.2575 & -.6263 \end{bmatrix}$$

$$ZPO = \begin{bmatrix} 0. & -.7615E-04 & -.1414E-03 & -.6160E-04 \\ 0. & -.3132E-03 & .4467E-03 & .2696E-03 \\ 0. & .6342E-03 & -.1612E-02 & -.1097E-02 \end{bmatrix}$$

$$IRPOS = \begin{bmatrix} 6 & 7 & 8 & 9 & 0 \\ 1 & 2 & 3 & 4 & 5 \\ 0 & 0 & 0 & 0 & 0 \end{bmatrix}$$

$$IRSEG = \begin{bmatrix} 2 & 2 & 2 & 2 & 0 \\ 1 & 1 & 2 & 2 & 4 \\ 0 & 0 & 0 & 0 & 0 \end{bmatrix}$$

$$LAST = \begin{bmatrix} 101 \\ 97 \\ 41 \\ 37 \end{bmatrix} \qquad PERIOD = \begin{bmatrix} 4959.2 \\ 9910.8 \\ 1497.84 \\ 1460.8 \end{bmatrix}$$

$$NRI = \begin{bmatrix} 4 \\ 5 \\ 0 \end{bmatrix} \qquad YR = \begin{bmatrix} 395. & 1369. & 1804. & 2406. & 0. \\ 120. & 746. & 1106. & 1804. & 20.3 \\ 0. & 0. & 0. & 0. & 0. \end{bmatrix}$$

Table 4 (Contd.)

Auxiliary Matrices

$$AXX = \begin{bmatrix} 220.545 \\ 0 \\ 0 \\ 0 \\ 0 \\ 0 \\ 0 \\ 0 \\ 0 \end{bmatrix} \quad AXANG = \begin{bmatrix} 1.157164 \\ 0 \\ 0 \\ 0 \\ 0 \\ 0 \\ 0 \\ 0 \\ 0 \end{bmatrix} \quad NFP = \begin{bmatrix} 2 \\ 0 \\ 0 \\ 0 \\ 0 \\ 0 \\ 0 \\ 0 \\ 0 \end{bmatrix}$$

$$LOC = \begin{bmatrix} 1 \\ 0 \\ 0 \\ 0 \\ 0 \\ 0 \\ 0 \\ 0 \\ 0 \end{bmatrix} \quad IXPOS = \begin{bmatrix} 1 \\ 2 \\ 0 \\ 0 \\ 0 \\ 0 \\ 3 \\ 5 \\ 7 \\ 0 \\ 0 \\ 0 \\ 0 \\ 0 \\ 0 \end{bmatrix} \quad IUPOS = \begin{bmatrix} 2 & 3 \\ 0 & 0 \\ 0 & 0 \\ 0 & 0 \\ 0 & 0 \\ 0 & 0 \\ 0 & 0 \\ 0 & 0 \\ 0 & 0 \end{bmatrix}$$

Table 4 (Contd.)

Auxiliary Matrices

$$YO = \begin{bmatrix} 60.0 \\ 277.5 \\ 405.57 \\ 20.3 \end{bmatrix} \qquad YEND = \begin{bmatrix} 1299.8 \\ 2755.2 \\ 780.03 \\ 385.5 \end{bmatrix}$$

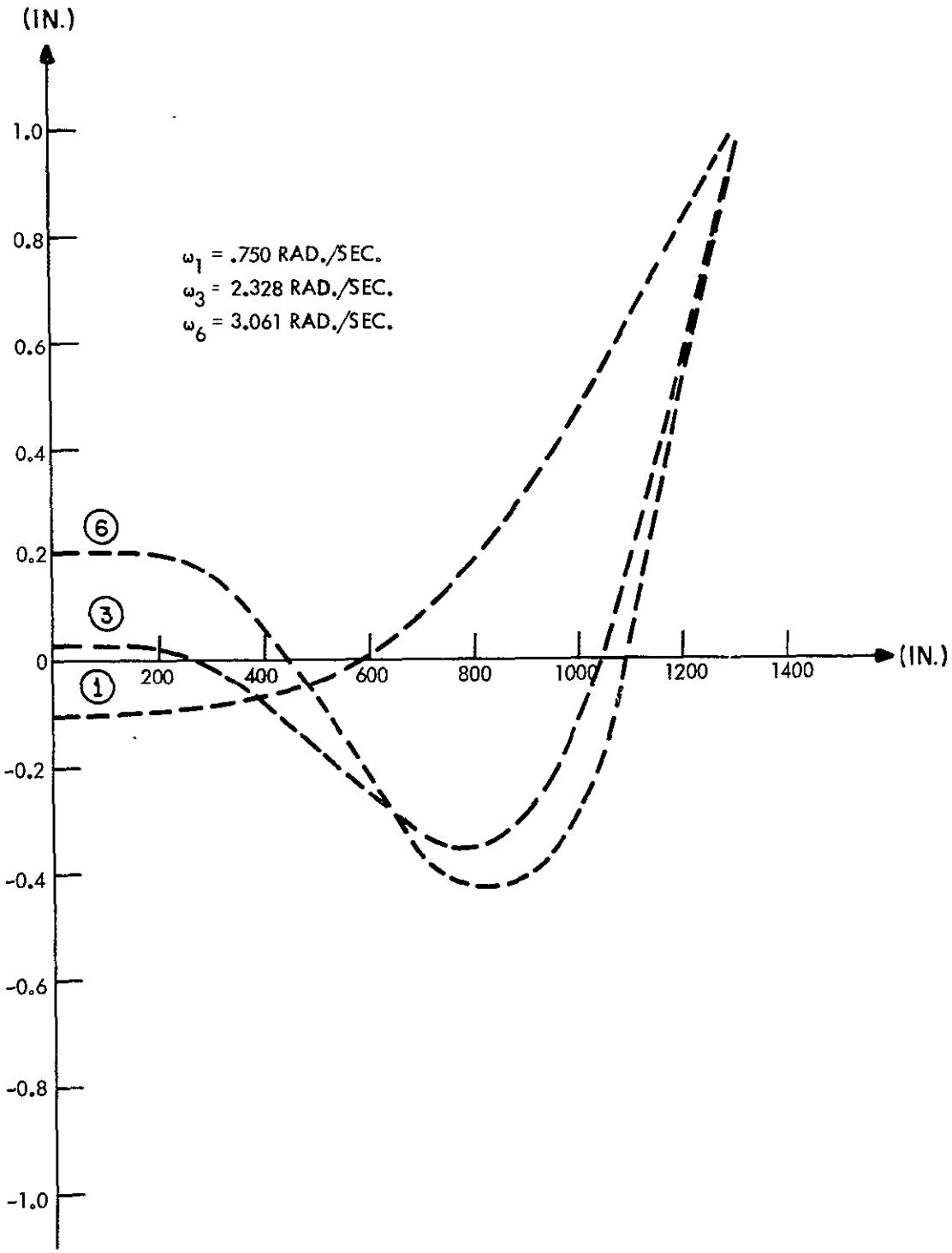

Chart 1 Vertical Deflection of Wing

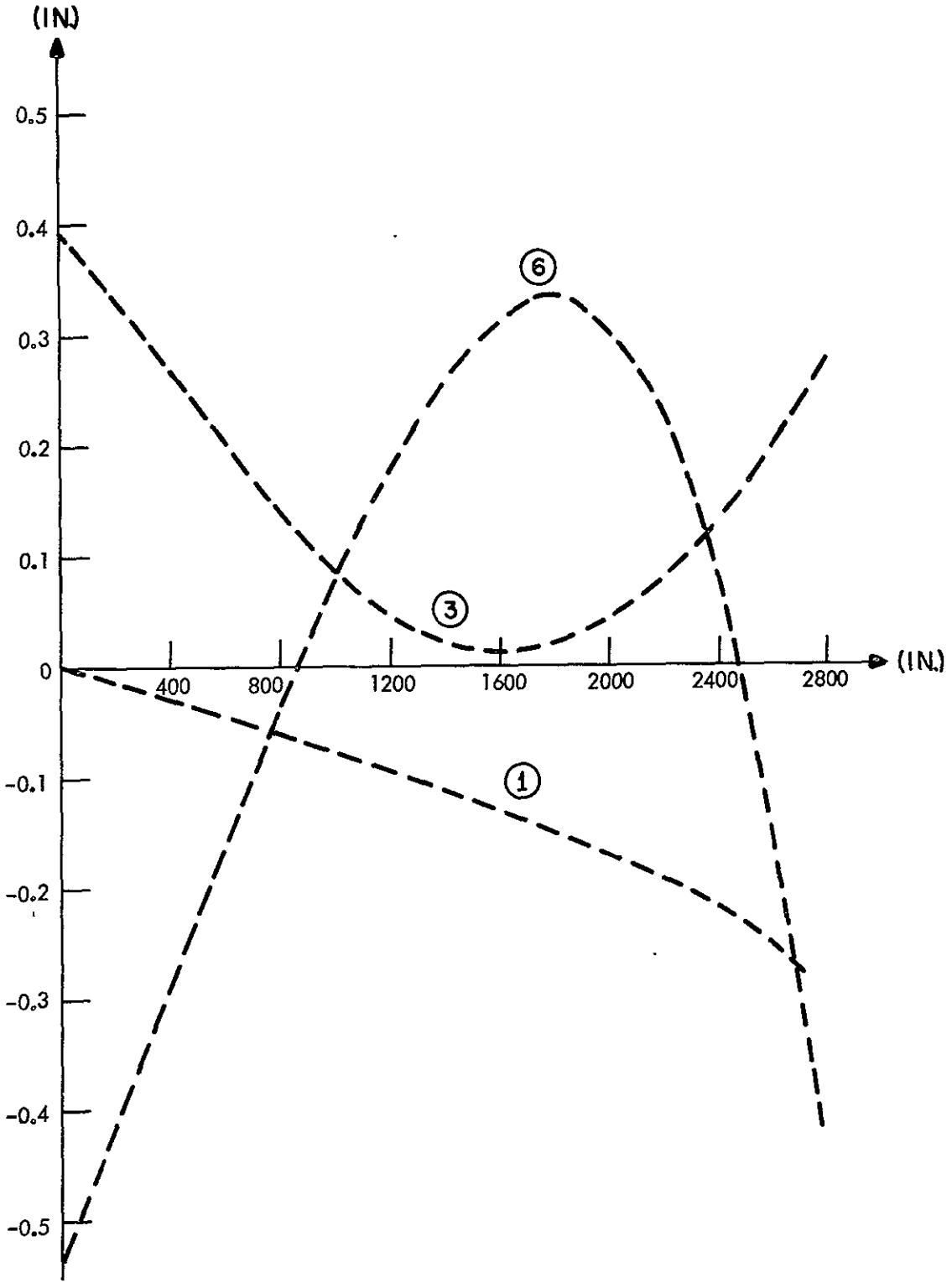

Chart 2 Vertical Deflection of Fuselage

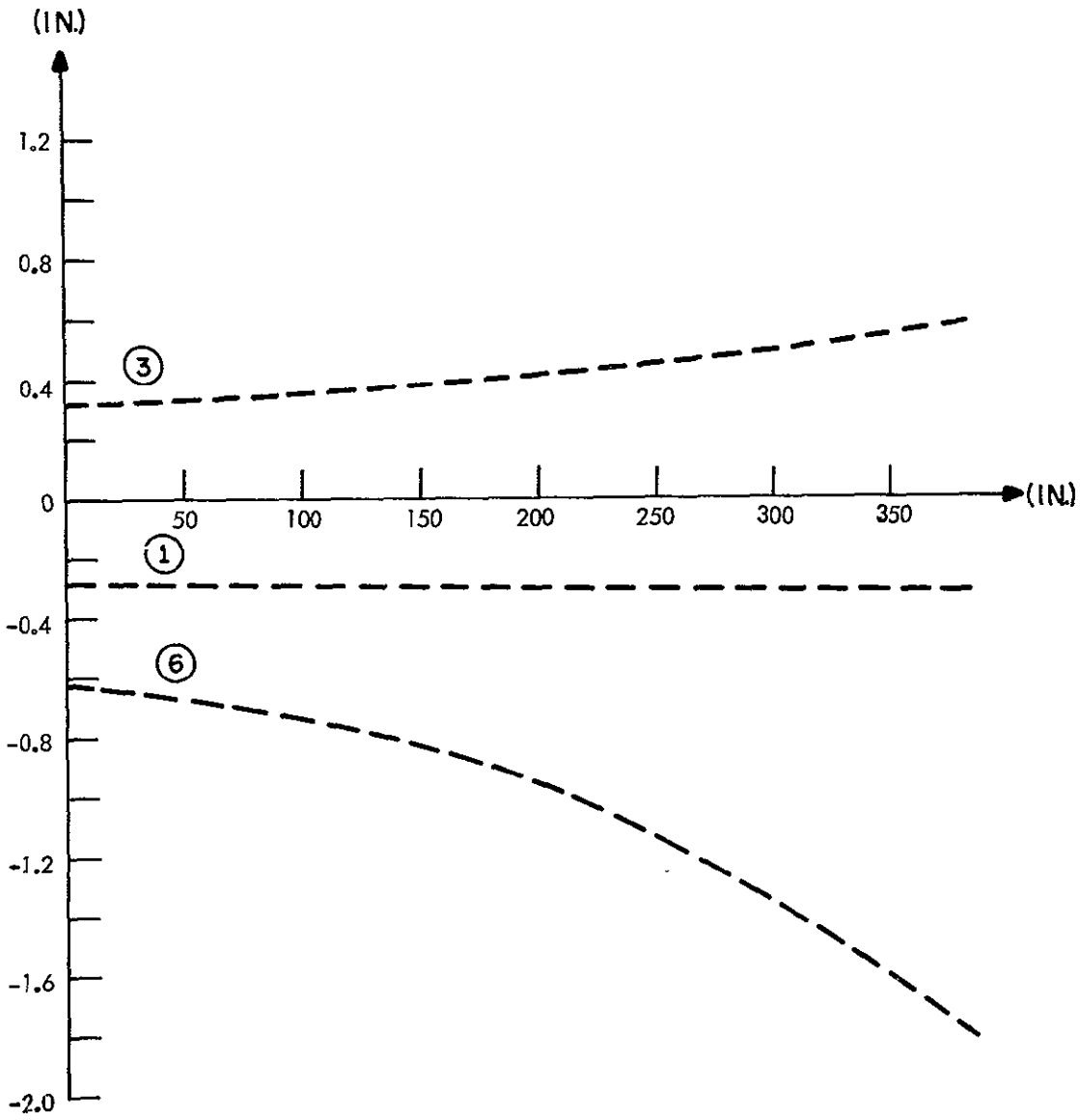

Chart 3 Vertical Deflection of Vertical Tail

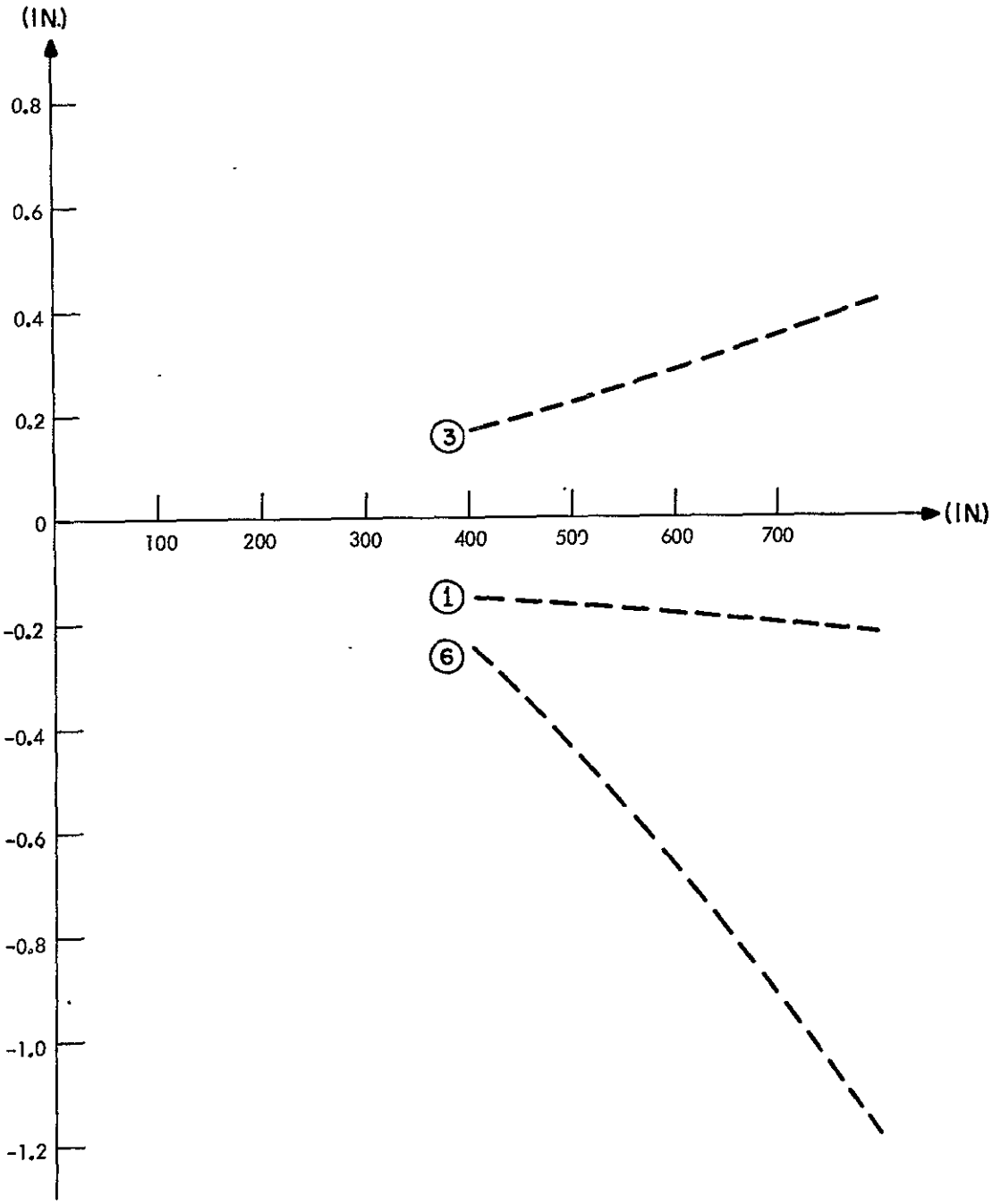

Chart 4 Vertical Deflection of Horizontal Tail

APPENDIX I

COMMENTS ON FORCE MATRIX PARAMETERS

This appendix contains miscellaneous notes on some of the more esoteric details of the modelling process.

1. Note on calculation of AXX, AXANG: The axis defined by AXX(I) and AXANG(I) corresponds neither to the hinge line nor the edge of control surface I. The axis should be calculated to correspond to the aerodynamic "center of pressure" due to the forces created by deflection of the surface. The book Foundations of Aerodynamics by Keuthe and Schetzer contains a derivation of center of pressure location for a flapped airfoil section (Sec. 5.5-5.8). If E is the ratio of flap chord to local chord (c(y)), then the center of pressure is a distance $x = c(y) \cdot K$ from the leading edge, where

$$K = \left[\frac{1}{4} + \frac{(1-E)\sqrt{E(1-E)}}{\pi - \sin^{-1}\sqrt{E(1-E)} + 2\sqrt{E(1-E)}} \right]$$

This has been derived from the expressions given in the above source. As E ranges from 0 to 1 the center of pressure starts at the quarter chord, moves back to about 35 percent of chord and returns to the quarter chord.

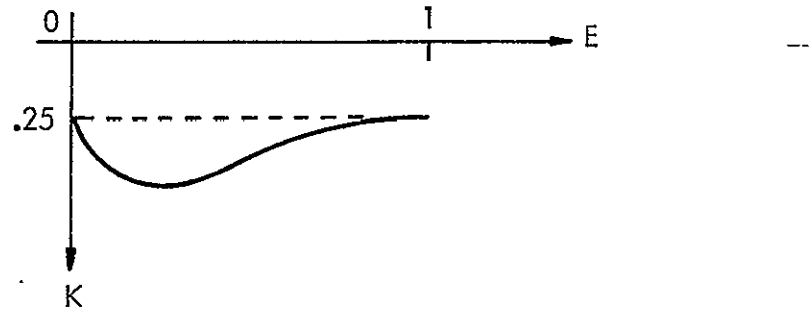

Fig. 1 Center of Pressure as Percent of Local Chord

The above source also gives the theoretical derivation of lift and moment coefficients which can be used in the linearized force equations if coefficients cannot be derived from the equations of motion for fixed locations. The magnitude of the vertical force exerted at the center of pressure due to a flap is

$$L = C_\ell q s(\alpha-\alpha_{LO}), \quad \text{where}$$

$$C_\ell = [\,2(\pi-\sin^{-1}(E\sqrt{1-E})) + 4E\sqrt{1-E}\,]\,\delta_f$$

δ_f = flap deflection (radians)

$q = \frac{1}{2}\rho V_\infty^2$ = dynamic pressure

$s = \ell_f c(y)$ = flap area

ℓ_f = flap length (span-wise)

$c(y)$ = local chord

α = local angle of attack

α_{LO} = zero lift angle of attack

2. A few comments on the simplifications in the mode shape are in order. First there is the distinction between free aircraft modes shapes (ξ_i) and the manufacturer's mode shape data for a specified flight condition. For a given flight condition there are distributed, velocity-dependent aerodynamic lift and damping terms on the right of Eqs. 1 and 2, Section III.A.2. These terms arise because of a change in local angle of attack and hence air flow (lift) pattern over the wing when a mode is excited. These are customarily brought to the left side (being constants of each flight condition) before mode shape data is generated. With aerodynamic effects included, the "modes" are coupled and the "natural" frequencies are changed slightly due to damping terms.

Aerodynamic terms are augmented by structural damping and coupling terms between torsion and bending modes (these cause further aerodynamic terms). Structural damping is usually approximated for lack of sufficient data by a constant on the order of .01 to .03. The structural coupling between bending and torsion modes depends on the specifics of basic structure of swept-wing aircraft. These structural effects are included in the equations for given flight conditions and for the free aircraft.

The net effect of aerodynamic and structural terms is to change the raw mode shape data given to the engineer and to add damping terms to the normal co-ordinate equations for the $\eta_1(t)$. Since these effects enter as data inputs (i.e., entries of the $\underline{F}$ matrix) rather than as computational modifications, they need be of no further concern.

REFERENCES

1. Athans, M., "The Matrix Minimum Principle," Information and Control, Vol. 11, No. 5, pp. 592-605.

2. Bisplinghoff, R. L., Aeroelasticity, Addison-Wesley Publishing Co., Reading, Mass., c 1955, pp. 106 ff.

3. Etkin, Bernard, Dynamics of Flight, John Wiley and Sons, Inc., New York, N. Y., c 1959, Ch. 4.

4. Francis, J. G. F., "The QR Transformation," The Computer Journal, October, 1961 (Part I), pp. 265-71, and January, 1962 (Part II), pp. 332-235.

5. Glasser, W. A., to M. A. Bender, "LAMS Optimization Study of the C-5A," Honeywell Interoffice Correspondence, Aerospace Division, April 19, 1968.

6. Honeywell, Inc., (Aerospace Division), Report to the Lockheed-Georgia Company," C-5A Data Base for Load Alleviation and Mode Stabilization Program," Honeywell Document 20564-DB1, April, 1968.

7. Kalman, R. E., "A New Approach to Linear Filtering and Prediction Problems," Journal of Basic Engineering, March, 1960, pp. 35-45.

8. Kalman, R. E., and Bucy, R. S., "New Results in Linear Filtering and Prediction Theory, " Journal of Basic Engineering, March 1961, pp. 95-108.

9. Keuthe, A. M., and Schetzer, J. D., Foundations of Aerodynamics, John Wiley and Sons, Inc., New York, N. Y., c 1950, pp. 79-87.

10. Landau, L. D., and Lifschitz, E. M., Mechanics, Addison-Wesley Publishing Co., Inc., Reading, Mass., c 1960 (by Pergamon Press), Ch. VI.

11. Press, H., Meadows, M. T., and Hadlock, I., "A Reevaluation of Data on Atmospheric Turbulence and Airplane Gust Loads for Application in Spectral Calculation," NACA Report 1272, 1956.

12. Potter, J. E., "Matrix Quadratic Solutions," SIAM Journal of Applied Mathematics, Vol. 14, No. 3, May 1966, pp. 496-501.

13. Rinzel, J. and Funderlic, R. E., ALLMAT computer subroutine, courtesy Union Carbide Corp., Central Data Processing Facility, Oak Ridge, Tenn.

REFERENCES (Contd.)

14. Schweppe, F., "Stochastic Dynamical Systems," Course Notes (6.606), M.I.T., Spring, 1969, Ch. 8.

15. Skelton, G. B., to Smith, F. B., "Distributed-Force Control," Honeywell Interoffice Correspondence (MR 10134), Systems and Research Center, Oct. 19, 1967.

16. Stein, G., To V. Levadi, "A Note on High-Speed Computation of Steady State Solutions to Linear Differential Equations," Honeywell Interoffice Correspondence (MRI0033), Systems and Research Center, July 14, 1967.

17. Stilley, G. D., and Pollack, "Method for Inclusion of Aeroelastic Degrees of Freedom in Solution of Equations of Motion of Aircraft," Minneapolis-Honeywell Aero Research Report (49174-21-TR3), March 8, 1957, pp. 64-89.

18. United States Air Force, Stability and Control Handbook, Flight Dynamics Laboratory, Wright-Patterson Air Force Base, Ohio, Oct., 1960.

19. United States Air Force Flight Dynamics Laboratory, Aircraft Load Alleviation and Mode Stabilization, Technical Report AFFDL-TR-68-158, December, 1968.

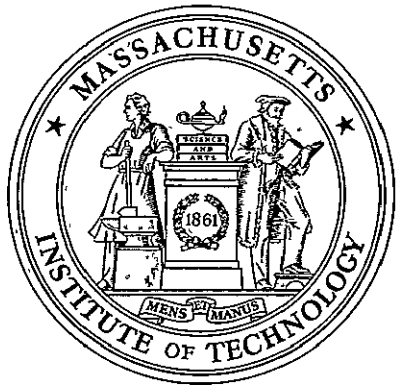
MASSACHUSETTS
INSTITUTE OF TECHNOLOGY
1861
MENS ET MANUS